2022

B Cell Receptor Signalng in Germinal Centers

Spencer T. Chen

B CELL RECEPTOR SIGNALING IN GERMINAL CENTERS

A Thesis Presented to the Faculty of
The Rockefeller University
in Partial Fulfillment of the Requirements for
the degree of Doctor of Philosophy

by

Spencer T. Chen

June 2022

B CELL RECEPTOR SIGNALING IN GERMINAL CENTERS

Spencer T. Chen, Ph.D.
The Rockefeller University 2022

Germinal centers (GC) are sites of B cell clonal expansion, diversification, and antibody affinity selection. This process is limited and directed by T follicular helper cells that provide helper signals to B cells that endocytose, process, and present cognate antigens in proportion to receptor affinity. GCs play a crucial role in immunity by generating an evolving B cell pool that serves as the origin of protective memory B and plasma cells. Therefore, understanding how the GC reaction is controlled and how high-affinity clones are selected within the GC is fundamental to our understanding of adaptive immunity and of crucial importance to the development of vaccines.

Under current models, GC selection is primarily determined by the antigen capture function of the B cell receptor (BCR). However, the BCR can also function as a signaling entity, and it is not well understood how signaling by the B cell receptor contributes to selection. The critical barriers to addressing this question have been a lack of specific BCR signaling reporters and models that do not compromise the initiation and maintenance of the GC reaction.

In the first part of my thesis, I developed and characterized a "tracker" to detect active antigen engagement *in vivo*. Crucially, this tracker does not confer any cognate antigen for presentation, thus uncoupling the signaling and antigen capture functions of the BCR. In the second part of my thesis, I used this tracker in combination with a c-Myc reporter to investigate the role of BCR signaling in positive selection. I found that BCR signaling itself enhanced the ability of cells to receive T cell help, even when antigen presentation had been normalized. Transcriptome analysis showed that continuous BCR engagement was necessary for full induction of positive selection pathways and identified a subset of pre-memory B cells associated with lower magnitudes of positive selection. GC BCR engagement per se also induces metabolic changes that may prime cells to receive T cell help.

To investigate the role of BCR selection in negative selection and survival, I developed a Bruton's tyrosine kinase (BTK) drug-resistant mouse model. I found that continuous BCR engagement was necessary for the survival of light zone B cells and that survival was intrinsic to BCR signaling by inhibiting BTK. Lastly, I investigated the synergy between BCR signaling and T cell help in the presence of antigen targeting and low levels of drug treatment. Dampening of BCR signaling impacted the proliferation of cells after migration, despite normalized antigen presentation capacity. In summary, selection in the GC is dependent on both the signaling and endocytic functions of the BCR.

To my Dad, Mom, and Brother.

Acknowledgements

Thanks first to the people directly involved in the work: Anna Gazumyan for producing Fabs, TM4-Core, and αDEC reagents; Melissa Cipolla for producing Fabs; Thiago Y. Oliveira for assisting with the RNA-seq analysis; Luka Mešin and Johanne Jacobsen for help with imaging; and Kai-hui Yao, Thomas Eisenreich, and Kristie Gordon for their research support. Thanks to Jennifer McQuillan, Adriana Barillas-Batarse, Zoran Janković, and Maša Janković for their help over the years. I was also very lucky to be supported by a fellowship from the NIH, NIAID grant F31A1147458.

I would like to thank my advisor Michel for his guidance, for challenging me, and for his critical mind which have sharpened my faculties as a scientist. I would also like to thank the members of my committee, Gabriel Victora and Daniel Mucida, for their advice, creativity, and mentorship, and for assembling a great group of colleagues.

To those that I am lucky to call friends, thank you for making this journey less lonely, for putting up with me, and for memories both good and bad.

To my family, thank you for your love, support, and patience.

Contents

List of Figures

Chapter 1

Introduction

1.1 Antibody Diversity

The mammalian immune system is characterized by its ability to produce specific, high-affinity antibodies to a diverse set of antigens, and this is crucial to protective immunity upon infection or vaccination. Antibody diversity is generated at several levels: primary diversification is determined by the combinatorial somatic rearrangement and joining of immunoglobulin Variable (V), diversity (D), and joining (J) segments during B cell development [1]; secondary diversification of the repertoire occurs by somatic hypermutation (SHM), in which nucleotide mutations are introduced into antibody genes by activation-induced cytidine deaminase (AID) [2–5].

1.1.1 Primary diversification generated by combinatorial and junctional diversity during V(D)J recombination

The V region of immunoglobulin light and heavy chains are encoded by two (V and J) and three segments (V, D, and J), respectively. During V(D)J recombination, each B cell generates a unique receptor through the random assembly and joining of segments, creating a continuous exon encoding the V region from an array of diverse V, (D), and J genes [6]. These arrays contain multiple copies of V, (D), and J gene segments and are organized into three clusters: the κ and λ loci; and the heavy-chain locus [7, 8]. The first level of antibody diversity is dictated by the random selection of these component segments during V(D)J recombination. In theory, because any rearranged heavy chain can be paired with any possible light chain, traditional estimates of the combinatorial diversity generated by rearrangement are in the range of $1.5 - 2.3 \times 10^6$ functional receptors [9, 10] (Table 1.1). In practice, however, the probability of specific rearrangements and heavy-light chain combinations is variable, and the diversity of the repertoire is likely under-expressed [11].

Additional diversity is generated at the junctions between gene segments during V(D)J recombination. V(D)J recombination is catalyzed by the activity of recombination-activating gene (RAG) recombinase that binds at recombination signal sequences (RSS) separated by 12 or 23 base pairs of spacer DNA next to V, D, and J elements [14–16]. Recombination occurs almost exclusively between a 12RSS and a 23RSS, thus ensuring the order of rearrangement in the generation of heavy (D-J followed by V-DJ) and

Locus	V	D	J	Minimum	Maximum
IGH	38-46	23	6	5244	6348
IGK	34-48	0	5	170	190
IGL	29-33	0	4-5	116	165

Table 1.1: Diversity generated by rearrangements of functional Immunoglobulin Genes [12, 13]

light (V-J) chains [16, 17]. RAG recombinase brings the two gene segments in close proximity and cleaves, generating DNA hairpins at the ends of the gene segments [18]. These hairpins are then nicked, and in the process of DNA repair, three additional mechanisms generate diversity at the junctions between gene segments: first, germline-encoded nucleotides can get deleted; second, missing palindromic nucleotides are filled in; and third, by terminal deoxynucleotidyl transferase (TdT) addition of non-templated nucleotides [19]. These changes introduce diversity between the D-J and V-DJ junctions in heavy chains and the V-J junction in light chains. These junctions, structurally, form the hypervariable **complementarity-determining region 3** (CDR3) of the antibody, responsible for conferring antibody-binding specificity. These random changes increase the diversity of possible receptors by several magnitudes ($> 10^{15}$).

1.1.2 Secondary diversification by Somatic Hypermutation in Germinal Centers

While combinatorial and junctional diversity is generated during B cell development, additional diversity is introduced in mature B cells by SHM within germinal centers. AID acts on immunoglobulin genes, deaminating cytosine substrates to uracil, creating U:G mismatches that are repaired by base-excision repair pathways [20, 21]. These gaps are filled in by error-prone DNA polymerase ɳ (Polɳ), creating additional mutations around the WRCY hotspot motif targeted by AID [22]. These mutations are the key to affinity maturation, as the mutations accrued via AID activity potentially enhance the affinity of the antibody receptor for antigen, allowing the pre-immune germline-encoded repertoire to adapt to infection or immunization.

1.2 B cell development and tolerance

1.2.1 Pre-Pro-B to Pro-B Cell Stages

B cell development begins in the bone marrow, and progression through developmental stages is directly linked to the ordered rearrangement of heavy and light chains and the generation of a functional surface B cell receptor (BCR) [23]. In the bone marrow, early progenitors turn on RAG1 and RAG2 and rearrange D-J_H segments on both alleles. These progenitors, now pro-B cells, initiate the joining of a V_H with the rearranged DJ_H segment. Rearrangement has a 1 in 3 chance of placing the V_H segment in frame with the DJ_H segment, and unsuccessful attempts at one allele can be rescued by rearrangement at the second allele [8]. The V_H chain pairs with surrogate light chains VpreB and $\lambda 5$ and

associate with Igα and Igβ to generate a pre-BCR complex [24–26]. Auto-aggregation and auto-signaling of the pre-BCR prevent further heavy chain rearrangement, turn off the expression of surrogate light chain genes, and in combination with signaling through the interleukin (IL-) 7 receptor (IL-7R), triggers cell division [27]. Notably, the prevention of further heavy chain rearrangement maintains **allelic exclusion**, the restricted expression of a single heavy and light chain pair [28, 29].

1.2.2 Pre-B Cell Stage and mechanisms of central tolerance

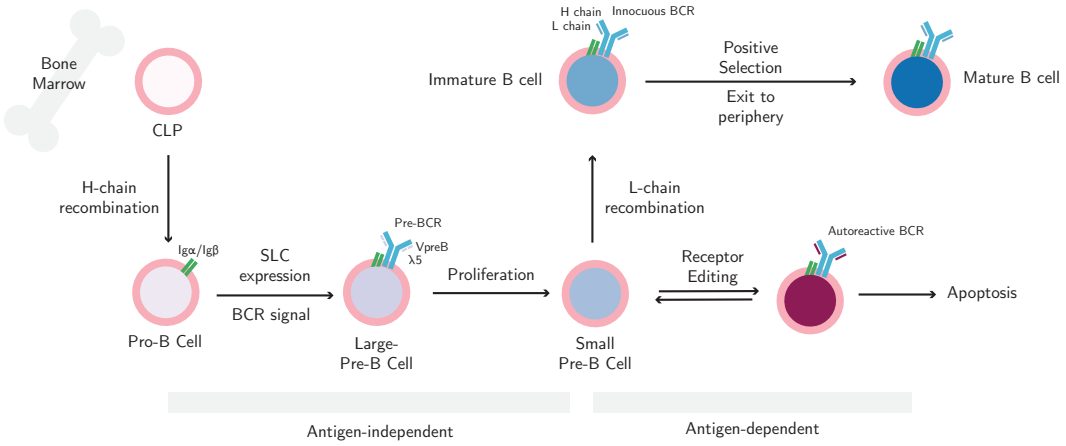

Figure 1.1: B cell development and central tolerance

Pre-B cells, marked by their expression of a pre-BCR complex, now initiate light chain rearrangement at the κ locus. RAG1 and RAG2 catalyze the joining of Vκ-Jκ segments. Successful light-heavy chain pairing generates a BCR that triggers tonic signaling and positive selection [27]. If, however, the rearrangement is unproductive or generates an autoreactive BCR, progression is arrested, and additional rearrangements can be attempted in a process known as **receptor editing** [9, 30, 31]. Receptor editing of light chains can continue as long as there are unrearranged V segments upstream and J segments downstream of the rearranged VJ [9]. This maximizes the potential to generate a functional BCR and maintains **central tolerance**, the negative selection mechanisms that prevent autoreactive B cells from progressing and entering the periphery [32]. B cells display **isotypic exclusion**, expressing either a κ or a λ light chain [33]. While most κ-expressing B cells retain germline configurations at their λ locus, λ-expressing B cells are frequently rearranged at the κ-locus and lack Cκ regions from recombination with the kappa deletion element or recombining sequence in humans and mice respectively [34–37]. This suggests that rearrangement at the λ locus occurs after attempts at the two κ loci have been exhausted. Immature B cells, expressing IgM receptors paired with either κ or λ light chains, exit the bone marrow and enter the periphery, becoming transitional B cells. Transitional B cells eventually mature into marginal zone B cells or follicular B cells [38].

1.2.3 Peripheral Tolerance

Central tolerance is imperfect and many autoreactive and polyreactive B cells slip through and make it to the periphery [39]. B cell development in the periphery is subject to antigen-dependent mechanisms that maintain **peripheral tolerance** [40–42]. Transitional B cells can no longer undergo receptor editing, and the fate of autoreactive B cells at this stage is controlled by the strength of receptor signaling received and the presence of secondary costimulatory signals. Autoreactive B cells with low-affinity receptors to “rare” autoantigens are "ignored," and there is little tolerization of these autoreactive B cells [41]. Responses to highly present self-antigens appear to be dominated by avidity. Encounter with lowly-multimerized and highly-multimerized self-antigen induce anergy or deletion respectively [43]. While transgenic studies have shown a range of anergic phenotypes, anergic B cells generally downregulate their levels of BCR, show a decreased lifespan, and are hyporesponsive to T cell help [44]. The induction of tolerance in developing B cells is also dependent on the presence of secondary signals from helper T cells. Consistent with the two-step model of B cell activation originally proposed by Bretscher and Cohn [45], it has been suggested that BCR signaling, signal 1, may be tolerizing by default, and B cells only contribute to immune responses in the presence of a secondary T cell cytokine or CD40L signal [41, 46]. Therefore, autoreactive B cells that bind to self-antigen in the absence of T cell help become tolerized.

1.3 Structure of the B cell receptor

1.3.1 Immunoglobulin Structure

V(D)J recombination during B cell development generates the two continuous exons encoding the immunoglobulin. Each “Y-shaped” immunoglobulin is composed of four polypeptides: two identical heavy chains; and two identical light chains. Immunoglobulins can be divided into three regions: the two identical **fragment antigen-binding** (Fab) regions which make up the “arms” of the “Y”; and the **fragment crystallizable** (Fc), which makes up the "trunk". The variable domains of the heavy (V_H) and light (V_L) chains pair to comprise the two **paratopes** or antigen-binding sites of the Fab. The remaining portion of the Fab is comprised of the C_H1 domain of the heavy chain and the C_L domain of the light chain. Each immunoglobulin domain is a sandwich of β-sheets linked by disulfide bonds. The framework regions encode the conserved regions of the V domain; these regions generate the β-sheet scaffold that makes up the structural core of the V domain. Looping between the β-sheets are the hypervariable CDR regions. Two of these regions, CDR1 and CDR2, are encoded in the V gene segment. The CDR3, encoded by the junction between the VJ and VDJ segments, displays a high degree of junctional diversity due to the imprecise joining and addition of P and N nucleotides during recombination. As the most variable portion of the antibody, the

CDRs, and most importantly, the CDR3, are crucial for the binding and specificity of the paratope [47, 48].

The Fc portion of the immunoglobulin is encoded by the heavy chain and is similarly constructed from a series of β-sheets [49]. Class-switch recombination, mediated by AID and DNA damage machinery, deletes constant gene segments and changes the isotype of the antibody while maintaining the specificity of the antigen-binding domain [50]. The Fc is comprised of three domains (C_H2-C_H4) in IgM and IgE isotypes, whereas IgG, IgA, and IgD Fc regions are comprised of two domains (C_H2-C_H3) [51]. While the Fab determines the specificity of the antibody, the Fc portion determines the effector function through its binding to Fc receptors expressed on immune cells. These responses are further modulated by the type of N-glycosylation present at the C_H2 domain [52, 53]. Antibodies can form high order structures in solution, increasing their avidity for antigen, with IgM and IgA antibodies forming pentameric (rarely hexameric) and dimeric complexes, respectively [51].

Connecting the two Fab regions with the Fc region of the antibody is a hinge region encoded by the CH2 exon in IgM and IgE antibodies and the C_H1-C_H2 exons in IgG, IgA, and IgD antibodies [54]. The hinge region is flexible, allowing each Fab arm to rotate to cover a range of angles [55]. Additional flexion is present between the V and C domains of the Fab, which can move angularly [56]. Altogether, the molecular motion of the Fab arms facilitates the binding of epitopes in different spatial rearrangements [57].

1.3.2 B cell receptor complex

The BCR is a multimeric complex of membrane-bound immunoglobulin associated with a heterodimer of Igα and Igβ [58]. Immunoglobulins are expressed in both membrane and secreted forms. Membrane-bound immunoglobulins (mIg) have an additional 26-residue transmembrane helical domain, relatively conserved across different isotypes, and a cytoplasmic tail. The length of the cytoplasmic domain differs depending on isotype; mIgM and mIgD have short cytoplasmic tails (3 residues), mIgA mid (14 residues), and mIgG and mIgE long cytoplasmic tails (28 residues) [59]. mIgs with short cytoplasmic tails, namely mIgM and mIgD, are unable to signal directly and require the association of kinases for the initiation of signaling [60].

Igα and Igβ are encoded by the *mb-1* and *B29* genes, respectively, and homologous in structure and function to CD3 chains in T cells [61]. Igα and Igβ have an N-terminal Ig-like domain, a transmembrane domain, and a C-terminal cytoplasmic domain. Igα and Igβ are linked by an intermolecular disulfide bond, but the mIg associates noncovalently with the Igα/Igβ heterodimer via the transmembrane domain of mIg and Igα respectively [58]. Igα and Igβ function as signal transducers, linking signals derived upon ligation of mIg with the activation of downstream protein tyrosine kinases (PTK) [62, 63]. This is mediated by the **Immunoreceptor Tyrosine-based Activation Motif** (ITAM) in their cytoplasmic tails; ITAMs have a conserved amino acid motif of two tyrosine residues separated by spacer residues, (D/E)XXYXX(L/I)X6–8 YXX(L/I), and are

similarly found in cytoplasmic domains of activating Fc receptors and in each of the CD3 chains in T cells [64].

The distribution of BCRs in resting B cells is an area of ongoing investigation. Tolar and colleagues used a fluorescence resonance energy transfer (FRET) approach to demonstrate that BCRs do not display higher-order oligomerization prior to antigen stimulation [65]. In the context of more contemporary views of the organization and function of the plasma membrane, the roughly 100,000 BCR molecules on the B cell surface can freely diffuse between zones dictated by "pickets" set by anchored transmembrane proteins and "fences" set by the cytoskeleton. In comparison, oligomeric BCRs formed spontaneously or in response to antigen binding are trapped and restricted within the "picket-fence" zones [66, 67].

1.4 B cell receptor signaling and B cell activation

B cell receptor signaling serves two interrelated functions: the initiation of signaling cascades that result in gene expression, survival, and metabolic changes in the cell; and the internalization of bound antigen for processing and presentation on major histocompatibility class II (MHC-II) molecules to cognate T helper cells, which in turn, provide helper signals necessary for full activation of the B cell. I first discuss the proteins and molecules involved in signaling through the BCR, beginning with the initiation of signaling, followed by propagation, and lastly, the integration of signaling with the induction of downstream pathways. Then I discuss how BCR binding triggers cytoskeletal rearrangements that promote membrane spreading over the surface of antigen presenting cells (APCs), contraction, and antigen extraction.

1.4.1 Activation of BCR signaling upon antigen encounter

The mechanism by which surface BCR encounter with antigen is relayed to trigger activation is an area of active investigation. However, tenets have been established regarding the nature of antigen required for signaling and the higher-order BCR oligomerization necessary to trigger signaling. Historically, biochemical studies of BCR signaling initiation were performed by soluble antigen stimulation. Multivalent, but not monovalent, stimulation was shown to efficiently trigger signaling after observing cap structures, the coalescence of multiple BCRs, which allows for widespread phosphorylation of Igα/Igβ ITAM tails [66]. However, B cells were observed to engage antigen displayed on the surface membranes of APCs, such as dendritic cells (DCs) or macrophages, *in vivo* [68–72]. *In vitro* studies also revealed that membrane-bound antigen is a more efficient activator of BCR signaling as even anchored monovalent antigen is capable of triggering signaling [73].

In light of these findings, one model that has received considerable traction is the **conformation-induced oligomerization model** of B cell activation. Under this model, the Cμ4 domain of the BCR exists in a default "closed" conformation that is not amenable to higher-order oligomerization of multiple BCRs. However, upon antigen

binding, the Cμ4 portion "opens" and is then receptive to oligomerization when in proximity with other antigen-bound BCR complexes. Oligomerization limits the diffusion capabilities of BCRs, allowing BCR microclusters to coalesce in a BCR-intrinsic manner. These microclusters are organized and maintained by cytoskeletal rearrangements and are necessary for the coordinated recruitment of kinases and signaling molecules associated with BCR signaling [66].

1.4.2 Initiation of the BCR signaling pathway

Upon antigen binding, the BCR is phosphorylated at the tyrosine residues within ITAM motifs of Igα and Igβ by the Src-family kinase Lyn [74]. Phosphorylation of the first tyrosine residue on Igα/Igβ recruits spleen tyrosine kinase (SYK), which phosphorylates the second tyrosine. SYK binds to the dual-phosphotyrosine motif via its two SH2 domains and triggers its own activation via autophosphorylation [75, 76]. The B cell linker protein, BLNK, is also recruited to Igα and binds via its C-terminal SH2 domain to phosphorylated Y204 outside of the Igα ITAM domain [77]. BLNK has five tyrosine residues in its central region which are phosphorylated by SYK kinase, generating docking sites for SH2-domain-containing proteins [78, 79].

1.4.3 Propagation of BCR signaling

Initiation of BCR signaling is propagated by the generation and dissemination of secondary messengers, including inositol triphosphate (IP_3), diacylglycerol (DAG), and free intracellular Ca^{+2} [80]. This requires the activation of the phosphatidylinositol-3-kinase (PI-3K) pathway. Upon BCR ligation, tyrosine residues in the cytoplasmic tail of the BCR coreceptor, CD19, are phosphorylated by Lyn, creating docking sites for the SH2 domains of the p85 subunit of PI-3K [81]. The association of PI-3K with CD19 increases the activation of the catalytic subunit of PI-3K, p110 [82]. PI-3K phosphorylates phosphatidylinositol 4,5-bisphosphate (PIP_2) to create phosphatidylinositol 3,4,5-triphosphate (PIP_3). PIP_3 is a substrate for proteins with pleckstrin homology (PH) domains, including Bruton's Tyrosine Kinase (BTK) [83, 84], the serine/threonine kinase AKT [85], and phospholipase Cγ-2 (PLCγ2) [86]. Recruitment of BTK and PLCγ2 to the plasma membrane puts them in proximity to SYK kinase and BLNK. BTK binds the phosphorylated Y96 residue on BLNK via its SH2 domain, and BTK is partially activated via phosphorylation by SYK kinase [84]. Subsequent autophosphorylation at Y223 leads to full activation of BTK [78].

Similarly, up to three PLCγ2 proteins are recruited to BLNK and are partially activated by SYK kinase activity. Complete activation of PLCγ2 requires BTK-mediated phosphorylation at residues Y753 and Y759 [87]. PLCγ2 cleaves PIP_2, generating IP_3, which binds to IP_3 receptors on the endoplasmic reticulum prompting the release of intracellular Ca^{+2} stores, and DAG, which activates protein kinase C beta (PKC-β) [88, 89]. Altogether, propagation of BCR signaling by secondary messengers requires the coordinated activation of PI-3K, BTK, and PLCγ2.

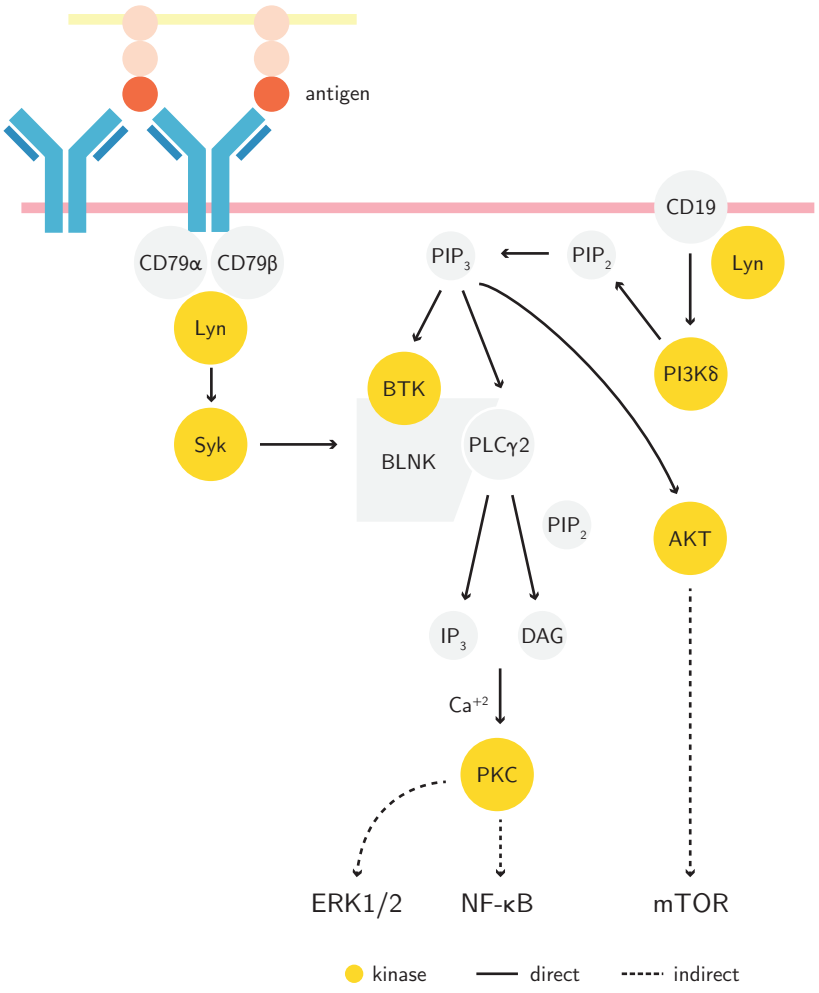

Figure 1.2: B cell receptor signaling: initiation, propagation, and integration.

1.4.4 Integration of BCR signaling

BCR signaling induces multiple transcription factors and signaling pathways. Here I discuss the induction of Akt downstream of PI-3K, mitogen-activated protein kinase (MAPK), and nuclear factor kappa B (NF-κB) pathways activated by BCR signaling.

AKT signaling leads to metabolic changes, which promote growth, survival, and proliferation pathways [86]. Generation of PIP_3 recruits AKT to the plasma membrane, where it is phosphorylated at its T308 residue by phosphoinositide-dependent kinase 1 (PDK1). AKT becomes fully activated upon additional phosphorylation at S473 via mechanistic target of rapamycin (mTOR) complex 2 (mTORC2) kinase. AKT phosphorylates and inactivates tuberous sclerosis complex 2 (TSC2), a component of the larger TSC complex. Inactivation of TSC2 disrupts TSC binding to the small G-protein Ras homologue enriched in brain (RHEB), which allows RHEB to bind to and activate mTORC1, leading to induction of downstream anabolic pathways associated with mTOR [90]. AKT also enters the nucleus and phosphorylates the transcription factor Forkhead box protein 01 (FOXO1), causing its exclusion from the nucleus and

preventing cell cycle inhibition and pro-apoptotic pathways downstream of FOXO1. Inhibition of FOXO1 and concurrent activation of Hypoxia-inducible factor 1α (HIF1α) downstream of mTORC1 promotes glycolysis and provides metabolites for other anabolic processes [86, 91, 92].

BCR signaling also activates the extracellular-signal-regulated kinase (ERK) MAPK pathway [93]. The Ras pathway is activated by binding to DAG and phosphorylation by PKC-β, leading to downstream activation of MAPK/ERK kinase 1(MEK1) and MEK2. MEK1 and MEK2 directly phosphorylate ERK1 and ERK2 [89]. ERK1 and ERK2 have numerous substrates, including other protein kinases, transcription factors, such as activator protein 1 (AP1), Fos, and Jun, and members of the B cell lymphoma-2 (BCL-2) family, which regulate apoptosis [94]. Activation of ERK by BCR signaling, therefore, has effects on cell cycle, proliferation, and growth.

PKC-β activation by DAG and Ca^{+2}, secondary messengers generated by PLCγ2, integrates BCR signaling with the activation of NF-κB pathways. NF-κB pathways govern several immune responses in B cells, including class-switch recombination, proliferation, and protection from apoptosis. In lymphocytes, activation of NF-κB pathways is mediated by a trimolecular protein complex consisting of CARMA1 (CARD-containing MAGUK protein 1), Bcl10, and MALT1 (Mucosa-associated lymphoid tissue lymphoma translocation protein 1) (CBM) [89]. Assembly of this protein complex is initiated by PKC-β phosphorylation of CARMA1 on S668, which allows the association of Bcl10 and MALT1 to form the CBM complex [95]. Activated CARMA1 associates with NF-kappa-B essential modulator (NEMO), or IKKγ , the regulator of the Inhibitor of NF-κB Kinase (IKK) complex. Association of the IKK complex, composed of IKKα-IKKγ, with CBM allows TRAF6 (TNF receptor-associated factor 6) to ubiquitylate the IKK and CBM complex, recruiting downstream signaling components transforming growth factor b-activated kinase 1 (TAK1) and the TAK1 binding protein [95]. TAK1 phosphorylates IKK, which in turn, phosphorylates IκB proteins, marking them for degradation and releasing NF-κB dimers to the nucleus where they can act as transcription factors [95]. This process is further enhanced by MALT1 proteolytic degradation of negative regulators of NF-κB, including the ubiquitin editing protein A20 and RelB, which inhibits canonical NF-κB signaling [96–98].

1.4.5 Negative Regulators of BCR signaling

The strength and quality of BCR signaling are modulated by negative regulators of BCR signaling. This is important in conveying different strengths of antigen-binding through the BCR and in the control of autoreactivity. Below, I discuss how the sialic acid-binding cell surface protein CD22 and the Fc receptor FcγRIIB receptor inhibit BCR signaling. CD22 and FcγrIIB possess **Immunoreceptor Tyrosine-based Inhibitory Motifs** (ITIM), the functional counterpart of the ITAMs found in Igα/Igβ, in their cytoplasmic tails [99]. Consistent with their roles as negative regulators of BCR signaling, both $CD22^{-/-}$ and $FcγRIIB^{-/-}$ mice show B cells hyperresponsiveness and auto-antibody production [100–102].

Sialic acids are sugar modifications present on cell surface proteins and lipids. Due to their widespread expression in mice and humans, sialic acids are considered self-ligands, and therefore their recognition should be tolerizing. CD22 binds to sialic acids via α2,6 linkages in *cis*, in *trans* on the surface of other cells, and to sialic acid modifications on Fc domains [103]. Upon BCR engagement, the Src-family kinase Lyn responsible for the phosphorylation of ITAM domains in Igα/Igβ, can also bind to and trigger the phosphorylation of tyrosine residues in the ITIM domains of CD22 [104]. Phosphorylation generates docking sites recognized by the SH2 domains of the phosphatase SHP-1. SHP-1 dephosphorylates key members of the BCR signaling pathway, including Igα/Igβ BLNK, and SYK, thus attenuating BCR signaling [105].

B cell activation thresholds are also regulated by FcγRIIB binding to Fc domains on IgG molecules. B cells recognizing antigens in the form of immune complexes are susceptible to co-ligation of the BCR and FcγRIIB, and ligation of FcγRIIB in the absence of BCR activating signals has been demonstrated to induce apoptosis [106]. FcγRIIB exerts inhibitory effects in several ways. Co-ligation of the BCR and FcγRIIB can disrupt early BCR oligomerization prior to the recruitment of Lyn kinase [106, 107]. Tyrosine residues in the ITIM domains of FcγrIIB can also be phosphorylated upon co-ligation, recruiting the phosphatase SHIP-1 [108]. Recruitment of SHIP-1 to the ITIM tail puts it in proximity to membrane PIP_3 generated by PI3-K activity. SHIP-1 dephosphorylates PIP_3 [109], thus inhibiting the activation of downstream signaling molecules dependent on PI3-K including BTK, AKT, and PLCγ2 [110]. Another regulator of PI3-K activity is the Phosphatase and tensin homolog, PTEN, which similarly dephosphorylates PIP_3, generating PIP_2 [93].

1.4.6 BCR-mediated antigen capture and processing

B cells function as efficient APCs in secondary lymphoid organs and present antigens to T cells in a class-II restricted manner. In contrast to other APCs, B cells are not phagocytic, and internalization is mediated by the antigen-specific BCR [111].

B cells encounter antigens *in vivo* in secondary lymphoid organs (SLOs) such as the lymph nodes and the spleen. Small soluble antigens that can readily diffuse through the subcapsular sinus (SCS) of the lymph node can be internalized and presented [112, 113]. Larger antigens, such as intact viruses or immune complexes, are presented by SCS macrophages or follicular dendritic cells (FDCs) via cell surface complement, Fc, and carbohydrate-binding scavenger receptors to follicular B cells [114]. Intact antigen is also displayed on the surface of FDCs within the germinal center [67].

BCR binding to tethered antigen triggers cytoskeletal changes at the site of contact, characterized by dissociation of the plasma membrane from the cytoskeleton through actin depolymerization and dephosphorylation of adapter ezrin and moesin proteins [115]. This is accompanied by the rapid polymerization of actin that radiates from the point of contact, leading to the protrusion of membrane lamellipodia and membrane spreading over the APC surface [116]. Membrane spreading increases the surface area of contact, increasing the probability of BCR-antigen interactions, which in turn propagate

local signaling and rearrangements through recruitment of kinases such as Lyn and SYK [66, 67, 117]. B cell adhesion to the APC cell surface is further enhanced by binding of the integrins Lymphocyte function-associated antigen 1 (LFA-1) and very late antigen-4 (VLA-4) to their corresponding ligands [118, 119]. Therefore, what begins as a single BCR-antigen interaction is quickly amplified. The spreading response is followed by synapse contraction, and the signalosome clusters are gathered to form a central supramolecular activation cluster (cSMAC) [120, 121]. B cells exert mechanical force on antigens [122], initiated by the contraction of myosin IIa, which extracts the antigen from the surface of the APC [121, 123]. Endocytosis of the bound BCR-antigen complex occurs via clathrin-coated pits (CCPs) [121]. It is still unclear the mechanism by which BCRs interact with and are internalized by CCPs, though it has been demonstrated that internalized BCRs retain signaling capacity [124]. These endosomes are trafficked to MHC processing compartments for processing and presentation [121].

1.5 The Germinal Center Reaction

While it was known that immunizations with protein antigens result in progressive increases in the ability of antisera to associate with antigen [125], it was unclear which properties were responsible. By focusing their investigation on the antibody response to a single epitope—the hapten DNP—Eisen and Siskind were able to demonstrate that there was a progressive increase in antibody affinity over time [126]. Subsequent studies replicated this result and supported the clonal selection hypothesis of antibody formation—namely that antigens activate B cells with corresponding antibody specificities [127, 128].

However, this increase in antibody affinity over time, **affinity maturation**, is not fully accounted for by the primary diversity of the pre-immune repertoire generated during B cell development. We now understand that affinity maturation occurs in structures called germinal centers, microanatomical structures located within SLOs that appear upon infection or immunization. These structures were first described by Walther Flemming in 1885 and postulated to be sites of lymphocyte development. Subsequent studies from Nieuwenhuis and others described the cellular constituents of the GC that we continue to study today [129]. Within these structures, B cells undergo secondary diversification of antibody genes by AID-mediated SHM coupled to division. SHM was first demonstrated to occur in GCs by Rajewsky and colleagues in studies where individual GC B cells were isolated and sequenced [130, 131]. This evolving B cell pool is subjected to Darwinian-like selection, where B cells of higher affinity progressively outcompete lower affinity counterparts, resulting in an overall increase in affinity for antigen [132]. The success of vaccination strategies hinges on their ability to generate GCs and drive B cell expansion and diversification. GC reactions are also crucial to the development of broadly neutralizing antibodies important in protection against viruses such as HIV-1 [133], and more recently, SARS-COV2 [134].

I begin by providing an overview of the cellular composition of the GC reaction and discuss models for how high-affinity B cells are selected.

1.5.1 Cellular Composition of the Germinal Center reaction

Germinal Center B cells

Naive B cells enter lymph nodes through high endothelial venules (HEV) and migrate to the follicle in response to the chemokine C-X-C motif ligand 13 (CXCL13) [113]. Within the follicle, B cells can encounter soluble antigens that freely diffuse through the afferent lymph vessel or intact antigens displayed on SCS macrophages and FDC membranes [135]. B cells that encounter their cognate antigen and are activated via their BCR upregulate the expression of chemokine receptors CCR7 (C-C chemokine receptor type 7) and EBI2 (Epstein-Barr virus-induced G-protein coupled receptor 2), which respond to the chemokines CCL19 or CCL21 [136], and the oxysterol 7α,25-HC respectively, guiding activated B cells to the T-B border [137–140]. Activated B cells concurrently downregulate surface S1P receptor 1 (S1PR1), which retains B cells in the follicle [141]. At the T-B border, B cells present cognate peptide on MHC-II to T helper cells and receive activation signals in the form of cytokines and CD40-CD40L interactions. T cell signals prompt an initial burst of proliferation and commitment to GC differentiation or an extrafollicular plasma or memory B cell fate [142, 143]. Recent work has demonstrated that class-switch recombination occurs predominantly, if not exclusively, among these pre-GC activated cells and rarely in the GC [144]. Activated B cells that commit to the GC reaction upregulate the transcription factor BCL-6 (B-cell lymphoma 6), which represses the expression of S1PR1 and EBI2 [145, 146]. GC-committed B cells migrate to the center of the follicle in response to CXCL13 and upregulate their expression of S1PR2, which promotes their confinement to the GC [147, 148].

Central to the differentiation and maintenance of the GC B cell phenotype is the master regulator, BCL-6, which is both necessary and sufficient for the GC B cell program [149–151]. BCL-6 is an oncogene, and transient expression of BCL-6 in hematopoietic stem cells is sufficient to induce mature B cell lymphoma, indicating that minute dysregulation in BCL-6 expression has extreme lymphomagenic potential [152]. In GC B cells, BCL-6 controls pleiotropic pathways, including B cell activation, apoptosis, the DNA damage response, and differentiation into plasma cells [151, 153, 154]. BCL-6 directly represses the transcription of *Myc*, *Ccnd2*, and *Nfkb1*, raising the threshold of helper signals needed to promote activation and proliferation [153, 154]. BCL-6 also regulates the expression of pro- and anti-apoptotic genes, including *Bcl-2*, which may underlie the high rate of apoptosis among GC B cells [153, 154]. Regulation of these apoptotic pathways is crucially linked to the repression of genes involved in the DNA damage response, including *Tp53*, *Cdkn1a*, and *Atr*, which is necessary for the ability of GC cells to tolerate damage accrued during SHM [155, 156]. Lastly, BCL-6 directly

represses the expression of *Prdm1* and *Irf4*, which encode transcription factors involved in plasma cell differentiation [157, 158].

GC B cells can be distinguished from naïve B cells by their high expression of the death receptor Fas, loss of glycoprotein CD38 and IgD expression, and binding to peanut agglutinin and the antibody GL-7 [159]. Phenotypically, GC B cells can be separated into two populations: the dark zone (DZ), or centroblast phenotype, composed of proliferative, cycling cells; and the light zone (LZ), or centrocyte phenotype, composed of activated cells. DZ cells can be distinguished by their high expression of the chemokine receptor CXCR4 and low expression of the activation molecules CD83 and CD86. In contrast, LZ cells are lower in their expression of CXCR4 but higher in their expression of CD83 and CD86 [160].

The DZ program is controlled by the transcription factor FOXO1, which is thought to suppress the "activated" LZ phenotype [161, 162]. Mice lacking FOXO1 are devoid of a DZ, owing in part to the dysregulated expression of CXCR4, necessary for the proper establishment of DZ polarization [162]. FOXO1 and BCL-6 cooperate in downregulating the expression of DNA damage genes *Tp53* and *Mdm2* [162]. This is crucial for affinity maturation because the DZ is the site of SHM. DZ cells express high levels of the cytidine deaminase AID, which targets cytosine residues within AID hotspot motifs [163]. These lesions are repaired by base excision and mismatch repair pathways and polymerase Polη activity, generating mutations that are the basis for affinity-based selection [22, 164]. AID activity is dependent on cell division, as the nucleus is only accessible to AID during early G1 [165]. DZ B cells are among the fastest cycling cells in mammals, with an estimated division time of 6-12 hours [166] and accumulate mutations in proportion to the amount of cell division [22].

The LZ program is characterized by activation gene signatures. LZ B cells extract intact antigen displayed on FDCs using their BCRs and process this antigen for presentation on MHC-II to LZ-resident Tfh cells; this interaction is enhanced by their high levels of CD83 and the costimulatory molecule CD86 [160]. LZ cells express high levels of CD69 and SLAMF1, consistent with their more activated phenotype relative to DZ cells [160]. A small population of LZ cells expresses *c-Myc*, representing cells that have received productive positive selection signals, and these cells enter S-phase before migrating to the DZ and progressing through cell cycle [167–169].

T follicular helper cells

T follicular helper (Tfh) cells are a specialized subset of $CD4^+$ T helper cells necessary for the maintenance and formation of the GC reaction [170]. Tfh cells provide T cell help to B cells within SLO structures, and dysregulation of Tfh frequencies leads to a lupus-like phenotype and the production of autoantibodies [171]. Tfh are required for the formation and maintenance of GC reactions, and their differentiation is a multi-step, multi-signal process that integrates initial priming from dendritic cells (DCs), TCR strength, cytokine signals, and T-B cognate interactions at the T-B border [172].

In addition to antigen presentation on MHC-II in the T cell zone, DCs provide costimulatory signals to surface CD28, ICOS, CD40L, and OX40 molecules on naïve T cells [173, 174]. DCs can also serve as a source of IL-6, which induces early expression of the transcription factor *Bcl-6*, necessary for induction and maintenance of the Tfh program [175]. Additionally, Tfh differentiation can be enhanced by IL-21 and antagonized by IL-2, which activate downstream transcription factors STAT1 and STAT3, and STAT5, respectively [176]. DC-priming upregulates the expression of BCL-6, promoting the expression of CXCR5 and EBI2 and downregulation of CCR7, prompting the migration of pre-Tfh cells to the T-B border where they can interact with activated B cells [173].

Cognate T-B interactions at the T-B border are the second step in Tfh differentiation. Activated B cells clonally expand and localize to the T-B border where they present cognate antigen on MHC-II to primed Tfh cells [177]. Activated B cells also express high levels of CD80, CD86, CD40, and ICOSL, which support the development of GC Tfh cells. Homophilic interactions between SLAM family proteins CD84 and SLAMF6 activate SLAM-associated protein, which is required for stable T-B interactions [178]. Cognate B-T interactions reciprocally lead to B cell proliferation and determine entry into the GC reaction [142, 143]. GC Tfh upregulate their expression of *Cxcr5*, and *S1pr2*, while downregulating their expression of *Ccr7*, which promotes their movement and confinement to the center of the follicle [179]. Tfh motility is amplified by bystander B cell provision of ICOSL to T cells [180].

GC Tfh can be identified by their high expression of CXCR5 and PD-1 [181]. Within the GC, GC Tfh provide survival signals in the form of costimulatory, crucially CD40L, and cytokine—IL-4 and IL-21—signals [182] and unlike GC B cells, can migrate between neighboring GCs [183]. Tfh form short cell-cell contacts via surface-expressed CD28, CD40L, ICOS, and integrins, among others [184], with GC B cells in the LZ which are prolonged when antigen density is increased [185]; these interactions are the basis for positive selection of LZ B cells.

T follicular regulatory cells

T follicular regulatory (Tfr) cells are a forkhead box P3 (FOXP3)-expressing subset of GC resident T cells that display features of both Treg and Tfh cells [186]. Tfr cells express Treg markers including Foxp3, GITR, Blimp1, and CTLA-4 but do not express B cell helper molecules CD40L, IL-4, and IL-21, characteristic of GC Tfh. However, like GC Tfh, Tfr express BCL-6, CXCR5, PD-1, and ICOS.

The origin and heterogeneity of Tfr cells is an area of active investigation. Initial parallel reports of this CXCR5$^+$ BCL6$^+$ FOXP3$^+$ PD-1$^+$ and ICOS$^+$ population concluded that Tfr cells develop from thymic derived Treg (tTreg) cells [187–189]. Development of these tTreg-derived Tfr occurs in a CD28 and SAP-dependent manner, similar to the development of GC Tfh [189]. However, subsequent studies have suggested that Tfr may be more heterogeneous in their origins and phenotypes than first reported. Tfrs can derive from peripherally induced Tregs and can also develop from GC Tfh cells in late-stage GCs [190, 191]. The development of Tfr was a conundrum given

that IL-2 activates FOXP3 while inhibiting BCL-6 expression, which are co-expressed in Tfr [192]. In the context of mouse influenza infection, Tfr development was inhibited early, coinciding with high levels of IL-2. The waning of IL-2 levels upon resolution of infection corresponded with a rise in Tfr numbers, indicating that Tfr development during an immune reaction is dynamic [193]. Whether Tfr development occurs in response to waxing and waning of IL-2 levels during other infections or immunization is unclear.

Tfr exert a suppressive function on the GC reaction though the exact mechanism of suppression is unclear. In the absence of Tfr, mice display augmented GC responses and can develop autoantibodies and spontaneous autoimmunity [189, 194]. *In vitro* co-culture assays have shown that Tfr suppress activation of Tfh and B cells as well as antibody production [195]. Similarly, *in vivo* suppression by Tfr has been demonstrated and is mediated in part by CTLA-4 [196]. Other mechanisms for suppression may be through the secretion of inhibitory cytokines [197]—though this has yet to be demonstrated *in vivo*—or a consequence of increased Tfr to Tfh ratios in the GC, which sequesters available Tfh help [191].

Follicular Dendritic Cells

First described by Miller and Nossal in 1964, follicular dendritic cells (FDCs) are specialized cells of stromal origin that reside within the center of the follicle [198]. FDCs require both tumor necrosis factor and lymphotoxin for their development and are essential for the initiation and maintenance of GC reactions [199–201]. FDCs establish the polarity of the GC reaction through their secretion of chemotactic factors CXCL13, the ligand for CXCR5 expressed on GC B and Tfh cells [202]. FDCs have been demonstrated to secrete the trophic factor B cell activating factor (BAFF) [203] when assessed *in vitro*, though ablation of FDCs *in vivo* does not affect the levels of BAFF in the tissue, suggesting that other stromal populations may serve as a source [201]. FDCs also secrete IL-6 [204], and they express integrin ligands Intercellular Adhesion Molecule 1 (ICAM-1) and vascular cell adhesion molecule 1 (VCAM-1), which can facilitate B cell adhesion and survival [184, 205].

However, the principal function of FDCs in the GCs is their presentation of intact antigen to GC B cells. FDCs express a wide array of Fc—FcγRIIB, FcεRII, FcμR, FcαR—and complement receptors 1 (CR1) and CR2 [114]. Shortly after immunization, FDCs in the LZ accumulate antigen in the form of antibody-antigen and complement coated complexes. Small, $<$70 kDa antigens can flow directly through the lymph and be deposited on FDC surfaces [112]. Larger antigens, such as viruses or bacteria, are thought to be captured via complement receptor 3 (CR3) or Fc receptors and transported across the SCS by SCS macrophages [114]. These antigens can then be captured by naïve B cells in a CR2-dependent manner and handed off to FDCs [71, 206]. The exact mechanism of this transfer is unclear but it is thought to be dependent on the higher density of CRs expressed on FDC surfaces, which captures the coated-antigen from B cells in an actin-dependent manner [207]. FDCs act as "antigen libraries" through their

retention and presentation of opsonized, native antigen [114]. These antigens are recycled by shuttling through a nondegradative endosomal compartment, allowing antigen to be presented in its native form to GC B cells over extended periods of time [208].

Tingible Body Macrophages

An understudied population in the GC microenvironment is DZ-resident tingible body macrophages (TBMs). TBMs are characterized by their phagocytosis of apoptotic cells, or "tingible bodies" [209]. This is mediated by FDC secretion of milk fat globule epidermal growth factor 8 (MFG-E8), which binds to exposed phosphatidylserine residues on apoptotic cells and integrin receptors on TBMs, thus facilitating the engulfment of apoptotic cells by TBMs [210]. This process is crucial for the maintenance of the GC reaction, and impairment of dead cell clearance is associated with autoimmune phenotypes, including systemic lupus erythematosus and autoimmune glomerulonephritis [211, 212].

1.6 Selection in the Germinal Center Reaction

1.6.1 Entry into Germinal Centers

Competition among B cells begins before they enter the GC reaction. Pre-GC B cells that capture and present the highest density of cognate antigen at the T-B border preferentially receive T cell signals necessary for differentiation to a GC phenotype [143]. This finding supported early observations that GCs elicited by hapten immunization appeared to be initiated by a small number of clones [213–215]. However, recent work has demonstrated that early GCs are seeded by tens to hundreds of different clones [216, 217]. This suggests that entry into the GC may not be as stringent as previously believed, and affinity maturation as the GC reaction proceeds depends on interclonal and intraclonal competition dynamics.

1.6.2 Positive Selection by T cell help

The increase in antibody affinity over time upon immunization or infection is dependent on the selective survival and expansion of high-affinity B cell clones in the GC reaction. A classic model of selection based on zonal segregation postulated that DZ GC B cells undergo rounds of cell division and diversification followed by migration to the LZ where they undergo affinity-dependent competition for survival and return to the DZ. However, the nature of this competition was unclear [159, 218]. Two leading hypotheses were raised: one, that GC B cells compete for and receive signals based on their engagement with antigen; and second, that GC B cells compete for T cell help based on their capture and presentation of antigen to T cells [218]. Imaging of GC B cell behavior indicated that LZ B cells travel over FDCs with little pausing. However, stable contacts between GC Tfh were infrequent, suggesting limited access to productive T cell help in the LZ [219, 220].

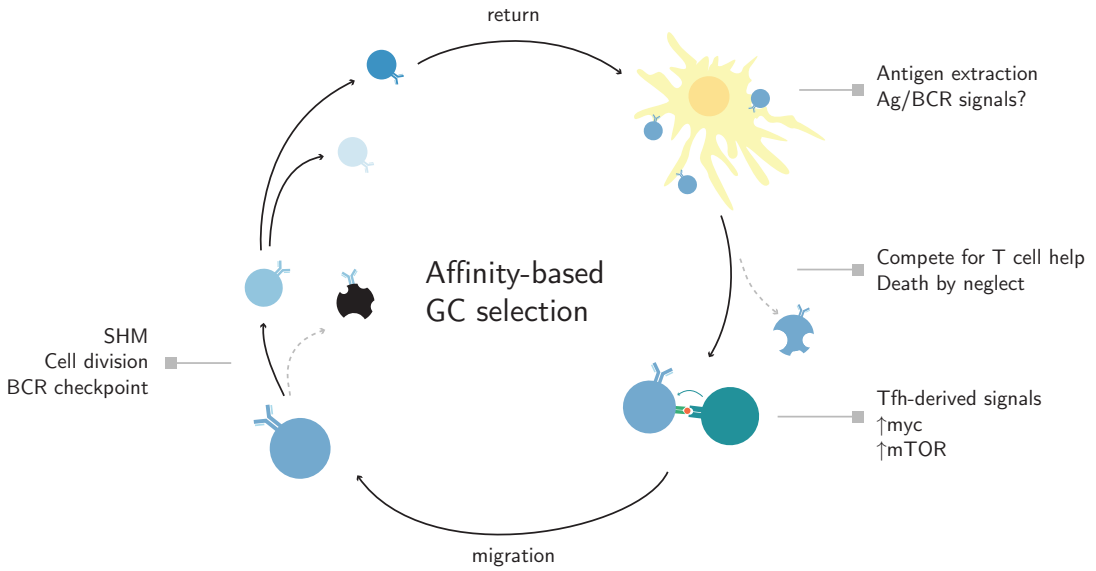

Figure 1.3: T cell centric model of affinity-based Germinal Center selection

Direct evidence for T cell mediated selection came from experiments where GC B cells were provided with increased amounts of antigen independently of BCR engagement [160]. This approach targets the surface lectin DEC205 with a chimeric anti-DEC205 antibody (αDEC) fused to a protein antigen such as ovalbumin (αDEC-OVA) [221, 222]. Antigen-targeted cells interact strongly with Tfh and migrate to the DZ where they proliferate extensively. Targeting T cell help to this population not only controls their zonal migration but allows them to dominate the reaction despite their initial minor representation in the GC [160].

Subsequent studies have refined our molecular understanding of the T cell-derived signals that drive positive selection. GC B cells have been shown to engage in "entanglement," a phenomenon characterized by increased surface area and duration of contact with Tfh cells. GC B-T cell interactions are subject to feed-forward loops along ICOS and CD40 signaling axes, allowing minute differences in pMHC density to be amplified [223]. Critically, CD40L signaling induces NF-κB necessary for proliferation in the DZ [224]. Tfh also secrete the cytokines IL-4 and IL-21 [182]—which can modulate the GC response and promote plasma cell responses [225]—and dopamine, which can enhance ICOS-CD40 feedback loops [226]. However, while some secreted molecules are concentrated via directed secretion across the immune synapse, how bystander activation from the non-directed secretion of factors is avoided is an area of continued investigation. A recent study has proposed a model where IL-4Rα expression on FDCs can act as a sink for secreted IL-4, limiting non-cognate activation [227]. Whether similar mechanisms exist for other secreted factors is unknown.

The strength of T cell signals received in the LZ directly correlates with the speed and number of cell divisions in the DZ, suggesting that selected cells retain a "memory" or record of the signals received [169, 228]. This is controlled in part by the magnitude of *Myc* induced—which determines the extent of proliferation [229]—and on biomass

accumulation in a mTORC1-dependent manner [230]. Selected LZ B cells turn on Myc and mTOR pathways and enter S-phase before their migration to the DZ where they continue to progress through cell cycle. Cycling in the DZ is sustained by Myc-dependent induction of the transcription factor AP4 [231] and occurs "inertially" in a cyclin D3 dose-dependent manner [232]. In this manner, affinity-dependent competition for T cell help results in the selective proliferation of high-affinity cells.

1.6.3 Negative Selection in the Germinal Center

Concurrent with proliferation in the DZ is the accumulation of mutation and DNA damage in an AID-dependent manner. While these random mutations diversify the repertoire and can result in affinity-enhancing mutations, they can also generate autoreactive antibodies [233]. Although much is known about the control of self-reactivity in immature B cells, the constraint of autoreactive GC B cells is less understood [234]. Germline reverted antibodies from self-reactive GC B cells demonstrate little binding to the final autoantigen, indicating that this self-reactivity originates from SHM in the GC [235–238]. Early attempts to model self-reactive signals in the GC introduced soluble antigen into ongoing GCs, which would mimic engagement of highly concentrated self antigen in the GC. GC B cells that experienced this extensive cross-linking of their surface BCRs underwent apoptosis, suggesting that GC B cells are sensitive to acute levels of BCR engagement [239–241]. Therefore, one mechanism for control may be clonal deletion via BCR-induced cell death that occurs upon strong engagement with self-antigen.

Another method of autoreactive control may be the "redemption" of self-reactive clones from recognition of self to foreign antigen [242–244]. This has been proposed as a rationale for the continued survival and retention of self-reactive anergic cells. Evidence for the recruitment and redemption in mice was shown using the HEL-HyHel10 model, where it was observed that self-reactive, reawakened anergic cells acquired mutations that lowered their affinity for HEL [245]. Clonal redemption was also observed in human antibodies using the IGHV4-34 heavy chain with pre-existing reactivity to glycans on erythrocytes [242] and B cells, and among malaria patients with insertions of collagen-binding LAIR1 insertions into antibody genes [246, 247].

Lastly, GC B cells that acquire self-reactivity during the GC reaction may fail to recruit necessary survival signals from Tfh and die by apoptosis. Using an apoptosis indicator mouse, Mayer and colleagues demonstrated that LZ cells that are "neglected" and fail to receive T cell help die by apoptosis [248].

1.6.4 Selection for export to post-Germinal Center fates

Although the generation of diverse, high-affinity antibodies occurs in the GC, GC B cells intrinsically possess little effector functions due to their minimal secretion of antibodies. Low-affinity, extrafollicular responses provide early protection during the immune

response [249, 250]. However, this response is transient, and immunity depends on GC-derived antibody-secreting cells, which secrete antibodies during infection, and memory B cells that rapidly differentiate to plasma cells upon re-exposure to antigen.

Plasmablast and Plasma cell Fate Decisions

The preponderance of high-affinity antibodies in the long-lived plasma cell (LLPC) compartment has been demonstrated in model antigen systems with well-defined high-affinity mutations [249, 251, 252]. This has led to the view that the plasma cell fate decision is instructive, such that cells with high-affinity BCRs receive signals that lead to their differentiation [250, 253]. Plasma cell differentiation is dependent on the induction of *Prdm1*, which in GC B cells is repressed by BCL-6 [254]. Therefore, a proposed molecular mechanism posits that commitment to the plasma cell fate results from strong BCR and T cell-derived CD40 signals that synergize to induce NF-κB and the PI3K pathway, activating IRF4 expression, which abates BCL-6 repression of Blimp1 [255–258]. Delivery of antigen via DEC205 targeting induces a wave of plasmablast production, suggesting that strong T cell help can induce differentiation [160]. This model is supported by work identifying pre-plasma cell precursors in the GC using Blimp1 and BCL-6 reporter systems, although disparate conclusions were drawn on the requirement for CD40 signaling [257, 259]. A competing, though not incompatible, model is supported by observations that the peak of LLPC export from the GC occurs at later timepoints [260]. GC B cell affinity increases in proportion to the time spent in the reaction and thus would explain the presence of high-affinity antibodies in the LLPC compartment. Outstanding questions include a better understanding of how particular isotypes, such as IgG [261] and IgE [262], and how GC B cell intrinsic [263] and extrinsic signals received by high-affinity cells favor plasma cell differentiation.

Memory B cell Fate Decisions

Recent work has advanced our understanding of the timing, precursor phenotype, and transcription factors associated with memory B cell differentiation [264–267]. A wave of low-affinity memory B cells is generated early from pre-GC and early GC B cells [260, 268, 269]. Memory precursors have also been identified by several groups and have been defined as LZ CCR6$^+$ Efnb1$^+$ cells with increased S1PR1, Ebi2, and CD38 expression, and decreased S1PR2 expression [270–273]. Memory differentiation has been associated with increased *Bach2* expression [273] and is dependent on transcription factors HHEX and TLE3 [274]. Together these studies suggest that memory B cells differentiate from predominantly low-affinity LZ cells that have received weak T cell help. This leads to lower mTORC1 activity, which favors memory differentiation versus DZ migration and proliferation in part by reduced activation of BCL-6 [271]. However, whether this operates at the absolute or relative levels of T cell signals received is unclear, particularly in the context of higher and lower memory B cell output during early and late GC

phases. How induction of apoptosis is counterbalanced by memory B cell differentiation remains a murky area of investigation.

1.6.5 Selection by Germinal Center B cell receptor signaling

Taken all together, a working model of affinity-based selection stipulates that antigen displayed on FDCs in the LZ is captured by the BCR, internalized, processed, and presented to Tfh. T cell help is limiting and differentially delivered to LZ B cells that display higher levels of cognate peptides on MHC. This interaction induces selected B cells to upregulate positive selection pathways and migrate to the DZ where they mutate their antibody genes and divide proportionally to the strength of the T cell signal received. B cells that have exhausted their division capacity return to the LZ, where they test their newly mutated antibody receptors for antigen capture [159, 275]. According to this model, GC selection is determined primarily by the ability of the BCR to bind to and endocytose antigen. However, the BCR is a dual-purpose receptor that is both a signal transducer and an endocytic receptor, and the role of BCR signaling in affinity-based selection remains poorly understood.

Initial experiments investigating GC BCR signaling suggested that GC B cells are insensitive to soluble antigens due to increased phosphatase activity. This, along with the low levels of surface BCR expression on GC B cells, led to the view that GC BCR signaling is silenced *in vivo* [276]. However, more recent work, in which GC B cells were exposed to membrane-tethered antigens that resemble the display on FDCs, showed that stimulating GC B cells in this manner activates BCR signaling [277–279]. The GC B cell differentiation program is associated with the rewiring of signaling pathways, which accounts for their general attenuation compared to other B cell populations. BCR and CD40 signaling pathways are rewired such that both are required in short succession in order to induce Myc and NF-κB pathways [224]. Signal propagation is also altered by differential phosphorylation of AKT1, which activates the phosphatase PTEN and other negative regulators of BCR signaling [280].

GC B cells also have altered synaptic architecture, which allows them to exert greater tensile forces during antigen extraction, resulting in enhanced affinity discrimination. In contrast to naïve B cells, extraction of antigen by GC B cells is not centralized and is uncoupled from endocytosis [277, 281]. These studies explain the underlying signaling rewiring associated with the GC B cell differentiation program. However, whether BCR signaling plays a direct role in selection remains to be determined.

Attempts to study the role of GC BCR signaling *in vivo* using constitutive or conditional knockouts of BCR signaling components have been hindered by the necessity of BCR signaling for the initiation and maintenance of the GC reaction [224, 282–285]. Some degree of tonic signaling is also necessary for return from the DZ as B cells with nonfunctional or structurally compromised BCRs are rarely found in the LZ [248, 286]. Nur77-GFP reporter mice have been used to identify a population of LZ B cells with active BCR engagement *in vivo* [287]. However, whether this reporter is specific to BCR engagement or can be induced by other activating signals, including T cell help, is uncertain. Therefore, one of the challenges in studying GC BCR signaling *in vivo* is a lack of BCR-specific tools and mouse models.

To examine the role of BCR engagement in GC selection, I developed a molecular tracker to detect antigen engagement and presentation *in vivo*. I combined this tracker with reporter models to uncouple B cell intrinsic changes upon antigen capture from T cell signals provided in response to antigen presentation. Lastly, I developed a drug-resistant mouse model that I used in combination with pharmacological inhibition to block or dampen BCR signaling *in vivo*.

Chapter 2

Results

2.1 Tracking germinal center BCR engagement *in vivo*

2.1.1 NP-Eα tracking identifies GC B cells engaging antigen *in vivo*

To track antigen binding and processing by GC B cells *in vivo*, I produced a tetrameric antigen consisting of fluorescently labeled streptavidin (SA-AF647), coupled to 4-hydroxy-3-nitrophenylacetyl (NP) and biotinylated I-E52-73 (Eα) peptide (NP-Eα) (Figure 2.1A). NP-specific B cells that bind and internalize NP-Eα will be AF647 fluorescent, and those that process and present the antigen as pMHC can be detected with an antibody specific to the Eα-pMHC (Y-Ae) [70, 143, 288, 289] (Figure 2.1B).

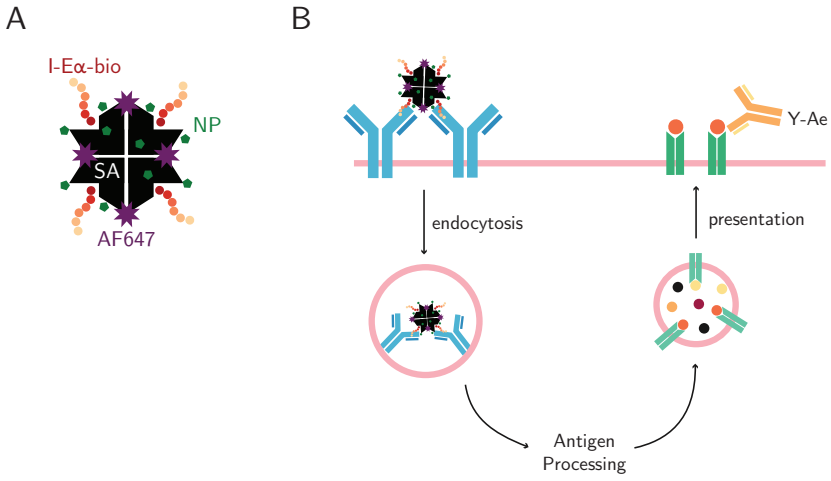

Figure 2.1: Binding, processing, and presentation of NP-Eα provides no additional T cell help.
(A) Cartoon representation of NP-Eα. (B) Binding, internalization, and processing of NP-Eα.

I elicited GC reactions using congenically-marked B cells carrying a knock-in heavy chain that, when paired with a lambda light chain (Igλ), produces a high-affinity receptor for NP (B1-8^{hi}) [290]. B1-8^{hi} B cells were adoptively transferred into ovalbumin (OVA)-primed mice that were subsequently boosted with NP-conjugated OVA (NP-OVA) (Figure 2.2A). This immunization scheme produces GCs containing OVA-specific Tfh cells, NP-specific B1-8^{hi} B cells, and host B cells [160, 220].

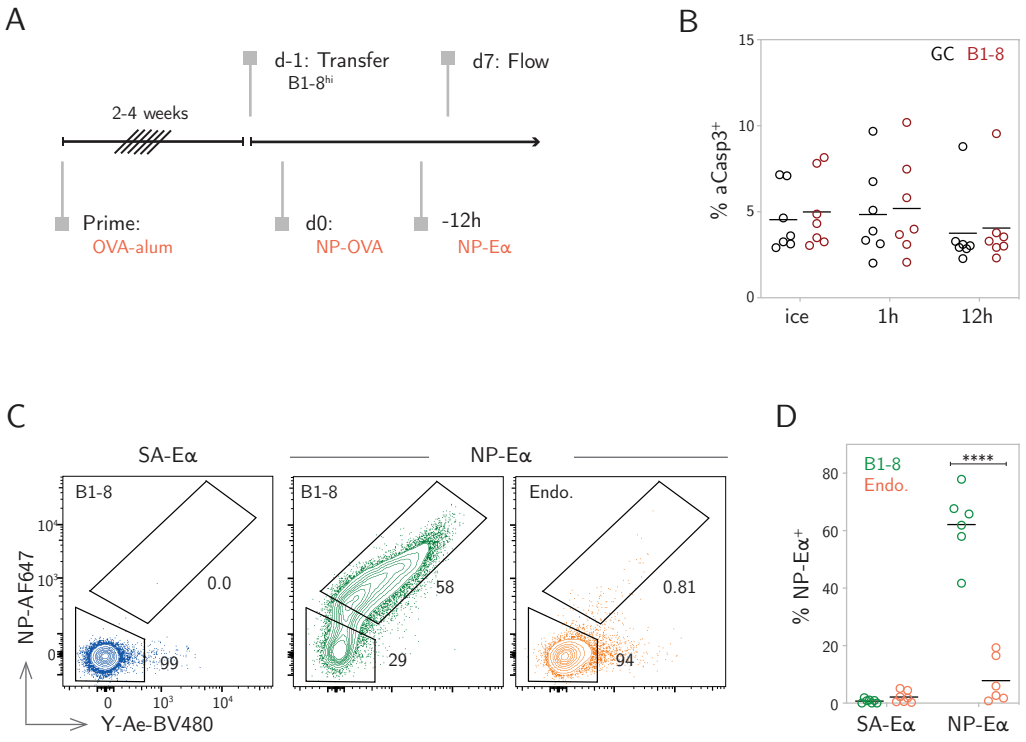

Figure 2.2: *In vivo* tracking of antigen engagement
(A) Experimental setup. (B) Frequency of aCasp3^{+} among total GC (black) or GC B1-8^{hi} (red) populations after NP-Eα injection, Two-way ANOVA with Šidák's multiple comparisons, ns. (C) Representative flow cytometry plots showing internalization and presentation of SA-Eα or NP-Eα by GC B cell populations. (D) Frequency of NP^{+} Y-Ae^{+} (NP-Eα^{+}) among B1-8^{hi} or host (endo) B cells after injection of ^{7}NP-Eα or SA-Eα, P-values calculated using two-tailed paired t-test, ****p<0.0001. (B, D) Data from two independent experiments. Each dot represents one mouse. Lines depict mean.

Introduction of high concentrations of soluble antigen into ongoing GC reactions can induce cell death due to extensive BCR crosslinking [239–241]. To circumvent this, I titrated and injected a small amount of low-valency NP-Eα for *in vivo* tracking and found no measurable increase in apoptosis (Figure 2.2B). Under these conditions, 40-80% of B1-8^{hi} GC cells were AF647 labeled, and cells that bound NP-Eα also presented it as indicated by staining with Y-Ae (NP-Eα^{+}) (Figure 2.2C and D). Control SA-AF647 labeled tetramers without NP showed little or no direct fluorescence staining (Figure 2.2C and D). Therefore, introduction of NP-Eα into ongoing GC reactions tracks antigen engagement in a BCR-specific manner.

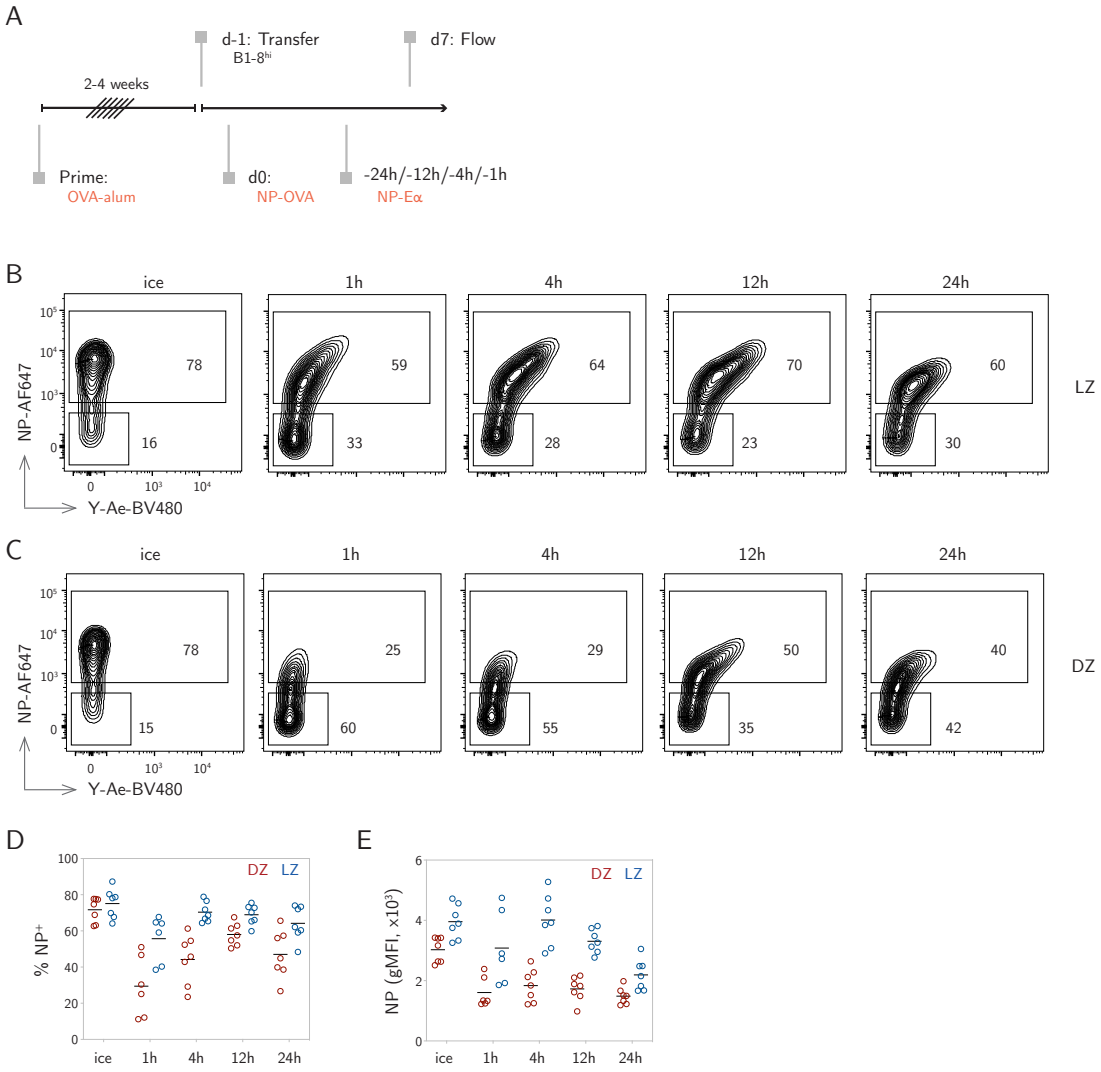

Figure 2.3: Kinetics of NP-Eα internalization and presentation
(A) Experimental setup. NP-Eα was injected 1h, 4h, 12h, or 24h before sacrifice. Control mice were injected with SA-Eα and cells were labeled with NP-Eα on ice. (B-C) Representative flow cytometry plots showing LZ (B) and DZ (C) B1-8^{hi} uptake and presentation of NP-Eα over time. (D) Summary of (B, C), frequency of NP^{+} DZ and LZ B1-8^{hi} over time. (E) gMFI of NP-AF647 in NP^{+} DZ and LZ cells over time (D-E) Data from two independent experiments. Each dot represents one mouse and lines depict mean.

Notably, I failed to detect NP-Eα binding and presentation by 15-40% of B1-8^{hi}

cells in GCs. To investigate the kinetics and dynamic range of NP-Eα tracking *in vivo*, I introduced NP-Eα into GC reactions at consecutive time points (Figure 2.3A-E). GC B cells isolated and labeled with NP-Eα *ex vivo* on ice were uniform in their AF647-labeling with no difference between LZ and DZ cells (Figure 2.3B and C). LZ B cells labeled *in vivo* were AF647-labeled but Y-Ae negative as early as one hour after injection and over time, the proportion of AF647$^+$ Y-Ae$^+$ cells increased (Figure 2.3B). The relative proportion of B1-8^{hi} cells that failed to bind NP-Eα was consistently higher in the DZ than in the LZ (Figure 2.3D).

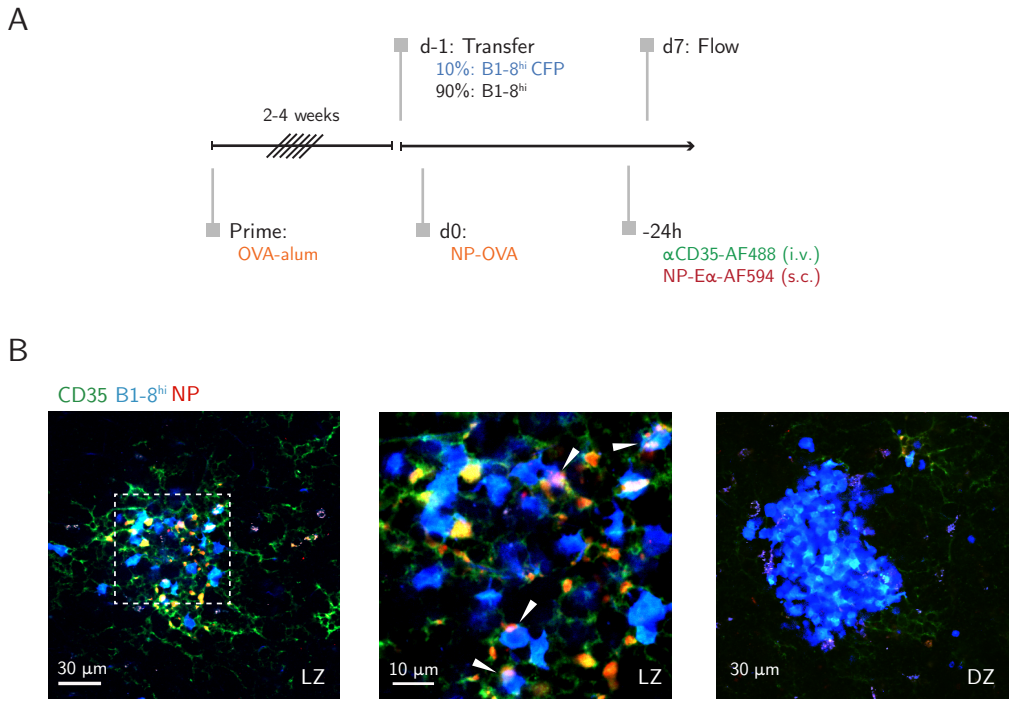

Figure 2.4: NP-Eα localizes to FDCs in the LZ
(A-B) Experimental setup and multi-photon images of GCs after prime-boost and transfer of B1-8^{hi}CFP cells. αCD35-AF488 and ^{7}NP-Eα-AF594 were injected intravenously and subcutaneously (s.c.) respectively 24 hours before imaging. LZs were identified by presence of FDC networks labeled with αCD35. LZ (leftmost panel); inset of LZ as marked with dashed line (center); and DZ (rightmost panel).

Imaging GCs revealed that NP-Eα is localized to FDCs in the LZ and bound and internalized by B1-8^{hi} cells (Figure 2.4A and B) but NP-Eα was not detectable in the DZ. Therefore, antigen access, in addition to phenotypic differences and BCR expression levels between LZ and DZ cells [291] may explain why the amount of antigen bound by LZ cells was higher (Figure 2.3). I conclude that the NP-Eα tracker identifies B cells binding and presenting antigen *in vivo* and can identify phenotypic difference otherwise missed by antigen-labeling on ice.

To determine if the apparent lack of binding was a consequence of lower surface BCR expression, I measured surface BCR by staining for Igλ (Figure 2.5A-F). Igλ surface expression was comparable in LZ-NP-Eα$^+$ and NP-Eα$^-$ populations. DZ cells showed lower levels of BCR surface expression compared to LZ cells, and DZ-NP-Eα$^-$

cells showed a bimodal distribution of Igλ, likely representing dilution of surface BCR among cells with different extents of cell division (Figure 2.5A-F). Consequently, absence of antigen binding by some DZ but not LZ cells might be explained by lower levels of surface BCR expression.

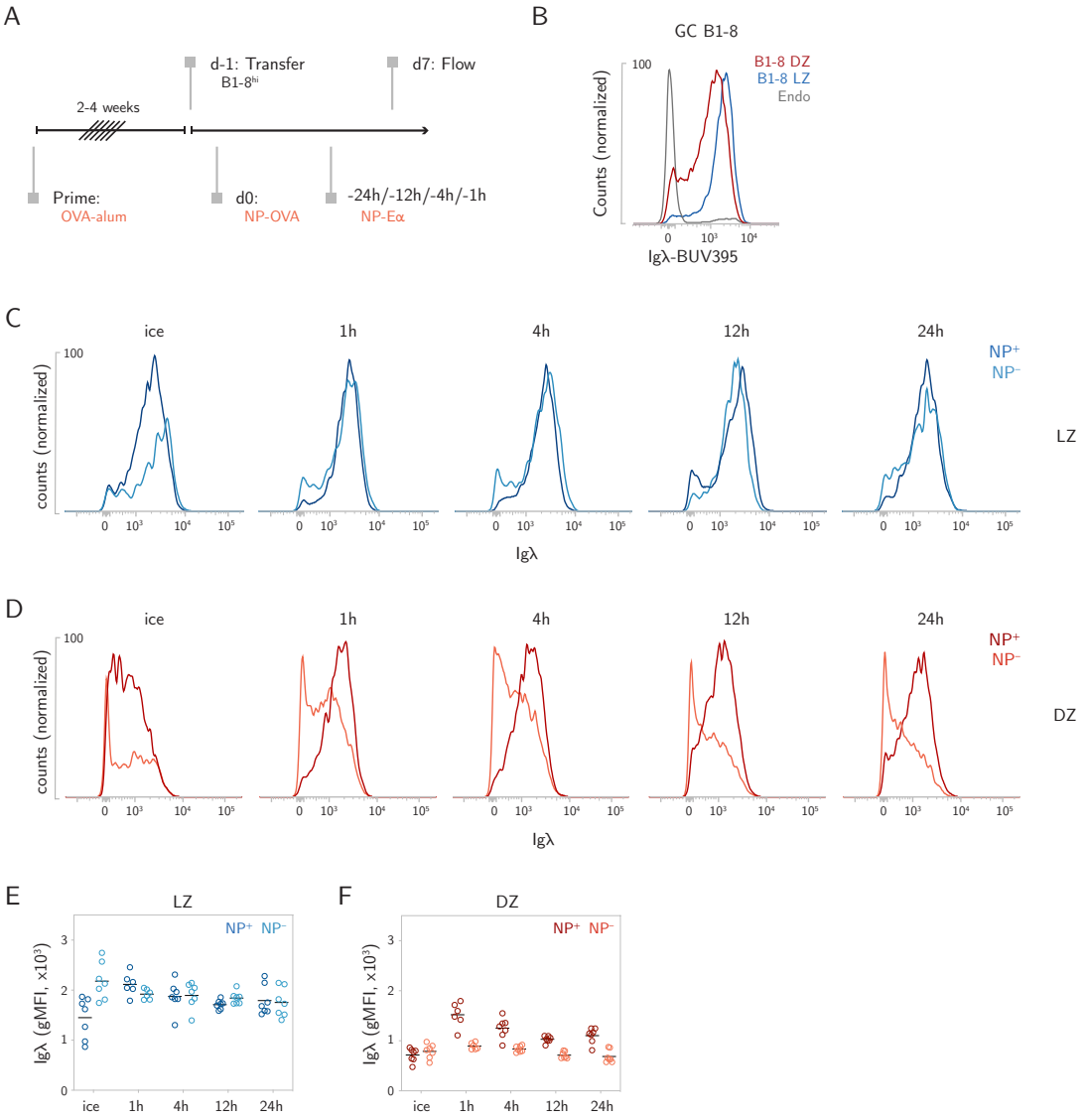

Figure 2.5: Kinetics of BCR expression with NP-Eα engagement
(A) Experimental setup. NP-Eα was injected 1h, 4h, 12h, or 24h before sacrifice. Control mice were injected with SA-Eα and cells were labeled with NP-Eα on ice. (B) Representative histograms showing Igλ surface levels between B1-8^{hi} and endogenous GC B cells. (C-D) Representative histograms showing Igλ surface levels of LZ (C) and DZ (D) B1-8^{hi} NP^{+} and NP^{-} populations over time. (E-F) Summary of Igλ gMFI of LZ (E) and DZ (F) NP^{+} and NP^{-} populations over time. Data from two independent experiments. Each dot represents one mouse and lines depict mean.

2.1.2 Loss of antigen engagement *in vivo* is not the result of recent zonal migration.

This persisting fraction of NP-Eα^{-} cells in the LZ may represent recent DZ to LZ emigrants that did not have sufficient time to engage with NP-Eα. To address this possibility, I performed sequential injections of NP-Eα labeled with two different fluorophores and two different conjugation ratios, which would allow labeling of recent emigrants that might otherwise be missed (Figure 2.6A and B). GC B cells that engaged with the first NP-Eα also engaged with the second, and there was little to no differential engagement with the second injection alone when both injections shared the same conjugation ratio. However, secondary injection with a higher avidity antigen, ^{14}NP-Eα, labeled a lower affinity population (Figure 2.6B). This indicates that the lack of engagement by the NP-Eα^{-} population is unlikely the result of recent zonal migration and lack of opportunity to bind to injected NP-Eα, but may represent differences in binding affinity.

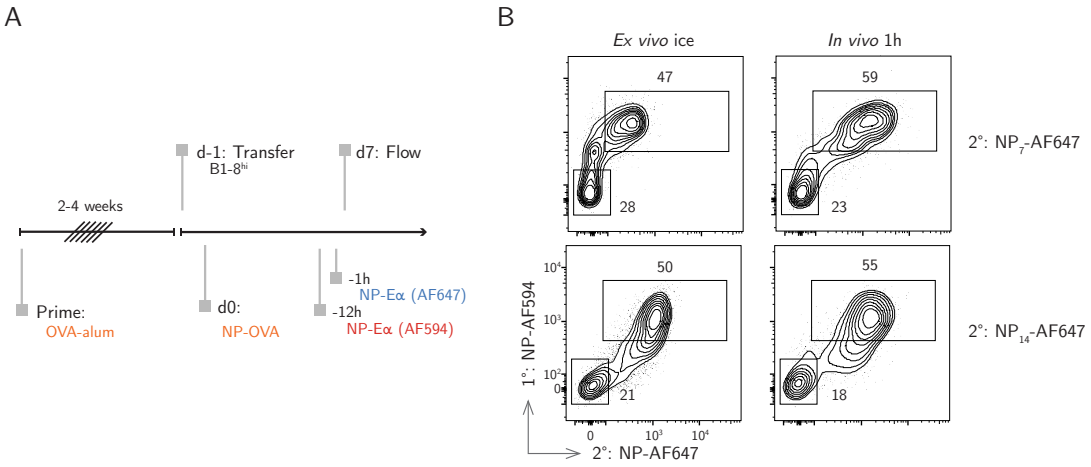

Figure 2.6: Sequential labeling with NP-Eα
(A)Sequential labeling setup. ^{7}NP-Eα-AF594 was injected 12h before assay while ^{14}NP-Eα-AF647 was injected 1h prior or incubated *ex vivo* on ice. (B) Lack of NP-Eα is not the result of recent LZ entry but tracking with higher avidity ^{14}NP-Eα-AF647 identifies a lower affinity population.

2.1.3 Loss of antigen engagement *in vivo* is associated with deleterious SHM.

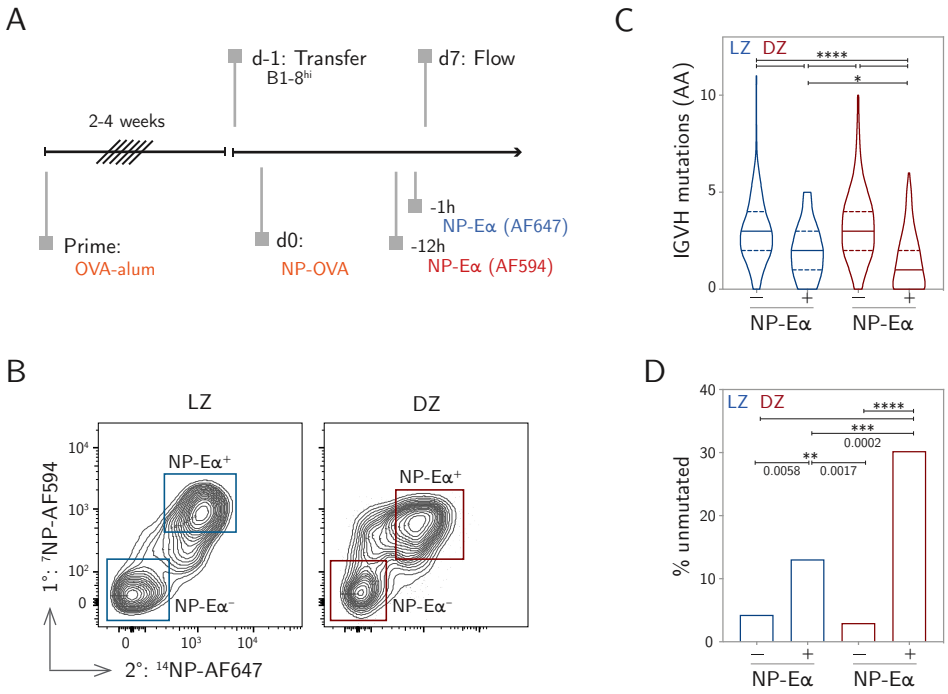

Figure 2.7: Inability to engage with NP-Eα is associated with higher frequencies of SHM. (A) Sequential labeling setup for sorting. (B) Sorting strategy. Two populations of binders and nonbinders were sorted from the LZ and DZ, respectively. (C) Number of amino acid (AA) mutations in IGVH chains of sorted populations, Violin plot depicts median and quartiles. *p=0.020, ****p<0.0001, Kruskall-Wallis with Dunn's multiple corrections test. (D) Fraction of unmutated cells in sorted populations, Fisher's exact test, ** and *** p-values indicated, ****p<.0001.

To determine if the loss of antigen engagement by the B1-8^{hi} population was the result of deleterious mutations I repeated the sequential NP-Eα labeling and isolated individual B cells for sequencing. Two groups of LZ and DZ cells were examined: double negative cells (LZ-NP-Eα$^-$ and DZ-NP-Eα$^-$) that were not labeled; and double positive cells (LZ-NP-Eα$^+$ and DZ-NP-Eα$^+$) that were (Figure 2.7A and B). NP-Eα$^-$ cells were more mutated than their antigen-binding counterparts (Figure 2.7C) and were also less likely to express the "germline" knock-in IGVH gene (Figure 2.7D).

To define the mutational landscape of NP-Eα$^-$ populations, I examined the accumulation of mutations across their IGVH sequences. Antibodies expressed by DZ-NP-Eα$^-$ cells showed greater accumulation of mutations throughout the sequence than their antigen-binding counterparts in the DZ (Figure 2.8A). This suggests that the DZ-NP-Eα$^+$ compartment is composed of cells that have recently been positively selected and yet to undergo cell division and SHM. As expected from the higher density of SHM accrued in the DZ-NP-Eα$^-$ population, non-productive Ig sequences containing stop or frameshift mutations were significantly enriched [248, 286] and were rarely found in LZ cells (p<0.0001) (Figure 2.8B). The frequency of mutations in FR3 and CDR3 was

also reduced in LZ-NP-Eα$^-$ cells compared to DZ-NP-Eα$^-$ cells (Figure 2.8C) and may represent selection against cells with structurally compromised BCRs [248].

The data suggest that in addition to producing cells that are unable to express the BCR, random somatic mutation in the DZ also generates cells that lose the ability to demonstrably bind to NP-Eα. The mutational profile of LZ antigen-binding and nonbinding cells differs primarily in the CDR3 (Figure 2.9A). Markedly, R55G and K66E, K66N, or K66Q accumulate in LZ nonbinders, suggesting that these replacements are associated with the loss of binding (Figure 2.9B), and these mutations were similarly present in the DZ-NP-Eα$^-$ compartment.

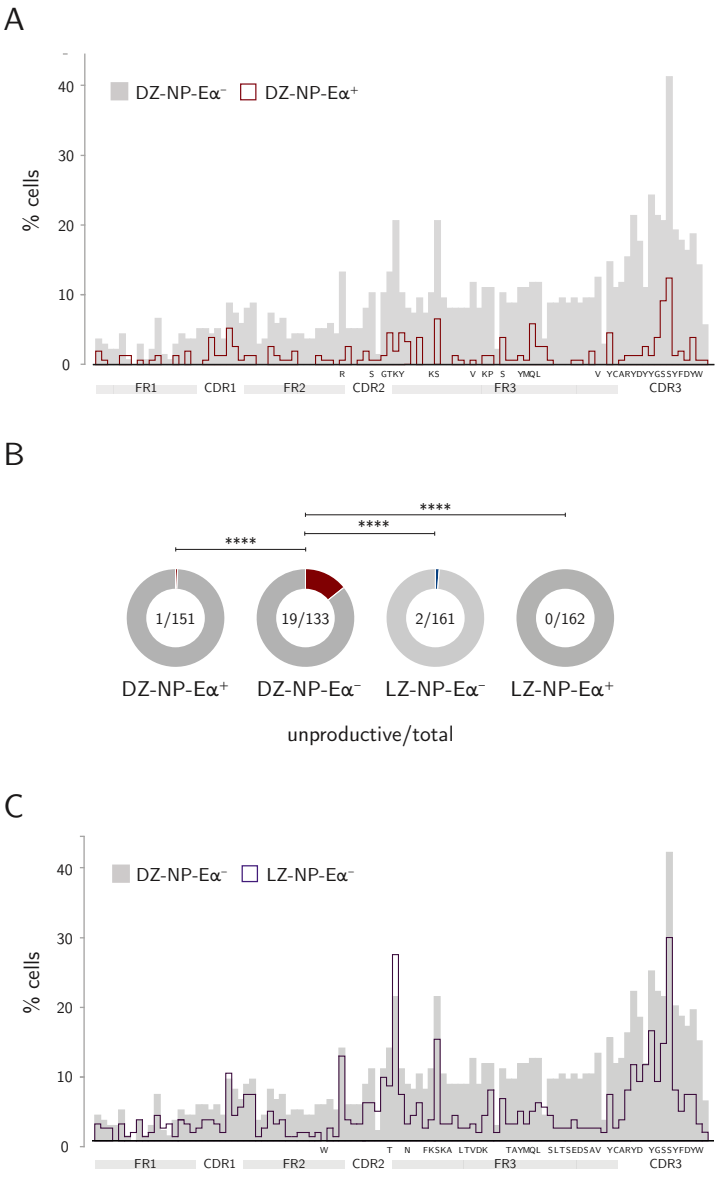

Figure 2.8: DZ nonbinders are enriched in SHM and unproductive BCRs.
(A) Overlapping histograms depicting distribution of mutations among DZ-NP-Eα$^-$ and DZ-NP-Eα$^+$ populations. Targeted AA residues found in ≥5% of DZ-NP-Eα$^-$ over DZ-NP-Eα$^+$ population are listed below axis. (B) Fraction of unproductive IGVH chains by compartment, Fisher's exact test, ****p<0.0001. (C) Distribution of mutations in DZ-NP-Eα$^-$ and LZ-NP-Eα$^-$ populations. Targeted AA residues found in ≥5% of DZ-NP-Eα$^-$ over LZ-NP-Eα$^-$ population are listed below axis.

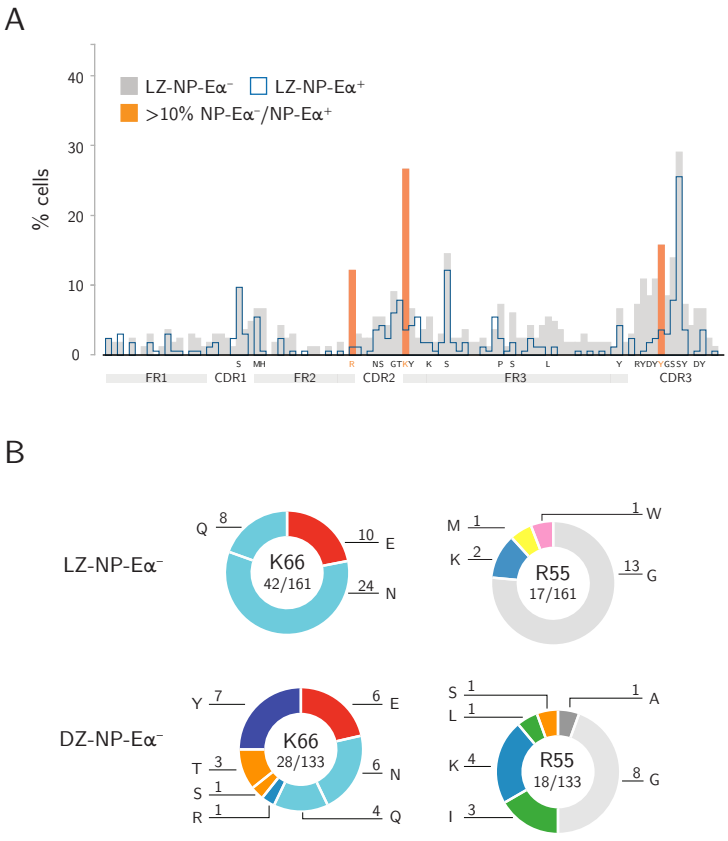

Figure 2.9: Mutational landscape analysis of LZ populations identifies targeted residues associated with lack of NP-Eα binding.
(A) Distribution of mutations in LZ-NP-Eα$^-$ and LZ-NP-Eα$^+$ populations. AAs targeted in 5% or more of LZ-NP-Eα$^-$ over LZ-NP-Eα$^+$ populations listed below axis; those targeted 10% or more are highlighted in orange. (B) Targeted K66 and R55 residues in LZ-NP-Eα$^-$ and DZ-NP-Eα$^-$ cells and their AA replacements.

2.1.4 Lack of antigen engagement *in vivo* results from the loss of binding affinity

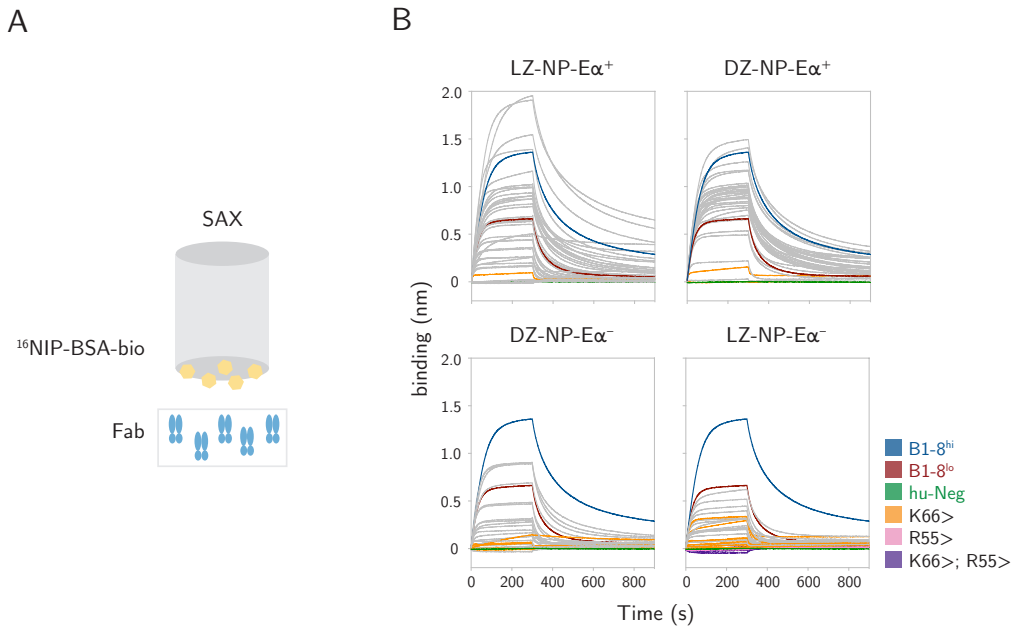

Figure 2.10: Monovalent binding traces of Fabs produced from LZ and DZ compartments. (A) Monovalent BLI setup. (B) BLI traces of Fabs [50nM] from LZ- and DZ-NP-Eα$^+$ and NP-Eα$^-$ compartments under monovalent setup.

To determine whether mutations associated with absence of NP-Eα binding impact affinity, I cloned and produced antibodies expressed by LZ and DZ cells and performed biolayer interferometry (BLI). Monovalent interactions were modeled by coupling ^{16}NIP-BSA-biotin to the sensor and using Fabs as the ligand (Figure 2.10A and B). Control B1-8^{hi} and its lower-affinity variant, B1-8^{lo} Fabs showed K$_D$s of 38nM and 50nM respectively in this assay (Figure 2.11A) [143, 290]. Fabs obtained from DZ-NP-Eα$^+$ cells showed relatively high affinities with geometric mean K$_D$ values of 49nM, supporting the hypothesis that these cells represent recently selected cells from the LZ (Figure 2.11A and B). Among the 29 Fabs from DZ-NP-Eα$^-$ cells, 10 showed affinities in the range of B1-8^{hi} supporting the hypothesis that some DZ cells that express low levels of high affinity BCRs may be missed by flow cytometry (Figure 2.11A and B, Figure 2.5).

Consistent with their inability to engage with NP-Eα *in vivo*, 36 Fabs from LZ-NP-Eα$^-$ cells showed lower affinities than B1-8^{lo} with a geometric mean K$_D$ value of 2.9μM (Figure 2.11A and B) when Fabs that showed no detectable binding were assigned a K$_D$ value of 10μM. In contrast, Fabs obtained from LZ-NP-Eα$^+$ cells showed a geometric mean K$_D$ value of 141nM (Figure 2.11A and B). Accumulation of IGVH mutations was negatively correlated with affinity (Figure 2.12) and antibodies with mutations in either R55 or K66, that are enriched among LZ nonbinders (Figure 2.9B), showed no measurable binding.

To model multivalent interactions found *in vivo*, I immobilized Fabs onto sensors

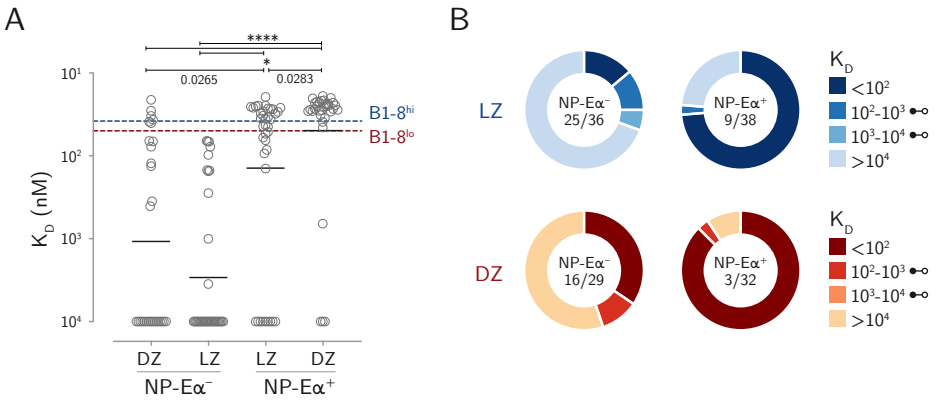

Figure 2.11: Binding affinities of Fabs produced from LZ and DZ compartments.
(A) K_D measurements of Fabs from LZ- and DZ-NP-Eα$^+$ and NP-Eα$^-$ compartments. Fabs with no detectable binding were assigned K_D values of 10 μM, *p-values as indicated, ****p<0.0001. (B) Distribution of K_D values of Fabs from LZ and DZ NP-Eα$^+$ and NP-Eα$^-$ compartments. Each dot represents one Fab with lines denoting geometric means. P-values calculated with Kruskall-Wallis with Dunn's multiple corrections test.

and measured binding to multivalent antigen (Figure 2.13). Of the 25 Fabs derived from LZ-NP-Eα$^-$ cells with undetectable monovalent binding, 18 bound to the higher valency substrate, but only one reached the apparent binding affinity of B1-8^{lo} (Figure 2.13D, Figure 2.14). Therefore, NP-Eα engagement is a reliable indicator of the relative antigen binding affinity of LZ cells and can therefore be used to identify cells able to engage antigen in the LZ.

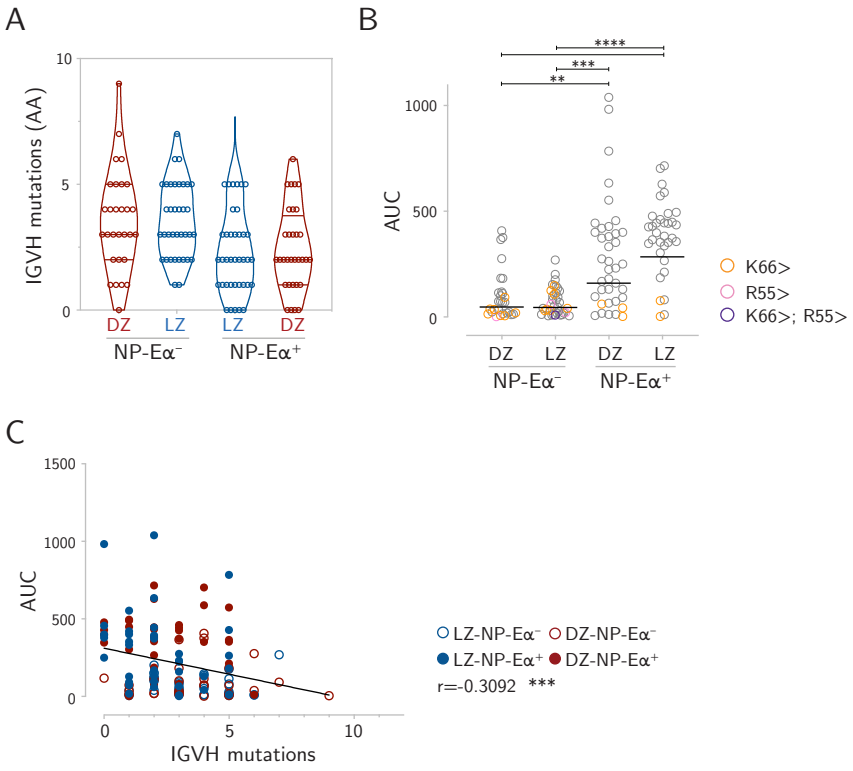

Figure 2.12: Decreased binding capacity is associated with increased SHM.
(A) Number of AA mutations in IGVH chains of Fabs produced from LZ- and DZ-NP-Eα$^+$ and NP-Eα$^-$ compartments. Violin plot depicts median and quartiles; each dot represents one Fab. (B) Area under the curve (AUC) calculations of BLI traces from (Figure 2.10B), **p=0.0027, ***p=0.0002, ****p<0.0001. Each dot represents one Fab (A and B) with lines denoting geometric means (B). P-values for (B) calculated with Kruskall-Wallis with Dunn's multiple corrections test.(C) Scatterplot showing correlation between number of IGVH mutations and AUC from monovalent BLI setup, Spearman correlation, r=-0.3092, ***p=.0003. Line depicts simple linear regression calculated from scatterplot (Y = -33.48X + 311.1).

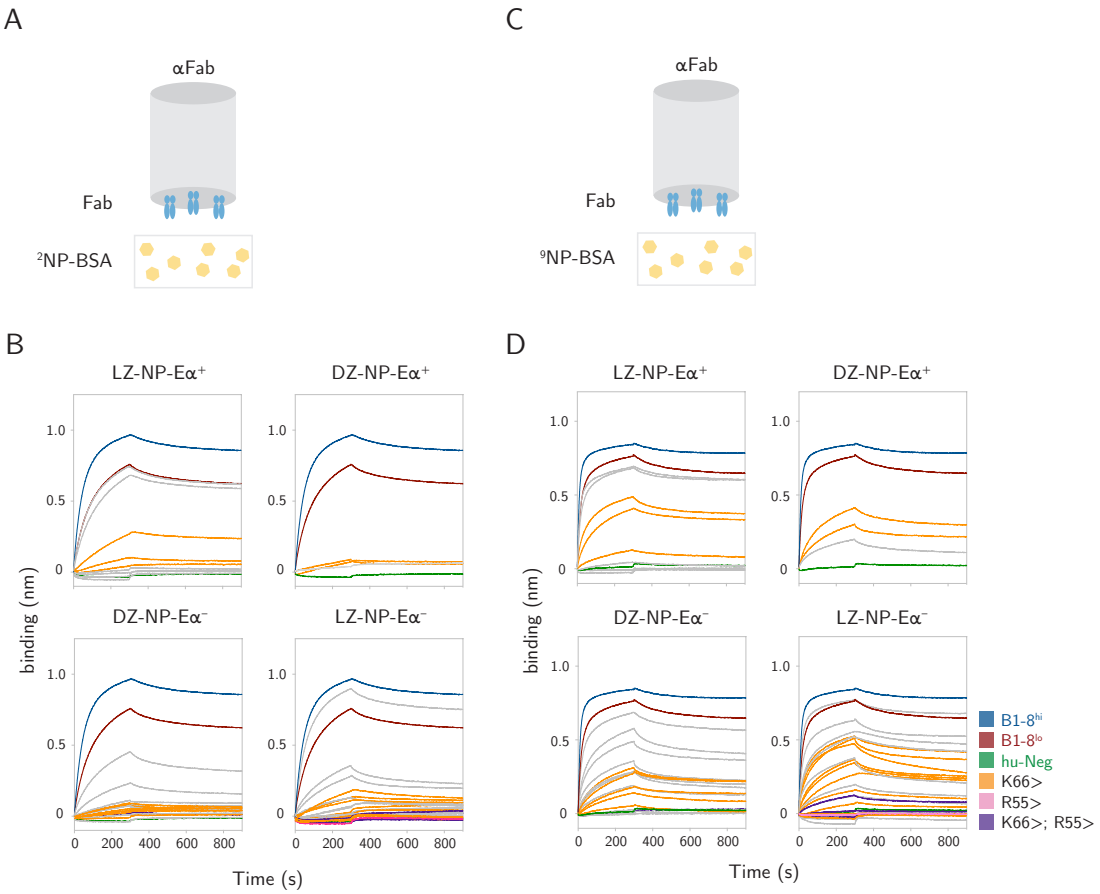

Figure 2.13: Modeling of polyvalent interactions of Fabs produced from LZ and DZ compartments by BLI.
(A) Low polyvalent BLI setup. Individual Fabs are immobilized to anti-human Fab sensors with ^{2}NP-BSA [0.33µM] in solution. (B) BLI traces of Fabs with no detectable monovalent binding (Figure 2.10) assayed with ^{2}NP-BSA. (C) High polyvalent BLI setup. Individual Fabs are immobilized to anti-human Fab sensors with ^{9}NP-BSA [0.11µM] in solution. (D) BLI traces of Fabs with no detectable binding under monovalent setup (Figure 2.10), assayed with ^{9}NP-BSA.

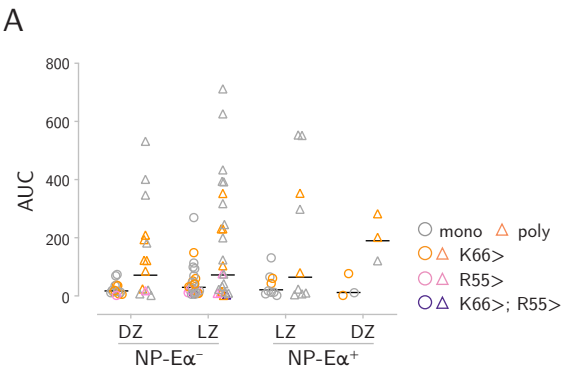

Figure 2.14: Monovalent vs polyvalent interactions of Fabs produced from LZ and DZ compartments by BLI.
(A) AUC comparison of Fabs that showed undetectable monovalent binding (circles) assayed under polyvalent condition with ^{9}NP-BSA (triangles) (Figure 2.10, Figure 2.12B, Figure 2.13D). Lines depict geometric means.

2.2 Role of BCR signaling in positive selection

2.2.1 Positive selection is enhanced among cells with active BCR engagement

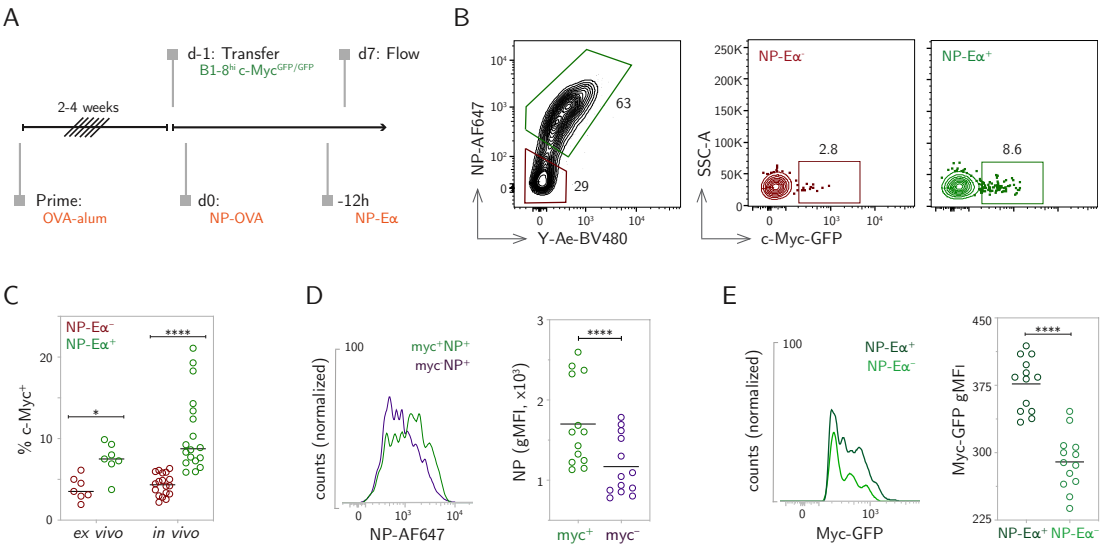

Figure 2.15: *c-Myc* expression is enriched among antigen-binding cells.
(A) Experimental setup. (B) Representative plots showing gating strategy for fraction of c-Myc$^+$ cells among NP-Eα$^+$ and NP-Eα$^-$ LZ B1-8^{hi} cells. (C) Frequency of c-Myc$^+$ cells among NP-Eα$^+$ and NP-Eα$^-$ LZ B1-8^{hi} cells stained either *ex vivo* on ice, or *in vivo*, Two-way ANOVA with Šidák's multiple comparisons, *p=0.0411, ****p<0.0001. (D) Representative flow cytometry histograms showing NP-Eα binding by c-Myc$^+$ NP-Eα$^+$ and c-Myc$^-$ NP-Eα$^+$ populations (left) and summary of gMFI intensity (right), ****p<.0001. (E) Representative histograms showing Myc-GFP expression in NP-Eα binding and nonbinding LZ B1-8^{hi} cells (left) and summary of gMFI intensity (right), ****p<0.0001. Data from five (D-E) independent experiments. Each dot represents one mouse. Lines depict mean. P-values (D-E) calculated by Two-tailed paired t-test.

c-Myc expression marks LZ cells that received Tfh activation signals associated with positive selection [167, 168]. To examine the role of BCR signaling in LZ B cell selection I used a c-Myc-green fluorescent protein (GFP) reporter (B1-8^{hi}c-Myc-GFP) [167, 292] and tracked antigen binding by injection of NP-Eα (Figure 2.15A and B). B1-8^{hi} tracking by NP-Eα confers no additional T cell selection advantage because processing and presentation of NP-Eα provides no cognate antigen for presentation to OVA-specific Tfh. As expected, the fraction of c-Myc$^+$ cells was significantly higher among LZ-NP-Eα$^+$ that retain the ability to bind NP when compared to LZ-NP-Eα$^-$ cells, irrespective of whether NP-Eα staining was done *in vivo* or *ex vivo* (Figure 2.15B and C) The amount of antigen captured, as measured by geometric mean fluorescence intensity (gMFI), was higher among LZ c-Myc$^+$NP-Eα$^+$ cells when compared to c-Myc$^-$NP-Eα$^+$ cells (Figure 2.15D). Furthermore, c-Myc expression by LZ-NP-Eα$^+$ cells was higher as measured by their gMFI (Figure 2.15E). Therefore, c-Myc expression and

by inference, positive selection, is enriched among LZ cells that bind antigen with higher affinity.

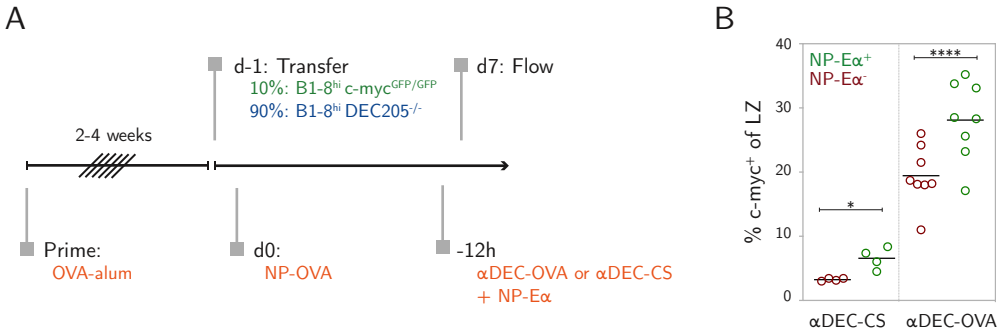

Figure 2.16: BCR signaling enhances positive selection, even when cognate antigen presentation is equal.
(A) Experimental setup for αDEC205 targeting. (B) Frequency of c-Myc^{+} cells among LZ B1-8^{hi} c-Myc-GFP NP-Eα^{+} and NP-Eα^{-} cells targeted with αDEC-CS (negative control, left) or αDEC-OVA (right), Two-tailed paired t-test, *p=0.0318, ****p<0.0001. Data from two independent experiments. Each dot represents one mouse. Lines depict means.

To uncouple the effects of antigen capture and cognate T cell interactions from BCR signaling, I normalized the amount of antigen presented by GC B cells in a BCR-independent manner using a chimeric antibody to deliver OVA antigen (αDEC-OVA) [160, 222]. After priming mice with OVA, I adoptively transferred a mixture of B1-8^{hi}c-Myc-GFP DEC205-sufficient and knockout B cells (B1-8^{hi}DEC205$^{-/-}$) and injected αDEC-OVA to deliver OVA to DEC205-sufficient GC B cells, irrespective of their ability to bind antigen as measured by NP-Eα (Figure 2.16A and B). Under these conditions, the fraction of *c-Myc* expressing LZ B cells was significantly higher among NP-Eα^{+} cells than their NP-Eα^{-} counterparts (Figure 2.16B). Thus, even when LZ B cells are loaded with similar amounts of antigen, irrespective of BCR affinity, selection is enriched among cells that demonstrably engage antigen suggesting that strong BCR signals renders these cells more competitive in receiving T cell help.

2.2.2 Transcriptome analysis of pathways induced upon BCR engagement and positive selection

To contextualize the molecular pathways induced upon BCR engagement in the GC, I isolated four populations of LZ B cells based on their engagement with NP-Eα and *c-Myc* expression and performed bulk mRNA-seq: c-Myc^{-} NP-Eα^{+}; c-Myc^{-} NP-Eα^{-}; c-Myc^{+} NP-Eα^{+}; and c-Myc^{+} NP-Eα^{-} (Figure 2.17).

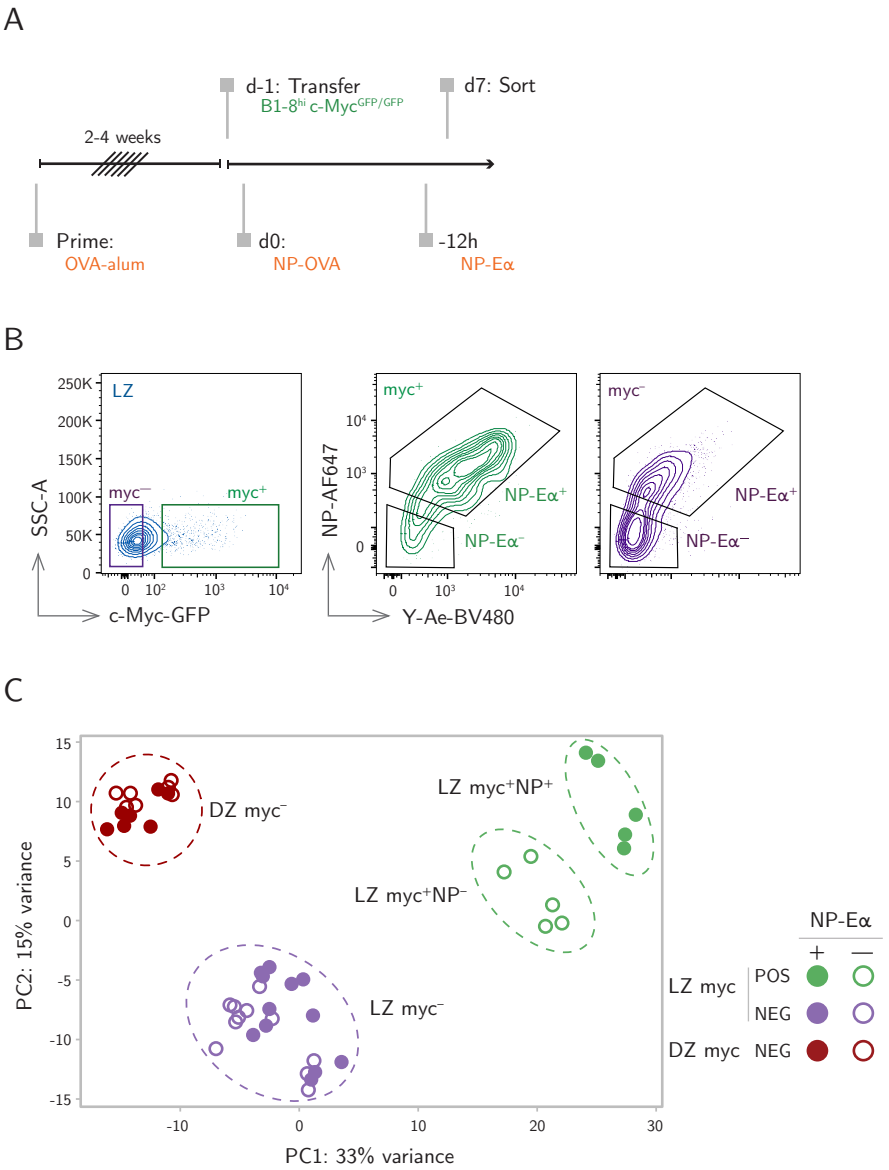

Figure 2.17: Sorting strategy and visualization of the gene expression similarities of c-Myc^{+} and c-Myc^{-}populations
(A-B) Experimental setup and sorting strategy. Cells were sorted on the basis of their *c-Myc* expression and NP-Eα engagement. (C) Principal components analysis visualization of sorted populations. Each dot represents a sorted population of 400 cells.

I initially compared the transcriptomes of c-Myc^{+} LZ cells that did or did not detectably bind antigen (Figure 2.18A). Gene Set Enrichment Analysis (GSEA) showed

that c-Myc$^+$ NP-Eα$^+$ cells were enriched in pathways induced by c-Myc, mTOR, and NF-κB relative to lower affinity c-Myc$^+$ NP-Eα$^-$ cells (Figure 2.18B). c-Myc$^+$ NP-Eα$^+$ cells also showed enriched expression of hallmark pathways associated with cell-cycle entry and energy metabolism (Figure 2.18C). In addition to cell-cycle entry and control genes like *Ccnd2*, *Batf*, *Socs2*, and *Socs3*, higher affinity cells showed greater expression of immune activation genes involved in cytokine responses such as *Il1r2*, *Socs2*, and *Sosc3*, and genes involved in metabolic regulation, *Uck2* [167] (Figure 2.19A and B). Altogether, the gene expression profile of the c-Myc$^+$ NP-Eα$^+$ population suggests these cells have received stronger selection signals relative to c-Myc$^+$ NP-Eα$^-$ cells and that the former are poised to enter cell cycle and migrate to the DZ.

Conversely, c-Myc-expressing LZ B cells with lower affinity BCRs were enriched in negative regulators of cell cycle entry *Cdkn1a* and *Id3* and signaling modifiers *Tbl1x*, *Cblb*, and *Trim56* (Figure 2.19C). This population also expressed more *Bach2*, which is inversely correlated with the strength of T cell help and positively correlated with memory B cell differentiation [267, 273] (Figure 2.20). Consistent with these observations, c-Myc$^+$ LZ B cells with lower affinity BCRs are enriched in expression of pre-memory associated transcription factors such as *Hhex*, *Mndal*, and *Tle3* [274], memory-associated markers, including *Efnb1*, *Cd38*, and *Lifr* [271, 272, 293], and the anti-apoptotic gene *Bcl2l1* [264] (Figure 2.20). Therefore, B cells with lower affinity receptors that receive T cell help display features associated with the pre-memory compartment [269, 270, 273, 274].

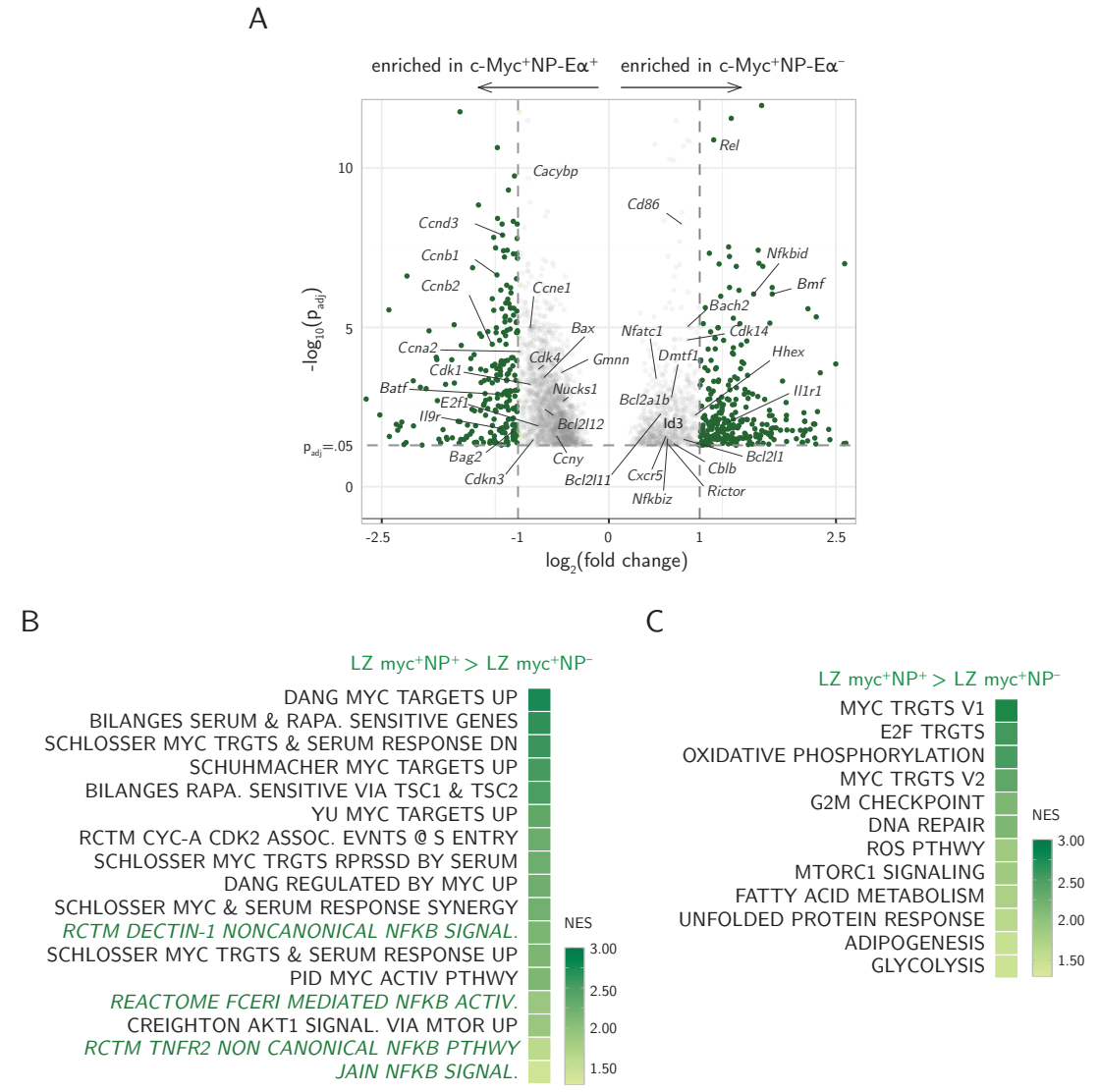

Figure 2.18: Continuous BCR engagement is necessary for full induction of positive selection pathways.
(A) Volcano plot depicting differentially expressed genes between c-Myc$^+$ populations. (B) GSEA summary of significantly varied canonical pathways between c-Myc$^+$ NP-Eα$^+$ and c-Myc$^+$ NP-Eα$^-$ populations, including Myc, mTOR, and NF-κB associated pathways. (C) GSEA summary of significantly varied hallmark pathways between c-Myc$^+$ NP-Eα$^+$ and c-Myc$^+$ NP-Eα$^-$ populations, including Myc, cell cycle, and energy metabolism pathways. (B and C) All enriched pathways had nominal p-values$<$.05 and FDR q-values$<$0.25.

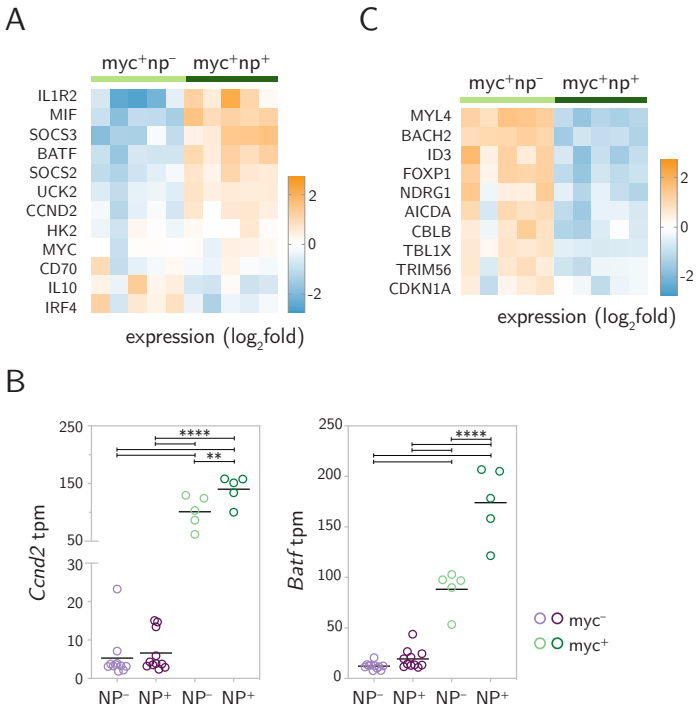

Figure 2.19: Expression of immune activation genes is enhanced among positively selected NP-Eα binders
(A) Heatmap depicting expression of "immune activation" genes associated with Myc activity among c-Myc$^+$ NP-Eα$^+$ and c-Myc$^+$ NP-Eα$^-$ populations. (B) Expression of *Ccnd2* and *Batf* mRNA, One-way ANOVA with Tukey's multiple comparisons test, **p=.0014, ****p<.0001. (C) Heatmap depicting expression of genes negatively correlated with Myc activity among c-Myc$^+$ populations.

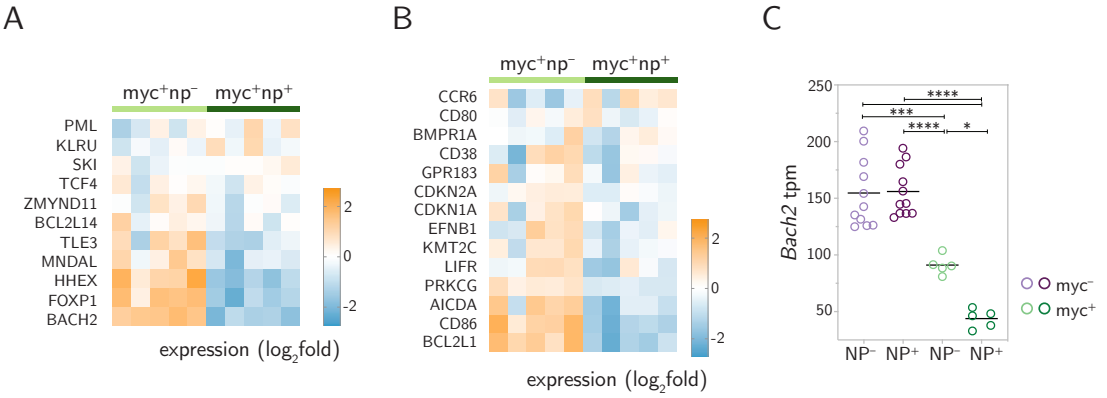

Figure 2.20: Lower magnitudes of T cell help may defer selected cells towards a memory fate
(A-B) Heatmap depicting expression of transcription factors (A) and genes (B) associated with pre-memory and memory B cell phenotypes among c-Myc$^+$ NP-Eα$^+$ and c-Myc$^+$ NP-Eα$^-$ populations. (C) Expression of *Bach2* mRNA, One-way ANOVA with Tukey's multiple comparisons test, *p=0.0161, ***p=0.0001, ****p<0.0001

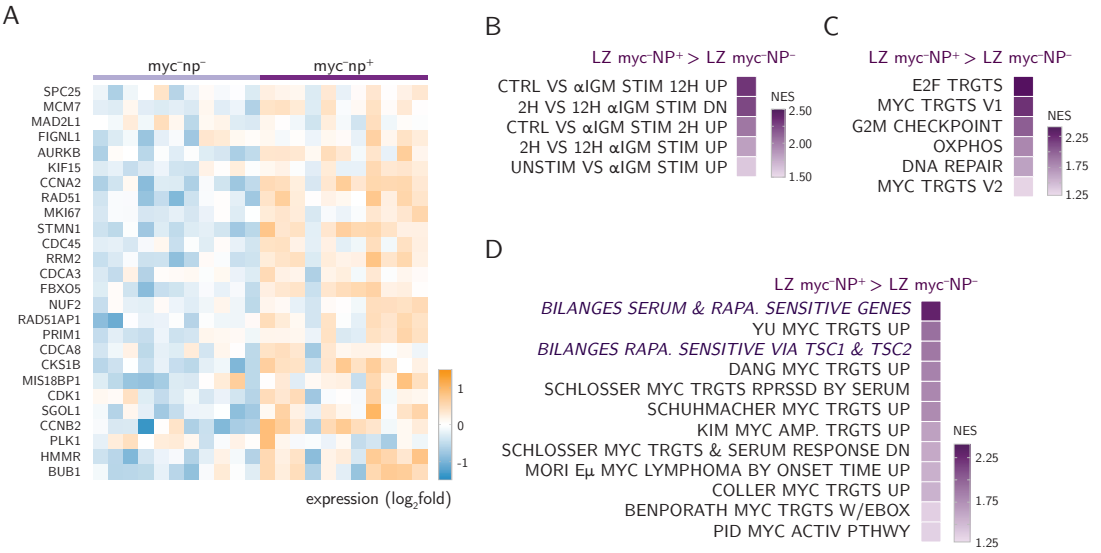

Figure 2.21: NP-Eα engagement is associated with BCR stimulation pathways and induction of metabolic changes.
(A) Heatmap depicting expression of BCR stimulation genes among c-Myc$^-$ NP-Eα$^+$ and c-Myc$^-$ NP-Eα$^-$populations. (B-D) GSEA summary of enriched BCR stimulation pathways (B), hallmark pathways (C), and canonical pathways (D) between c-Myc$^-$ NP-Eα$^+$ and c-Myc$^-$ NP-Eα$^-$ populations. (B-D) All enriched pathways had nominal p-values<.05 and FDR q-values<0.25.

To examine the gene expression profiles of antigen binding and nonbinding LZ B cells in the absence of detectable positive selection, I compared the transcriptomes of c-Myc$^-$ cells. GSEA showed that c-Myc$^-$ antigen-binding cells were enriched in pathways associated with BCR stimulation and activation (Figure 2.21A and B) and hallmark and canonical pathways indicative of metabolic changes (Figure 2.21D and E). These gene signatures were induced even in the relative absence of positive selection and c-Myc expression (Figure 2.22), indicating that LZ B cells that engage antigen signal through the BCR, activating metabolic pathways that may enhance positive selection.

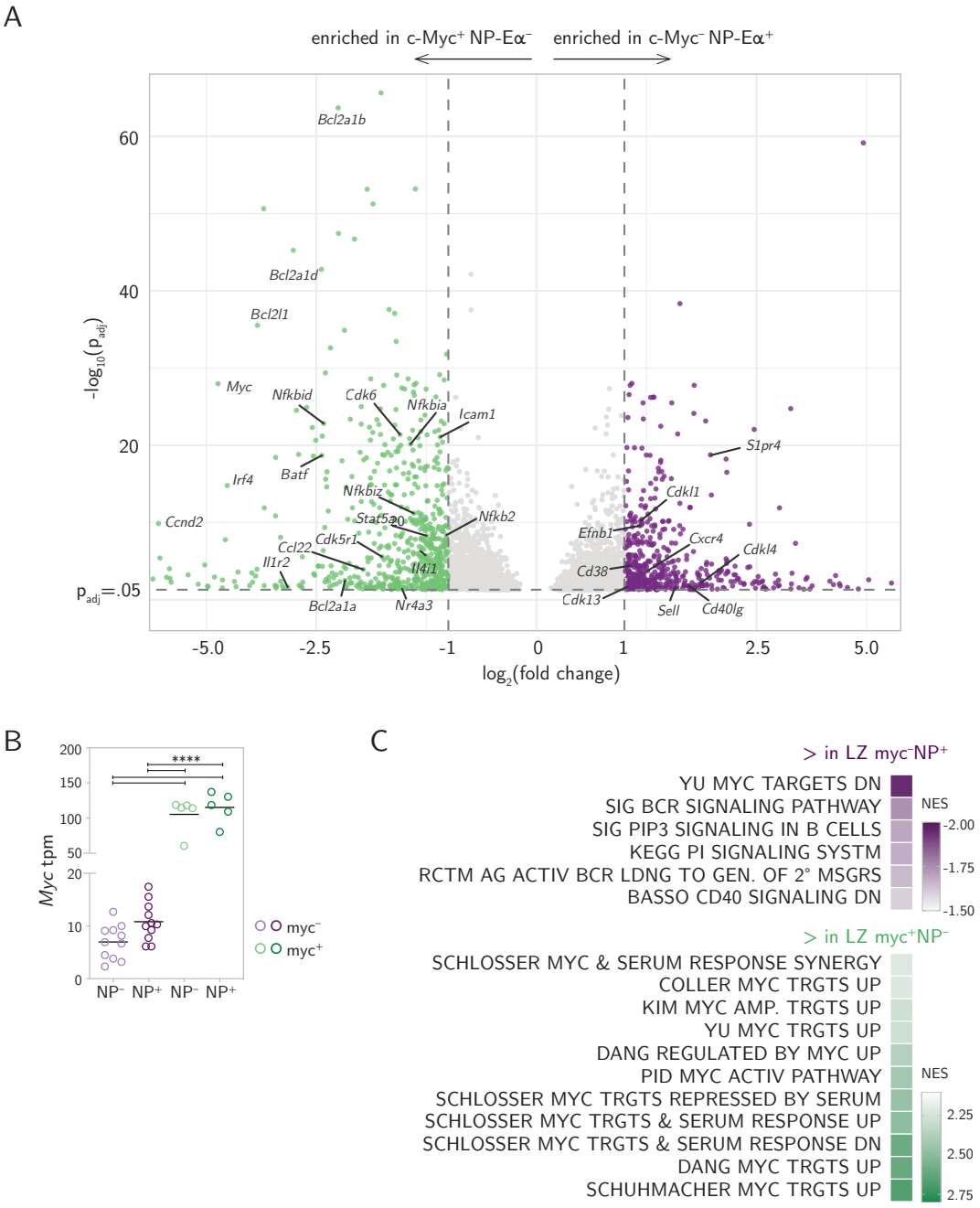

Figure 2.22: c-Myc$^-$ population shows little evidence of T cell positive selection.
(A) Volcano plot depicting differentially expressed genes between c-Myc$^+$ NP-Eα$^-$ (green, left) and c-Myc$^-$ NP-Eα$^+$ (purple, right) populations. (B) Expression of Myc mRNA, One-way ANOVA with Tukey's multiple comparisons test, ****p<.0001. Lines depict means. Each dot represents a population of 400 cells. (C) GSEA summary of significantly varied canonical pathways between c-Myc$^+$ NP-Eα$^-$ and c-Myc$^-$ NP-Eα$^+$ populations. Pathways depicted in purple (left) are enriched among c-Myc$^-$ NP-Eα$^+$ cells and pathways depicted in green (right) are enriched in c-Myc$^+$ NP-Eα$^-$ cells. All enriched pathways had nominal p-values<.05 and FDR q-values<0.25.

2.3 Role of BCR signaling in negative selection

2.3.1 Germinal Center BCR engagement protects LZ cells from apoptosis

To determine whether antigen binding confers a survival advantage to LZ B cells in the absence of positive selection, I measured cell death by apoptosis using activated caspase 3 expression (aCasp3) as a marker [248]. Antigen-binding LZ and DZ B cells showed lower frequencies of aCasp3$^+$ cells than their NP-Eα$^-$ counterparts (Figure 2.23A and B). This effect was independent of selection because c-Myc$^-$ LZ B cells that bound antigen were protected from apoptosis compared with lower affinity cells (Figure 2.23C). To determine whether a similar survival advantage is observed in a polyclonal immune response, I immunized mice with an HIV-1 antigen, TM4-Core [294], and identified cells capable of antigen binding by flow cytometry using TM4-Core-AF488 (Figure 2.24A-C). Polyclonal GC LZ B cells unable to bind TM4-Core-AF488 were significantly more likely to undergo apoptosis than antigen-binding cells (Figure 2.24C). Theefore, LZ B cells that engage antigen have a survival advantage.

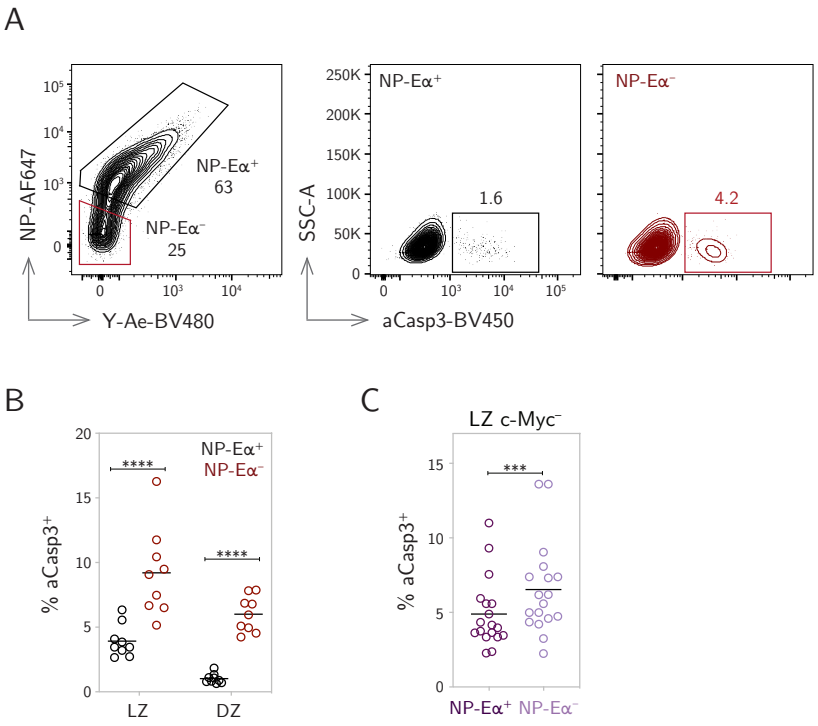

Figure 2.23: Apoptosis is enriched among cells lacking active BCR engagement.
(A) Gating strategy for identification of aCasp3$^+$ cells among NP-Eα$^+$ and NP-Eα$^-$ B1-8^{hi} cells. (B) Frequency of aCasp3$^+$ cells among NP-Eα$^+$ (black) and NP-Eα$^-$ (red) cells labeled *in vivo* with ^{14}NP-Eα, Two-way ANOVA with Šidák's multiple comparisons, ****p<0.0001. (C) Frequency of aCasp3$^+$ cells among c-Myc$^-$ NP-Eα$^+$ and c-Myc$^-$ NP-Eα$^-$ LZ B1-8^{hi} cells, Two-tailed paired t-test, ***p=0.0006. Data from three (B) and five (C) independent experiments. Each dot represents one mouse. Lines depict means.

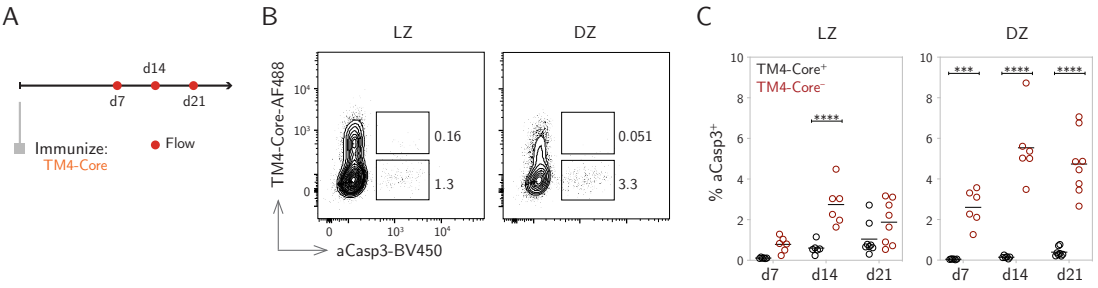

Figure 2.24: Apoptosis is enriched among nonbinding populations in a polyclonal setting. (A) TM4-Core immunization scheme (B) Flow cytometry plots of LZ and DZ populations. aCasp3 is enriched among TM4-Core nonbinders. (C) Frequency of aCasp3$^+$, gated on TM4-core binding and nonbinding populations in the LZ and DZ over time, Two-way ANOVA with Šidák's multiple comparisons, ***p=0.0004, ****p<0.0001. Data from two independent experiments. Each dot represents one mouse. Lines depict means.

2.3.2 LZ GC B cells are susceptible to ibrutinib treatment

To determine if continuous BCR signaling in GC B cells is required for survival, I inhibited BTK activity with a short pulse of the BTK inhibitor, ibrutinib [295–297]. BTK is directly downstream of the BCR and is required for physiologic levels of tonic and antigen-dependent receptor signaling (Figure 2.25A) [298–301]. Moreover, BTK is not expressed in T cells [302]. To determine whether inhibition of BCR signaling can alter LZ B cell survival, I treated mice with ibrutinib by subcutaneous injection (Figure 2.25B and C). As little as 1.6 µg of ibrutinib was sufficient to produce a significant increase in aCasp3$^+$ in LZ B cells within 1 hour after injection (Figure 2.25C). Moreover, LZ B cells were significantly more sensitive to ibrutinib than DZ B cells in a dose-dependent manner (Figure 2.25C). The increase in cell death upon this short interruption of signaling suggests that LZ B cells need continuous BCR engagement for survival.

To determine whether the effect of ibrutinib on BTK is B cell autonomous, I produced knock-in mice that carry a C481S mutation in BTK, which renders the enzyme insensitive to the drug [303–305] (Figure 2.25D). Development of BTK^{C481S} B cells was indistinguishable from their wild type counterparts in the bone marrow (BM) and the periphery. As expected, BTK^{C481S} B cells were resistant to ibrutinib-mediated inhibition of Ca^{+2} flux upon BCR crosslinking (Figure 2.26).

To determine whether BCR signaling in LZ GC B cells is required for survival, I made mixed BM chimeras with BTK^{C481S} and BTK^{WT} mice. Chimeras were immunized with an HIV-1 Env protein, TM4-core, and treated with acalabrutinib, a second-generation version of ibrutinib with improved specificity and reduced off-target binding to other Tec family kinases [306–309] (Figure 2.27). Whereas inhibitor treatment did not measurably increase apoptosis of DZ cells in either BTK^{C481S} or BTK^{WT} cells, BTK^{WT} LZ cells showed a significant dose-dependent increase in aCasp3$^+$ staining (Figure 2.27C).

To determine the kinetics of BCR inhibition, mice were treated with acalabrutinib at several timepoints. LZ B cells showed a peak of apoptosis 2 hours with rapid recovery

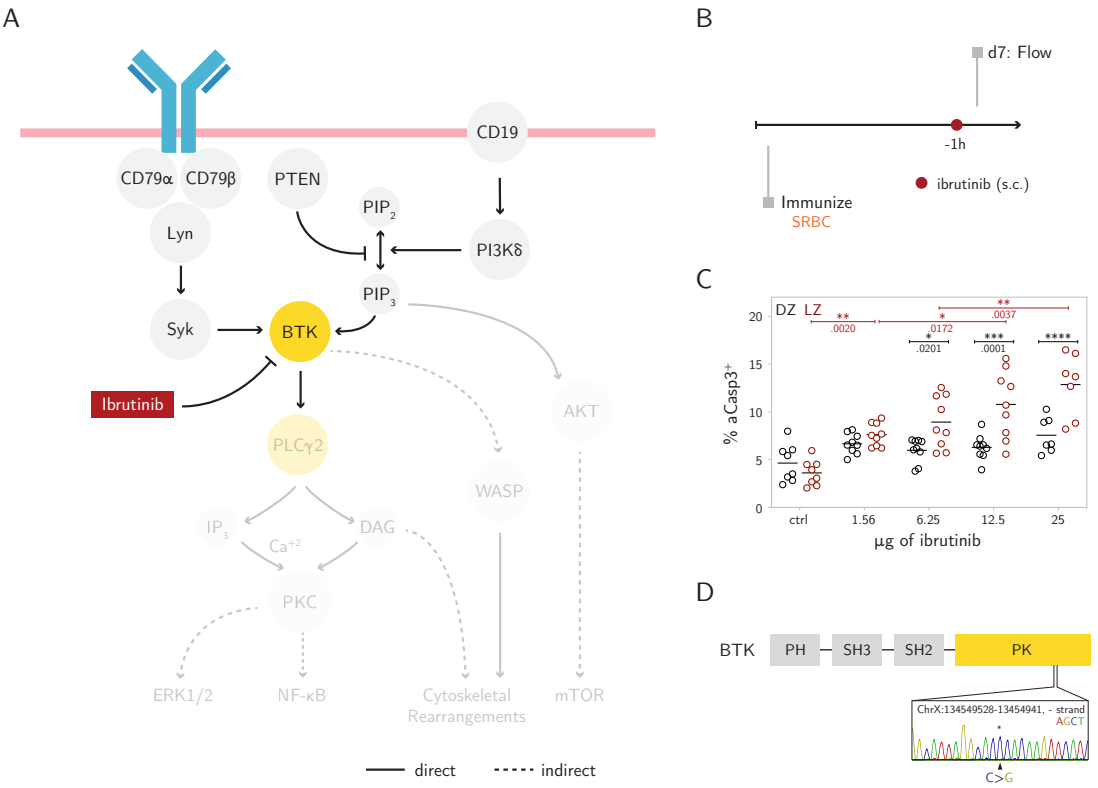

Figure 2.25: LZ GC B cells are differentially susceptible to ibrutinib treatment.
(A) Inhibition of BCR signaling pathways by ibrutinib treatment. (B) Experimental setup for SRBC immunization with ibrutinib subcutaneous pulse. (C) Frequency of aCasp3^{+} cells among LZ and DZ populations one hour after ibrutinib treatment, Two-way ANOVA with Šidák's multiple comparisons (within dose) and Tukey's multiple comparisons (across doses), * and **p-values as marked, ****p<.0001. Data from two independent experiments, each dot represents one mouse. Lines depict means. (D) Schematic depicting BTK^{C481S} point mutation mouse model.

by 12 hours (Figure 2.28). Altogether, the data indicate that BCR signaling is necessary for survival in the LZ.

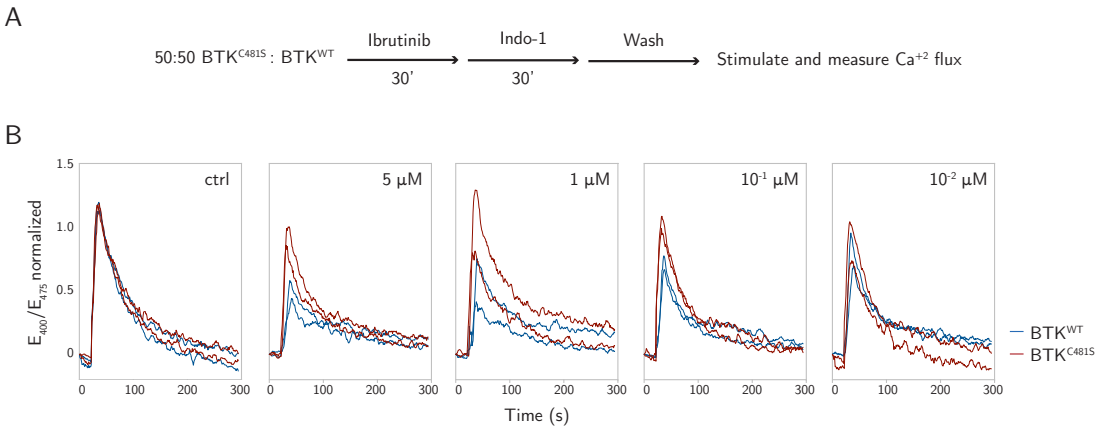

Figure 2.26: BTK^{C481S} confers resistance to ibrutinib inhibition of BCR-mediated calcium flux.
(a) Schematic depicting experimental setup for *ex vivo* Ca^{+2} flux assay. (b) Ca^{+2} flux traces comparing BTK^{C481S} (red) and BTK^{WT} (blue) after ibrutinib treatment and BCR stimulation. Data representative of two independent experiments.

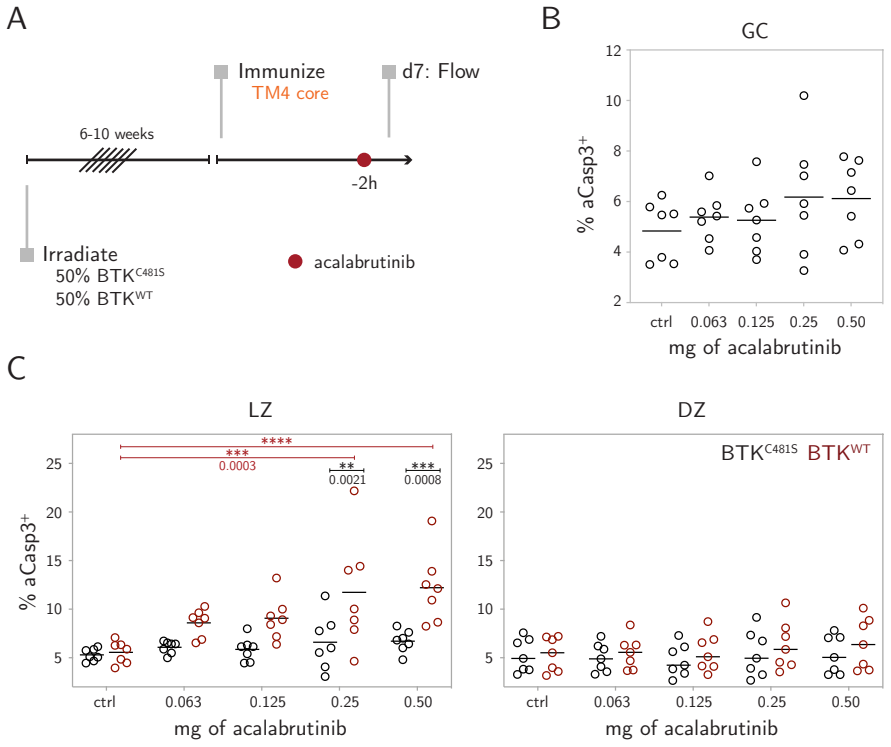

Figure 2.27: Continuous BCR engagement is necessary for survival of LZ B cells.
(A) Schematic of experimental setup for TM4-core immunization of mixed BTK^{C481S}:BTK^{WT} BM chimeras with different doses of acalabrutinib. (B) Frequency of aCasp3$^+$ among GC cells with acalabrutinib treatment, Two-way ANOVA with Šidák's multiple comparisons, ns. (C) Frequency of aCasp3$^+$ cells among LZ BTK^{C481S} and BTK^{WT} (left) and DZ BTK^{C481S} and BTK^{WT} (right) cells with acalabrutinib treatment, Two-way ANOVA with Šidák's multiple comparisons (within dose) or Tukey's multiple comparisons (across doses), ** and ***p-values as marked, ****p<.0001. Data from two independent experiments. Each dot represents one mouse. Lines depict means.

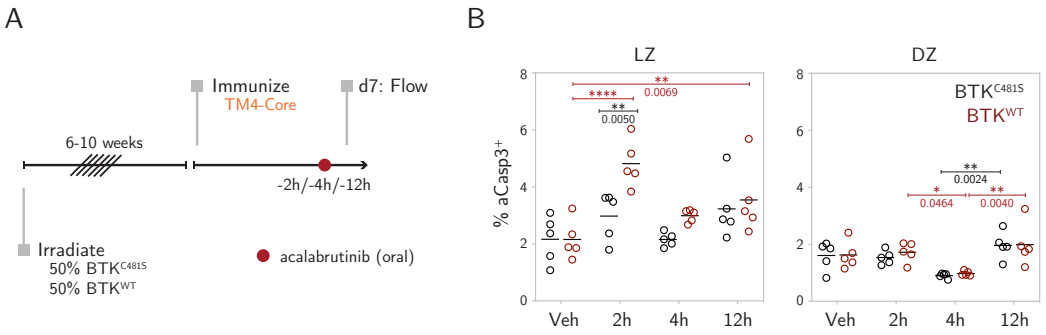

Figure 2.28: Kinetics of BTK blockade with acalabrutinib treatment.
(A) Experimental setup for TM4-core immunization of mixed BTK^{C481S}:BTK^{WT} BM chimeras with 0.0625 mg acalabrutinib treatment (oral) for different amounts of time. (F) Frequency of $aCasp3^{+}$ cells among LZ and DZ BTK^{C481S} and BTK^{WT} cells across timepoints, Two-way ANOVA with Šidák's multiple comparisons (within timepoint) or Tukey's multiple comparisons (across timepoints), * and **p-values as marked, ****p<.0001. Data from two independent experiments. Each dot represents one mouse. Lines depict means.

2.3.3 BCR signaling synergizes with T cell help to drive positive selection.

To determine a dose of acalabrutinib that would dampen but not block BCR signaling, I performed mixed transfer experiments with B1-8^{hi} BTK^{C481S} and BTK^{WT}, and treated mice with a low dose of acalabrutinib. Treatment did not alter cell survival of either population at the peak of drug inhibition (Figure 2.28, Figure 2.29B) but did slightly impair the ability of BTK^{WT} cells to bind and internalize NP-Eα (Figure 2.29C).

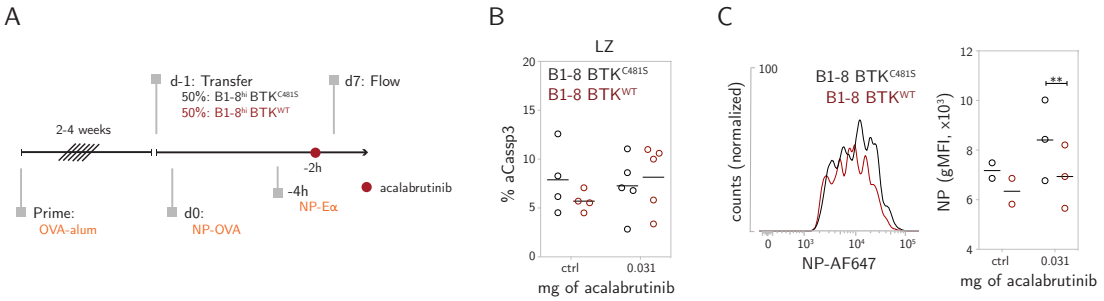

Figure 2.29: Treatment with low doses of acalabrutinib dampens BCR signaling without affecting LZ cell survival
(A) Experimental setup for prime-boost and mixed transfer of B1-8^{hi} BTK^{C481S} and B1-8^{hi} BTK^{WT} cells. Four hours prior to readout, NP-Eα was injected and followed by oral gavage with acalabrutinib (0.03125 mg) two hours later. (B) Frequency of LZ aCasp3^{+} cells among B1-8^{hi} BTK^{C481S} and B1-8^{hi} BTK^{WT} populations. (C) NP gMFI of LZ B1-8^{hi} BTK^{C481S} and B1-8^{hi} BTK^{WT}, RM Two-way ANOVA with Šidák's multiple comparisons, **p=0.0090.

To examine the synergy between BCR signaling and T cell help, I transferred DEC205-sufficient drug-resistant B1-8^{hi}BTK^{C481S} and drug-sensitive B1-8^{hi}BTK^{WT} cells and delivered antigen in a BCR-independent manner using αDEC-OVA (Figure 2.30A). Acalabrutinib did not measurably alter the relative frequency of wild-type and resistant LZ B cells at the cessation of drug treatment prior to DZ migration (Figure 2.30B). Nevertheless, the proliferation of B1-8^{hi}BTK^{WT} drug-sensitive cells in the DZ 48 hours after αDEC-OVA delivery (36h drug treatment) was significantly reduced compared to B1-8^{hi}BTK^{C481S} drug-resistant cells (Figure 2.30C and D). Therefore, the magnitude of T cell help received is not solely determined by antigen presentation and LZ BCR signaling directly impacts GC B cell selection.

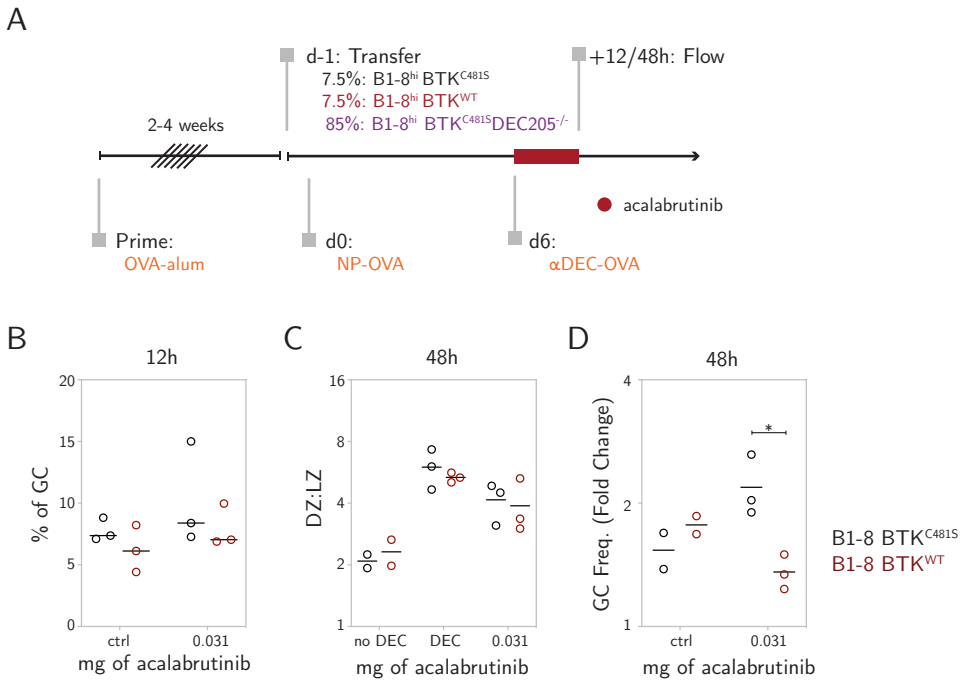

Figure 2.30: BCR signaling synergizes with T cell help to determine the extent of DZ proliferation

(A) Experimental setup. Day six after boost, 5 µg of αDEC-OVA was delivered (t=0) with 0.03125 mg of acalabrutinib by oral gavage at t=0 and t=6h, t=12h. Readout by flow at t=12h or t=48h. (B) Frequency of B1-8^{hi} BTK^{C481S} and B1-8^{hi} BTK^{WT} 12 hours after αDEC-OVA treatment. (C) DZ-LZ ratio of B1-8^{hi} BTK^{C481S} and B1-8^{hi} BTK^{WT} 48h after αDEC-OVA treatment and (D) frequency of B1-8^{hi} BTK^{C481S} and B1-8^{hi} BTK^{WT} 48h after αDEC-OVA treatment (right) Two-way ANOVA with Šidák's multiple comparisons, *p=0.016. (B-D) Data representative of two independent experiments. Each dot represents one mouse. Lines represent means.

Chapter 3

Discussion

Affinity maturation is contingent on iterative cycles of diversification and affinity-based selection in GCs [126, 159, 275]. Current models for GC B cell selection posit that antibody affinity is selected indirectly when B cells with higher affinity receptors extract, process, and present antigen to Tfh [310]. Tfh play an essential role in this process by physically engaging with B cells through cell surface receptor-ligand interactions and secretion of cytokines [182, 184, 223, 311]. Positive selection directs migration to the DZ, where selected cells undergo a proliferative burst proportional to the amount of antigen presented and the magnitude of T cell help [228].

In addition to antigen capture, the BCR is also a signaling receptor, and BCR stimulation synergizes with Tfh signals such as CD40 *in vitro* to activate positive selection pathways [224]. However, GC B cells show attenuated BCR signaling in response to soluble antigen due to increased SHP-1 and SHIP-1 phosphatase activity [276]. GC BCR signaling is rewired, showing poor signal propagation through PKC-β, resulting in altered synapse formation and inefficient activation of NF-κB [277, 278]. GC B cells also express elevated levels of PTEN, which alters the ratio of secondary signaling messengers, redirecting the specificity of AKT, leading to activation of negative regulators of BCR signaling [280].

Studying the role of BCR signaling *in vivo* has been difficult because its two functions, signaling and endocytosis, are inextricably coupled. Because BCR signaling is required for the formation and maintenance of the GC reaction, constitutive or conditional knockouts of BCR signaling components lead to cell death, limiting their use in this context [224, 282–285]. Genetic reporters such as Nur77-GFP have been used to identify a population of LZ B cells with active BCR engagement. However, it is unclear if this population more accurately represents selected B cells that have received Tfh signals [287]. Furthermore, the low frequency of BCR engagement reported is at odds with the observation that B cells are constantly traversing over FDC surfaces [219, 220].

To address these shortcomings and investigate BCR signaling in the context of positive selection *in vivo*, I introduced a tracker, NP-Eα, into ongoing GC reactions as a dynamic reporter of BCR engagement *in vivo*. NP-Eα acts as a surrogate antigen, providing a BCR signal without conferring additional cognate antigen for presentation to OVA-specific Tfh responses [143]. Furthermore, the small amounts of NP-Eα injected did not alter GC B cell survival or dynamics. Because it is conjugated at a low ratio of

NP to carrier, NP-Eα should not provide an enhanced BCR signal when compared to the immunizing antigen [239].

3.1 NP-Eα tracking allows snapshot of selection in action.

Despite using knock-in B cells with defined specificity and affinity for antigen, GC residence resulted in a substantial proportion of these cells with receptors that failed to bind to NP-Eα. Sequencing revealed that this loss of engagement is due to SHM. Using the mutational landscape of the sequenced populations, their zonal location, and their NP-Eα binding capacity, it is possible to plot the trajectories of populations as they cycle through the GC reaction. The mutational landscape of nonbinders in the DZ underscores the random nature of SHM and indicates that DZ-NP-Eα$^-$ cells have undergone cycles of division and mutation. These DZ cells represent the most likely candidates for migration to the LZ. Consistent with previous work, I observed that nonproductive BCRs are rarely present in the LZ, indicating that a functional BCR and some degree of tonic signaling are required to leave the DZ [248, 286]. It has been proposed that BCR signaling in the DZ inactivates FOXO1 control of the DZ program, allowing migration to the LZ [224]. While this is an appealing hypothesis, the data was derived from *ex vivo* stimulation of GC B cells, with no separation of LZ or DZ cells. Furthermore, there is little known about tonic signaling in GC B cells and whether it would be sufficient to inactivate FOXO1. Nonetheless, my results suggest that DZ to LZ migration is not dependent on an antigen-derived BCR signal, as cells that have lost the ability to bind antigen are present in both zones. DZ to LZ transition is also not affinity-dependent, as Fabs produced from DZ and LZ nonbinders showed no significant difference in affinity. These findings suggest that DZ to LZ migration is permissive, consistent with a strong net flux of cells from the DZ to the LZ [160].

In contrast, the LZ-NP-Eα$^+$ represents cells licensed to receive T cell help, while DZ-NP-Eα$^+$ cells are likely those that have recently been positively selected and migrated to the DZ. The DZ-NP-Eα$^+$ compartment expresses, on average, the highest affinity BCRs of the four compartments sequenced and is also the least mutated. Therefore, by compartmentalizing populations based on their engagement with NP-Eα and zonal location, we can observe a snapshot of selection within the GC reaction.

While the NP-Eα tracker reliably identifies low and high-affinity cells, it does not exclude that NP-Eα nonbinders may bind to the immunizing antigen. GC B cells engage with antigen displayed on FDC surfaces in the form of immune complexes [114, 208, 312, 313], and the threshold for survival in the GC may be set by avidity rather than by affinity for antigen. Polyvalent modeling of Fab binding showed that many of the Fabs produced from NP-Eα nonbinders showed detectable binding, suggesting that a fraction of low-affinity cells can capture antigen and receive T cell help. This is also evident using the c-Myc reporter, which allows identification, albeit at low frequencies, of c-Myc$^+$ cells with no NP-Eα binding; these cells must have presented cognate antigen to Tfh in order to receive productive T cell signals. However, none of the Fabs produced

from nonbinding cells in the LZ reached the binding capacity of the germline B1-8^{hi} Fab. Therefore, tracking with NP-Eα is a dynamic process and presents a snapshot of cells engaging with antigen, exposing *in vivo* competition dynamics resulting from affinity and antigen capture over time.

3.2 Role of BCR signaling in Positive Selection

By combining NP-Eα with a c-Myc reporter, I could directly associate the capacity to engage antigen with different magnitudes of T cell help. Among selected cells, those with less NP-Eα engagement, reflecting lower affinity BCRs or a lack of continuous antigen engagement, showed lower induction of positive selection pathways when compared to higher-affinity cells. Consistent with having received a lower magnitude of T cell help c-Myc^{+} NP-Eα^{-} cells had higher expression of *Bach2*, which is negatively correlated with the strength of T cell signals received [273]. Expression of *Hhex* and *Tle3*, transcription factors that promote memory B cell differentiation, was also enriched in this population [274]. This coincided with higher expression of memory B cell associated markers such as *Bcl2l1*, though the expression of previously identified markers such as *Ccr6* was mixed [264, 270]. Therefore, a subset of cells that receive lower amounts of T cell help may adopt a memory fate, consistent with previous findings that many memory B cells show low affinity for antigen [270, 273, 314].

In contrast, c-Myc^{+} NP-Eα^{+} cells showed significantly enhanced induction of Myc, mTOR, and NF-κB pathways associated with positive selection. Whereas lower-affinity cells seem poised to adopt a memory phenotype, these signatures suggest that high-affinity cells that receive a strong BCR signal and T cell help are positioned to migrate to the DZ and proliferate. This is consistent with *ex vivo* studies demonstrating that both BCR and CD40 signaling are required to induce NF-κB in GC B cells [224]. Previous work has suggested that plasma cell differentiation is initiated by a strong BCR signal, followed by T cell help signals, and the induction of *Irf4* [255–257]. Although I found no significant difference in bulk *Irf4* or *Prdm1* expression among c-Myc^{+} cells, future experiments with more stringent gating on the highest *c-Myc* expressing and NP-Eα binding population might uncover pre-plasma cells missed by our bulk analysis. To better understand fate decisions among positively selected cells, increased resolution using single-cell RNA-seq and trajectory analysis may better identify and characterize pre-Memory, pre-Plasma, and pre-DZ cells.

3.3 Role of BCR signaling in Negative Selection

Previous work from the Nussenzweig lab suggested that the default state of LZ B cells is to die, and survival is controlled by access to T cell help [248]. However, I found an active role for BCR signaling in conferring a survival advantage to LZ B cells. LZ B cells that retained the ability to engage antigen were less likely to die by apoptosis, and a short inhibition of BCR signaling by ibrutinib differentially affected LZ B cell survival.

This survival advantage was independent of productive T cell signals because it was present even among c-Myc$^-$ cells. Furthermore, by using the ibrutinib-resistant mouse model, BTK^{C481S}, I was able to show that this susceptibility was intrinsic to the BCR signaling pathway in LZ GC B cells. A similar role for BCR signaling has previously been observed in rescuing and preventing Fas-dependent apoptosis in activated B cells [315–317], though further work would be necessary to support this mechanism in GC B cells.

Though BTK blockade experiments demonstrate that rescue from apoptosis is dependent on BCR engagement, it does not exclude that synaptic interactions with FDCs may also impart signals that promote survival [184]. In cell culture studies, signaling through the integrins VLA-4 and LFA-1 has been shown to facilitate GC B cell survival [318]. Ablation of FDCs leads to GC B cell death, though this has pleiotropic effects, including loss of antigen for BCR engagement and secretion of soluble factors [201]. However, whether these signals alone can prevent apoptosis or if they are required in concert with BCR engagement is unknown.

In the context of affinity-based selection, high-affinity B cells that receive a strong BCR signal have an increased probability of receiving T cell help by virtue of their rescue from apoptosis. Conversely, low-affinity B cells, or B cells that have lost affinity for antigen, do not engage their BCRs and are less competitive at receiving T cell help due to their lower antigen presentation. From a teleological perspective, B cells that can continuously receive signals through their BCR would be retained but otherwise lost if survival was only dependent on receiving help from the limited Tfh population. T cell neglect would still represent a checkpoint against autoreactive B cells that encounter their self-ligand in the GC. Therefore, survival in the LZ depends on the endocytic and signaling function of the BCR.

3.4 Synergy between BCR signaling and T cell help

BCR engagement, prior to T cell help, may also serve to prime or license high-affinity B cells to receive T cell help, independently of their pMHC densities. I observed that positive selection is enriched among antigen-binding cells, even when competition on the basis of antigen presentation was normalized using anti-DEC205 targeting. Despite antigen targeting, proliferative capacity was similarly impaired when BCR signaling by drug treatment was dampened, indicating that priming was intrinsic to the BCR signaling pathway. Together, these experiments suggest that independent of its endocytic function, BCR signaling provides a selection advantage prior to receiving T cell help.

Ex vivo BCR stimulation of follicular B cells induces metabolic and mitochondrial changes, intended to prepare cells as they transition to a more active, proliferative state upon receiving a second costimulatory signal [319]. Despite no *c-Myc* expression, LZ B cells with active engagement showed increased induction of Myc and mTOR-associated signatures, along with oxidative phosphorylation and cell cycle entry pathways, though the contribution of short-lived T cell interactions cannot be ruled out. Induction of

these pathways may offer a molecular explanation for the survival advantage observed among antigen-engaged LZ B cells. However, further investigations into the involvement of pro and anti-apoptotic players, which are regulated at the protein, not transcription level, are necessary. In GC B cells, which require synergy from BCR and CD40 signals to induce *Myc*, this initial induction may amplify T cell help by lowering the threshold of signals needed to induce positive selection pathways.

BCR engagement may also alter the expression of cell surface molecules that may license and enhance Tfh interactions. T-B interactions are subject to feed-forward loops, and minute differences in the levels of these costimulatory molecules may be amplified to enhance positive selection pathways, as has been demonstrated along the CD40 and ICOS signaling axes [223]. Expression of cell surface molecules such as the integrin ligand ICAM-1 [320], members of the SLAM family [178], costimulatory molecules CD80 and CD86, cytokine receptors, or negative regulators of T cell activation may be enhanced with BCR engagement [311]. Bulk RNA-seq analysis did not reveal notable differences though a more nuanced investigation at the single-cell level either by RNA-seq or by surface staining might yield valuable insights.

Together, the data indicate that BCR signaling plays an integral role in GC selection by enhancing positive selection and in combination with Tfh signals, influences DZ recycling or memory fate decisions. BCR engagement activates metabolic pathways that may play a role in priming LZ B cells for selection. GC BCR signaling is protective and continuous signaling is necessary for LZ survival. Lastly, GC BCR signaling synergizes with Tfh signals to determine the extent and magnitude of proliferation in the DZ. Therefore, selection is dependent on both the signaling and endocytic functions of the BCR.

Chapter 4

Materials and Methods

4.1 Mice

4.1.1 Strains

Wild-type C57BL/6J and B6.SJL male mice were purchased from Jackson Laboratories. B1-8^{hi}, B1-8^{hi} DEC205$^{-/-}$, B1-8^{hi} CFP, and B1-8^{hi} c-Myc-GFP have been described previously [160, 167, 191]. BTKC481S point mutation mice were generated by microinjection of gRNA, hCas9, and single-stranded donor oligonucleotides into B6 zygote pronuclei (RU CRISPR and Genome Editing Center, RU Transgenic and Reproductive Technology Center [321]. Mutants were backcrossed to B6.SJL for 5+ generations to remove possible CRISPR off-target effects. B1-8^{hi} BTK^{C481S} and B1-8^{hi} DEC205$^{-/-}$ BTK^{C481S} were generated by crossing to B1-8^{hi} and B1-8^{hi} DEC205$^{-/-}$.

4.1.2 Bone Marrow Chimeras

Recipient mice were irradiated with two doses of 5 Gy each, with a resting period of 3-4 hours after the first dose. Bone marrow from BTK^{C481S} or BTK^{WT} mice was extracted by flushing tibias and femurs of mice. Erythrocytes were lysed by resuspension in 1 mL of ACK buffer, and suspensions were filtered by passing through a 70-µm filter. Single-cell suspensions were injected retro-orbitally into recipient mice following the second radiation dose. Mice were put on amoxicillin-laden chow for six weeks post-irradiation.

4.1.3 B cell transfer

Resting B cells were isolated from spleen tissue of donor mice. Spleens were passed through a 70-µm filter into complete RPMI media supplemented with Fetal Bovine Serum (2% v/v) and 1M HEPES (1% v/v). Erythrocytes were lysed by resuspension in 1-2 mLs of ACK buffer. B cells were purified by negative selection using MACS CD43 beads (Miltenyi Biotec) as per manufacturers' instructions. Cells were quantified, and $2 - 5 \times 10^6$ B cells were transferred by intravenous injection into recipient hosts.

4.1.4 Immunization and treatments

Host C57BL/6J and B6.SJL mice, six weeks of age, were primed by intraperitoneal injection of 50 µg Ovalbumin (Biosearch Technologies) precipitated in Imject Alum at

a 1:2 ratio as described [160]. 2-4 weeks after priming, resting B cells were adoptively transferred as described. Host mice were boosted by subcutaneous injection of 25 µg ^{17}NP-OVA in hind footpads one day later. Popliteal lymph nodes were collected, and single-cell suspensions were labeled for flow cytometry seven days after boost. When indicated, 2 µg NP-Eα in 1× DPBS was injected in hind footpads. 5 µg of αDEC-OVA or αDEC-CS in 1× DPBS were injected into mouse hind footpads when indicated [322]. For sheep red blood cell (SRBC) (Colorado Serum) immunizations, SRBCs were washed twice with 1× DPBS, quantified, and 5×10^6 SRBCs were injected into mouse hind footpads. For TM4-Core immunizations [294], 3-5 µg of TM4-Core (produced in our lab) was mixed with Alhydrogel adjuvant 2% (InvivoGen) at a 1:2 ratio and injected in hind footpads.

4.1.5 BTK Inhibition

Ibrutinib (S2680, Selleckchem) or acalabrutinib (S8816, Selleckchem) were solubilized in DMSO (0.5 µg/µL). Inhibitor solution was then dissolved in a solution of 10% (2-hydroxypropyl)-β-cyclodextrin (Sigma) in 1× DPBS. Mice were treated either by oral gavage (200 µL) or by injection into hind footpads (25 µL) as indicated.

4.2 Reagents

4.2.1 NP-Eα

4-Hydroxy-3-nitrophenylacetic acid Succinimide Ester (NP-Osu, Biosearch Technologies) was conjugated to Alexa Fluor 647 Streptavidin or Alexa Fluor 594 Streptavidin at a hapten: streptavidin molar ratio of 10:1 or 20:1. Biotinylated Eα 52-73 peptide (N-biotin-GSGFAKFASFEAQGALANIAVDKA-COOH) [143, 288] was synthesized at the Proteomics Resource Center (The Rockefeller University). NP-Streptavidin conjugates were incubated with a 6× molar excess of biotinylated Eα peptide, and excess peptide was removed by dialysis. Hapten-protein conjugation ratios were calculated by measuring the absorbance value at 430 nm.

4.2.2 Fab Production

Heavy and Light chain eBlocks were ordered from IDT and cloned into human Fab and human lambda expression vectors by restriction cloning [323, 324]. His6-tagged Fabs and lambda light chains were expressed by transient transfection in Expi293F cells, and Fabs were purified using Ni Sepharose 6 Fast Flow resin (GE Healthcare).

4.3 Methods

4.3.1 Flow Cytometry

Popliteal lymph nodes were isolated from immunized mice and resuspended in 1× DPBS supplemented with 1% BSA and EDTA [2mM final] (PBE). Single-cell suspensions were achieved by mechanical disruption of lymph nodes with disposable micro-pestles. For staining of Eα presentation on MHC-II, suspensions were stained with Fc-block and Y-Ae-biotin for 30 minutes. Cells were washed and passed through a 100-μm filter before staining with surface antibodies and fluorescently-labeled streptavidin as indicated. For aCasp3 staining, suspensions were washed in 1× DPBS before resuspension in BD fixation/permeabilization solution. Cells were fixed on ice for 30 minutes then washed twice with 1× Perm buffer. Cells were stained at 4C with aCasp3 antibodies in 1× Perm buffer for 45 minutes. Data were acquired on a BD FACSymphony instrument. Data were analyzed using FlowJo software (BD).

4.3.2 Multiphoton Imaging

Imaging was performed as previously described [216] using an Olympus FV1000 upright microscope fitted with a 25X 1.05NA Plan water-immersion objective and a Mai-Tai DeepSee Ti-Sapphire laser. Lymph nodes were collected, excess adipose tissue was removed under a dissecting microscope, and nodes were sandwiched between two coverslips adhered with vacuum grease for imaging. FDC networks were identified by intravenous injection of αCD35-AF488 24 hours prior to imaging. For tracking antigen localization and engagement, 2 μg of NP-Eα-AF594 was injected s.c. into hind footpads 24 hours prior to imaging. Imaging was performed at λ=910 nm. CFP and AF488 fluorescence emissions were collected in two channels, using a pair of CFP (480/40 nm) and YFP (525/50 nm) filters separated by a 505-nm dichroic mirror, with AF488 appearing as positive in both channels. A third filter was used for AF594 emissions (605/70 nm).

4.3.3 Cell Sorting

All cell sorting was performed on a BD FACSAria II. For single-cell sorting, single B cells were sorted into 96-well plates containing 5 μL of TCL Buffer (Qiagen), supplemented with 1% β-mercaptoethanol (Sigma-Aldrich). Plates were flash-frozen on dry ice. For sorting of GC populations for bulk RNA-seq, up to 400 cells were sorted into 25 μL of TCL Buffer, supplemented with 1% β-mercaptoethanol.

4.3.4 Single-Cell BCR sequencing

Single-cell RNA was purified using magnetic beads (RNAclean XP, Beckman Coulter). RNA was reverse transcribed to cDNA using oligodT primers and Maxima H- reverse transcriptase (Thermo Scientific). Heavy chain and lambda light chains were amplified separately using consensus V_H and V_L forward primers and reverse constant primers

[323, 324]. Well-specific 9-nucleotide barcodes were introduced via PCR to the 5' end. Plate-specific indexing was introduced via PCR by adapting Illumina Nextera DNA index sequences. PCR products from each plate were pooled, and individual plates were purified using magnetic beads (Ampure XP, Beckman Coulter). Plates were pooled at equal concentrations and sequenced with a 500-cycle reagent Nano kit v2 (Illumina) on the Illumina Miseq platform.

4.3.5 Bulk RNA-Seq

RNA was purified using magnetic beads (RNAclean XP, Beckman Coulter). RNA was reverse transcribed to cDNA using oligodT primers and Maxima H- reverse transcriptase (Thermo Scientific) to generate "template-switched" cDNA and amplified as previously described [325–327]. Libraries were prepared and indexed using a Nextera XT DNA Library Prep kit (Illumina) and sequenced on an Illumina NovaSeq platform (RU Genomics Resource Center).

4.3.6 Ca^{+2} Flux Assay

Resting B cells were isolated from spleen tissue of BTKC481S and BTKWT mice. Spleens were passed through a 70-µm filter into complete RPMI media supplemented with Fetal Bovine Serum (2% v/v) and 1M HEPES (1% v/v). Erythrocytes were lysed by resuspension in 1-2 mLs of ACK buffer. B cell suspensions were purified by negative selection using MACS CD43 beads (Miltenyi Biotec) as per manufacturers' instructions. Cells were quantified and mixed at equal concentrations. B cells were resuspended to 10^7 cells/mL in PBE with 1× PowerLoad Concentrate (Thermo Fisher) and Indo-1 AM [2µM] (Thermo Fisher). Cells were incubated, protected from light, at 37C for 30 minutes. After loading, cells were washed 2× and 2×10^6 cells were plated in a 96 well plate with ibrutinib (concentrations as indicated) and surface staining antibodies for 30 minutes at 37C. Cells were washed 2× with RPMI 1640 medium, no phenol red (Thermo Fisher), 1% BSA, and then allowed to rest in RPMI buffer on ice for 30 minutes. Stimulation was performed by addition of biotinylated Goat-Anti-mouse IgM [20 µg/mL] (Jackson ImmunoResearch) followed by Streptavidin (Jackson ImmunoResearch) [40 µg/mL].

4.4 Analysis

4.4.1 BCR Sequence Analysis

Sequences were demultiplexed, paired using Panda-Seq [328], and processed using FastX-toolkit. Sequences were submitted to IMGT [12] for analysis of somatic mutations, light chain usage and rearrangements, and unproductive sequences. Unmutated B1-8^{hi} sequences were identified by CDR3 sequences and the number of mutations.

4.4.2 RNA-seq analysis

Transcript abundance was quantified using kallisto v0.44.0 [329] and subsequently summarized to the gene amount using the R package tximport v.1.12.3 [330] and Ensembl gene database (release 94). Differential gene expression analysis was performed using DESeq2 v.1.24 [331].

4.4.3 Biolayer Interferometry

All biolayer interferometry measurements were performed using a ForteBio Octet Red96 (Sartorius). Monovalent binding assays were performed using High precision streptavidin biosensors (Sartorius), loaded with ^{16}NIP-BSA-biotin (Biosearch Technologies) [5.86nM]. Fabs were diluted in 1× Kinetics Buffer (KB) (Sartorius) and assayed at 100, 50, and 25 nM. Ligand-coated biosensors were regenerated by short incubation in HCl buffer followed by neutralization in 1× KB. Biosensors loaded with ligand alone were used as a reference for subtraction of background signals. Affinities were determined by modeling binding using a 1:1, partial dissociation model. For avidity measurements, Anti-human Fab-CH1 biosensors (Sartorius) were loaded with Fabs diluted in 1× KB [100 nM] and assayed with either ^{2}NP-BSA or ^{9}NP-BSA (Biosearch Technologies) at 0.33 and 0.11 μM. Biosensors loaded with individual Fabs were used as references for subtraction of background signals. Quality of fit for all curves was determined by three criteria: visual examination, R2 values, and χ^2 values. Dissociation constants were reported only from curves that had R2 0.97 and χ^2<0.5. Area under the curve calculations were performed in GraphPad Prism.

Bibliography

1. Tonegawa, S., Steinberg, C., Dube, S. & Bernardini, A. Evidence for Somatic Generation of Antibody Diversity. *Proceedings of the National Academy of Sciences* **71,** 4027–4031. ISSN: 0027-8424 (1974).
2. McKean, D *et al.* Generation of antibody diversity in the immune response of BALB/c mice to influenza virus hemagglutinin. *Proceedings of the National Academy of Sciences* **81,** 3180–3184. ISSN: 0027-8424 (1984).
3. Muramatsu, M. *et al.* Specific Expression of Activation-induced Cytidine Deaminase (AID), a Novel Member of the RNA-editing Deaminase Family in Germinal Center B Cells*. *Journal of Biological Chemistry* **274,** 18470–18476. ISSN: 0021-9258 (1999).
4. Petersen-Mahrt, S. K., Harris, R. S. & Neuberger, M. S. AID mutates E. coli suggesting a DNA deamination mechanism for antibody diversification. *Nature* **418,** 99–104. ISSN: 0028-0836 (2002).
5. Revy, P. *et al.* Activation-Induced Cytidine Deaminase (AID) Deficiency Causes the Autosomal Recessive Form of the Hyper-IgM Syndrome (HIGM2). *Cell* **102,** 565–575. ISSN: 0092-8674 (2000).
6. Early, P., Huang, H., Davis, M., Calame, K. & Hood, L. An immunoglobulin heavy chain variable region gene is generated from three segments of DNA: VH, D and JH. *Cell* **19,** 981–992. ISSN: 0092-8674 (1980).
7. Alt, F. W., Blackwell, T. K. & Yancopoulos, G. D. Development of the Primary Antibody Repertoire. *Science* **238,** 1079–1087. ISSN: 0036-8075 (1987).
8. Jung, D., Giallourakis, C., Mostoslavsky, R. & Alt, F. W. MECHANISM AND CONTROL OF V(D)J RECOMBINATION AT THE IMMUNOGLOBULIN HEAVY CHAIN LOCUS. *Annual Review of Immunology* **24,** 541–570. ISSN: 0732-0582 (2006).
9. Nemazee, D. Receptor editing in lymphocyte development and central tolerance. *Nature Reviews Immunology* **6,** 728–740. ISSN: 1474-1733 (2006).
10. Lefranc, M.-P. & Lefranc, G. *The Immunoglobulin FactsBook* ISBN: 9780124413511 (Academic Press, London, UK, 2001).
11. Mikocziova, I., Greiff, V. & Sollid, L. M. Immunoglobulin germline gene variation and its impact on human disease. *Genes & Immunity* **22,** 205–217. ISSN: 1466-4879 (2021).

12. Lefranc, M.-P. Immunoglobulin and T Cell Receptor Genes: IMGT® and the Birth and Rise of Immunoinformatics. *Frontiers in Immunology* **5,** 22. ISSN: 1664-3224 (2014).

13. Aouinti, S., Malouche, D., Giudicelli, V., Kossida, S. & Lefranc, M.-P. IMGT/HighV-QUEST Statistical Significance of IMGT Clonotype (AA) Diversity per Gene for Standardized Comparisons of Next Generation Sequencing Immunoprofiles of Immunoglobulins and T Cell Receptors. English. *PLoS ONE* **10** (ed Allen, R. L.) e0142353. http://journals.plos.org/plosone/article/file?id=10.1371/journal.pone.0142353\&type=printable (Nov. 2015).

14. Gent, D. C. v. *et al.* Initiation of V(D)J recombination in a cell-free system. *Cell* **81,** 925–934. ISSN: 0092-8674 (1995).

15. McBlane, J. *et al.* Cleavage at a V(D)J recombination signal requires only RAG1 and RAG2 proteins and occurs in two steps. *Cell* **83,** 387–395. ISSN: 0092-8674 (1995).

16. Eastman, Q. M., Leu, T. M. J. & Schatz, D. G. Initiation of V(D)J recombination in vitro obeying the 12/23 rule. *Nature* **380,** 85–88. ISSN: 0028-0836 (1996).

17. Alt, F. W. *et al.* Ordered rearrangement of immunoglobulin heavy chain variable region segments. *The EMBO Journal* **3,** 1209–1219. ISSN: 0261-4189 (1984).

18. Schatz, D. G. & Ji, Y. Recombination centres and the orchestration of V(D)J recombination. English. *Nature Reviews Immunology* **11,** 251–263. ISSN: 1474-1733 (2011-04).

19. Benedict, C. L., Gilfillan, S., Thai, T. & Kearney, J. F. Terminal deoxynucleotidyl transferase and repertoire development. *Immunological Reviews* **175,** 150–157. ISSN: 1600-065X (2000).

20. Muramatsu, M. *et al.* Class Switch Recombination and Hypermutation Require Activation-Induced Cytidine Deaminase (AID), a Potential RNA Editing Enzyme. English. *Cell* **102,** 553–563. ISSN: 0092-8674 (2000-09).

21. Wagner, S. D. & Neuberger, M. S. SOMATIC HYPERMUTATION OF IMMUNOGLOBULIN GENES. *Annual Review of Immunology* **14,** 441–457. ISSN: 0732-0582 (1996).

22. Peled, J. U. *et al.* The Biochemistry of Somatic Hypermutation. *Annual review of immunology* **26,** 481–511. ISSN: 0732-0582 (2008).

23. Hardy, R. R. & Hayakawa, K. B CELL DEVELOPMENT PATHWAYS. *Annual Review of Immunology* **19,** 595–621. ISSN: 0732-0582 (2001).

24. Sakaguchi, N & Melchers, F. Lambda 5, a new light-chain-related locus selectively expressed in pre-B lymphocytes. *Nature* **324,** 579–82. ISSN: 0028-0836 (1986).

25. Karasuyama, H, Kudo, A & Melchers, F. The proteins encoded by the VpreB and lambda 5 pre-B cell-specific genes can associate with each other and with mu heavy chain. *The Journal of experimental medicine* **172,** 969–972. ISSN: 0022-1007 (1990).

26. Winkler, T. H. & Mårtensson, I.-L. The Role of the Pre-B Cell Receptor in B Cell Development, Repertoire Selection, and Tolerance. *Frontiers in Immunology* **9,** 2423 (2018).

27. Rickert, R. C. New insights into pre-BCR and BCR signalling with relevance to B cell malignancies. English. *Nature Reviews Immunology* **13,** 578–591. ISSN: 1474-1733 (2013-08).

28. Nussenzweig, M. C. *et al.* Allelic Exclusion in Transgenic Mice That Express the Membrane form of Immunoglobulin μ. *Science* **236,** 816–819. ISSN: 0036-8075 (1987).

29. Nussenzweig, M. C., Shaw, A. C., Sinn, E, Campos-Torres, J & Leder, P. Allelic exclusion in transgenic mice carrying mutant human IgM genes. *The Journal of Experimental Medicine* **167,** 1969–1974. ISSN: 0022-1007 (1988).

30. Tiegs, S. L., Russell, D. M. & Nemazee, D. Receptor editing in self-reactive bone marrow B cells. *The Journal of experimental medicine* **177,** 1009–1020. ISSN: 0022-1007 (1993).

31. Gay, D, Saunders, T, Camper, S & Weigert, M. Receptor editing: an approach by autoreactive B cells to escape tolerance. *The Journal of experimental medicine* **177,** 999–1008. ISSN: 0022-1007 (1993).

32. Nemazee, D. Mechanisms of central tolerance for B cells. English. *Nature Reviews Immunology* **17,** 281–294. ISSN: 1474-1733 (Apr. 2017).

33. Gorman, J. R. & Alt, F. W. Regulation of Immunoglobulin Light Chain Isotype Expression. *Advances in Immunology* **69,** 113–181. ISSN: 0065-2776 (1998).

34. Hieter, P. A., Korsmeyer, S. J., Waldmann, T. A. & Leder, P. Human immunoglobulin κ light-chain genes are deleted or rearranged in λ-producing B cells. *Nature* **290,** 368–372. ISSN: 0028-0836 (1981).

35. Korsmeyer, S. J. *et al.* Normal human B cells display ordered light chain gene rearrangements and deletions. *The Journal of experimental medicine* **156,** 975–985. ISSN: 0022-1007 (1982).

36. Siminovitch, K. A., Bakhshi, A., Goldman, P. & Korsmeyer, S. J. A uniform deleting element mediates the loss of κ genes in human B cells. *Nature* **316,** 260–262. ISSN: 0028-0836 (1985).

37. Siminovitch, K. A., Moore, M. W., Durdik, J. & Selsing, E. The human kappa deleting element and the mouse recombining segment share DNA sequence homology. *Nucleic Acids Research* **15,** 2699–2705. ISSN: 0305-1048 (1987).

38. Hardy, R. R., Kincade, P. W. & Dorshkind, K. The Protean Nature of Cells in the B Lymphocyte Lineage. English. *Immunity* **26,** 703–714. ISSN: 1074-7613 (2007-06).

39. Wardemann, H. *et al.* Predominant Autoantibody Production by Early Human B Cell Precursors. English. *Science* **301,** 1374–1377. ISSN: 0036-8075 (Sept. 2003).

40. Goodnow, C. C., Adelstein, S. & Basten, A. The Need for Central and Peripheral Tolerance in the B Cell Repertoire. *Science* **248,** 1373–1379. ISSN: 0036-8075 (1990).

41. Goodnow, C. C. Transgenic Mice and Analysis of B-Cell Tolerance. *Annual Review of Immunology* **10,** 489–518. ISSN: 0732-0582 (1992).

42. Klinman, N. R. The "Clonal Selection Hypothesis" and Current Concepts of B Cell Tolerance. *Immunity* **5,** 189–195. ISSN: 1074-7613 (1996).

43. Hartley, S. B. *et al.* Elimination from peripheral lymphoid tissues of self-reactive B lymphocytes recognizing membrane-bound antigens. English. *Nature* **353,** 765–769. ISSN: 0028-0836 (Oct. 1991).

44. Cambier, J. C., Gauld, S. B., Merrell, K. T. & Vilen, B. J. B-cell anergy: from transgenic models to naturally occurring anergic B cells? *Nature Reviews Immunology* **7,** 633–643. ISSN: 1474-1733 (2007).

45. Bretscher, P. & Cohn, M. A Theory of Self-Nonself Discrimination. *Science* **169,** 1042–1049. ISSN: 0036-8075 (1970).

46. Parker, D. C. T Cell-Dependent B Cell Activation. *Annual Review of Immunology* **11,** 331–360. ISSN: 0732-0582 (1993).

47. Williams, A. F. & Barclay, A. N. The Immunoglobulin Superfamily—Domains for Cell Surface Recognition. *Annual Review of Immunology* **6,** 381–405. ISSN: 0732-0582 (1988).

48. Kirkham, P. M. & Schroeder, H. W. Antibody structure and the evolution of immunoglobulin V gene segments. *Seminars in Immunology* **6,** 347–360. ISSN: 1044-5323 (1994).

49. Chiu, M. L., Goulet, D. R., Teplyakov, A. & Gilliland, G. L. Antibody Structure and Function: The Basis for Engineering Therapeutics. *Antibodies* **8,** 55 (2019).

50. Xu, Z., Zan, H., Pone, E. J., Mai, T. & Casali, P. Immunoglobulin class-switch DNA recombination: induction, targeting and beyond. *Nature Reviews Immunology* **12,** 517–531. ISSN: 1474-1733 (2012).

51. Matsumoto, M. L. Molecular Mechanisms of Multimeric Assembly of IgM and IgA. *Annual Review of Immunology* **40,** 1–27. ISSN: 0732-0582 (2022).

52. Ravetch, J. V. & Bolland, S. IGG FC RECEPTORS. English. *Annual Review of Immunology* **19,** 275–290. ISSN: 0732-0582 (2001).

53. Nimmerjahn, F. & Ravetch, J. V. Fcγ receptors as regulators of immune responses. English. *Nature Reviews Immunology* **8,** 34–47. ISSN: 1474-1733 (2008-01).

54. Edmundson, A. B., Guddat, L. W. & Andersen, K. N. Crystal Structures of Intact IgG Antibodies. *ImmunoMethods* **3,** 197–210. ISSN: 1058-6687 (1993).

55. Lesk, A. M. & Chothia, C. Elbow motion in the immunoglobulins involves a molecular ball-and-socket joint. *Nature* **335,** 188–190. ISSN: 0028-0836 (1988).

56. Dangl, J. L. *et al.* Segmental flexibility and complement fixation of genetically engineered chimeric human, rabbit and mouse antibodies. *The EMBO Journal* **7,** 1989–1994. ISSN: 1460-2075 (1988).

57. Huber, R. & Bennett, W. S. Antibody–antigen flexibility. *Nature* **326,** 334–335. ISSN: 0028-0836 (1987).

58. Kurosaki, T. GENETIC ANALYSIS OF B CELL ANTIGEN RECEPTOR SIGNALING. English. *Annual Review of Immunology* **17,** 555–592. ISSN: 0732-0582 (1999).

59. Reth, M. Antigen Receptors on B Lymphocytes. *Annual Review of Immunology* **10,** 97–121. ISSN: 0732-0582 (1992).

60. Xu, Y. *et al.* No receptor stands alone: IgG B-cell receptor intrinsic and extrinsic mechanisms contribute to antibody memory. English. *Cell Research* **24,** 651–664. ISSN: 1001-0602 (2014-06).

61. Burkhardt, A. L. *et al.* Ig alpha and Ig beta are functionally homologous to the signaling proteins of the T-cell receptor. *Molecular and Cellular Biology* **14,** 1095–1103. ISSN: 0270-7306 (1994).

62. Sanchez, M *et al.* Signal transduction by immunoglobulin is mediated through Ig alpha and Ig beta. *The Journal of experimental medicine* **178,** 1049–1055. ISSN: 0022-1007 (1993).

63. Monroe, J. G. ITAM-mediated tonic signalling through pre-BCR and BCR complexes. *Nature Reviews Immunology* **6,** 283–294. ISSN: 1474-1733 (2006).

64. Reth, M. Antigen receptor tail clue. *Nature* **338,** 383–384. ISSN: 0028-0836 (1989).

65. Tolar, P., Sohn, H. W. & Pierce, S. K. The initiation of antigen-induced B cell antigen receptor signaling viewed in living cells by fluorescence resonance energy transfer. *Nature Immunology* **6,** 1168–1176. ISSN: 1529-2908 (2005).

66. Pierce, S. K. & Liu, W. The tipping points in the initiation of B cell signalling: how small changes make big differences. English. *Nature Reviews Immunology* **10,** 767–777. ISSN: 1474-1733 (2010-11).

67. Harwood, N. E. & Batista, F. D. Early Events in B Cell Activation. English. *Annual Review of Immunology* **28,** 185–210. ISSN: 0732-0582 (2010).

68. Carrasco, Y. R. & Batista, F. D. B Cells Acquire Particulate Antigen in a Macrophage-Rich Area at the Boundary between the Follicle and the Subcapsular Sinus of the Lymph Node. English. *Immunity* **27,** 160–171. ISSN: 1074-7613 (2007-07).

69. Junt, T. *et al.* Subcapsular sinus macrophages in lymph nodes clear lymph-borne viruses and present them to antiviral B cells. *Nature* **450,** 110–114. ISSN: 0028-0836 (2007).

70. Pape, K. A., Catron, D. M., Itano, A. A. & Jenkins, M. K. The Humoral Immune Response Is Initiated in Lymph Nodes by B Cells that Acquire Soluble Antigen Directly in the Follicles. English. *Immunity* **26,** 491–502. ISSN: 1074-7613 (2007-04).

71. Phan, T. G., Grigorova, I., Okada, T. & Cyster, J. G. Subcapsular encounter and complement-dependent transport of immune complexes by lymph node B cells. English. *Nature Immunology* **8,** 992–1000. ISSN: 1529-2908 (2007-09).

72. Qi, H., Egen, J. G., Huang, A. Y. C. & Germain, R. N. Extrafollicular Activation of Lymph Node B Cells by Antigen-Bearing Dendritic Cells. English. *Science* **312,** 1672–1676. ISSN: 0036-8075 (June 2006).

73. Tolar, P., Hanna, J., Krueger, P. D. & Pierce, S. K. The Constant Region of the Membrane Immunoglobulin Mediates B Cell-Receptor Clustering and Signaling in Response to Membrane Antigens. *Immunity* **30,** 44–55. ISSN: 1074-7613 (2009).

74. Gauld, S. B. & Cambier, J. C. Src-family kinases in B-cell development and signaling. *Oncogene* **23,** 8001–8006. ISSN: 0950-9232 (2004).

75. Kurosaki, T *et al.* Role of the Syk autophosphorylation site and SH2 domains in B cell antigen receptor signaling. *The Journal of Experimental Medicine* **182,** 1815–1823. ISSN: 0022-1007 (1995).

76. Geahlen, R. L. Syk and pTyr'd: Signaling through the B cell antigen receptor. *Biochimica et Biophysica Acta (BBA) - Molecular Cell Research* **1793,** 1115–1127. ISSN: 0167-4889 (2009).

77. Kabak, S. *et al.* The Direct Recruitment of BLNK to Immunoglobulin α Couples the B-Cell Antigen Receptor to Distal Signaling Pathways. *Molecular and Cellular Biology* **22,** 2524–2535. ISSN: 0270-7306 (2002).

78. Fu, C., Turck, C. W., Kurosaki, T. & Chan, A. C. BLNK a Central Linker Protein in B Cell Activation. *Immunity* **9,** 93–103. ISSN: 1074-7613 (1998).

79. Kurosaki, T. & Tsukada, S. BLNK Connecting Syk and Btk to Calcium Signals. *Immunity* **12,** 1–5. ISSN: 1074-7613 (2000).

80. Scharenberg, A. M., Humphries, L. A. & Rawlings, D. J. Calcium signalling and cell-fate choice in B cells. *Nature Reviews Immunology* **7,** 778–789. ISSN: 1474-1733 (2007).

81. Tuveson, D. A., Carter, R. H., Soltoff, S. P. & Fearon, D. T. CD19 of B Cells as a Surrogate Kinase Insert Region to Bind Phosphatidylinositol 3-Kinase. *Science* **260,** 986–989. ISSN: 0036-8075 (1993).

82. So, L. & Fruman, D. PI3K signalling in B- and T-lymphocytes: new developments and therapeutic advances. *Biochemical Journal* **442,** 465–481. ISSN: 0264-6021 (2012).

83. Chung, J. K. *et al.* Switch-like activation of Bruton's tyrosine kinase by membrane-mediated dimerization. *Proceedings of the National Academy of Sciences* **116,** 10798–10803. ISSN: 0027-8424 (2019).

84. Hendriks, R. W., Yuvaraj, S. & Kil, L. P. Targeting Bruton's tyrosine kinase in B cell malignancies. *Nature Reviews Cancer* **14,** 219–232. ISSN: 1474-175X (2014).

85. Otero, D. C., Omori, S. A. & Rickert, R. C. CD19-dependent Activation of Akt Kinase in B-lymphocytes*. *Journal of Biological Chemistry* **276,** 1474–1478. ISSN: 0021-9258 (2001).

86. Hoxhaj, G. & Manning, B. D. The PI3K–AKT network at the interface of oncogenic signalling and cancer metabolism. *Nature Reviews Cancer* **20,** 74–88. ISSN: 1474-175X (2020).

87. Kim, Y. J., Sekiya, F., Poulin, B., Bae, Y. S. & Rhee, S. G. Mechanism of B-Cell Receptor-Induced Phosphorylation and Activation of Phospholipase C-γ2. *Molecular and Cellular Biology* **24,** 9986–9999. ISSN: 0270-7306 (2004).

88. Hikida, M. & Kurosaki, T. Regulation of Phospholipase C-γ2 Networks in B Lymphocytes. *Advances in Immunology* **88,** 73–96. ISSN: 0065-2776 (2005).

89. Kurosaki, T., Shinohara, H. & Baba, Y. B Cell Signaling and Fate Decision. English. *Annual Review of Immunology* **28,** 21–55. ISSN: 0732-0582 (2010-03).

90. Valvezan, A. J. & Manning, B. D. Molecular logic of mTORC1 signalling as a metabolic rheostat. *Nature Metabolism* **1,** 321–333 (2019).

91. Limon, J. J. & Fruman, D. A. Akt and mTOR in B Cell Activation and Differentiation. *Frontiers in Immunology* **3,** 228 (2012).

92. Zhang, X., Tang, N., Hadden, T. J. & Rishi, A. K. Akt, FoxO and regulation of apoptosis. *Biochimica et Biophysica Acta (BBA) - Molecular Cell Research* **1813,** 1978–1986. ISSN: 0167-4889 (2011).

93. Tanaka, S. & Baba, Y. B Cells in Immunity and Tolerance. *Advances in Experimental Medicine and Biology* **1254,** 23–36. ISSN: 0065-2598 (2020).

94. Caunt, C. J., Sale, M. J., Smith, P. D. & Cook, S. J. MEK1 and MEK2 inhibitors and cancer therapy: the long and winding road. *Nature Reviews Cancer* **15,** 577–592. ISSN: 1474-175X (2015).

95. David, L. *et al.* Assembly mechanism of the CARMA1–BCL10–MALT1–TRAF6 signalosome. *Proceedings of the National Academy of Sciences* **115,** 201721967. ISSN: 0027-8424 (2018).

96. Shembade, N. & Harhaj, E. W. Regulation of NF-κB signaling by the A20 deubiquitinase. *Cellular & Molecular Immunology* **9,** 123–130. ISSN: 1672-7681 (2012).

97. Ruland, J. & Mak, T. W. Transducing signals from antigen receptors to nuclear factor κB. *Immunological Reviews* **193,** 93–100. ISSN: 1600-065X (2003).

98. Yang, C., David, L., Qiao, Q., Damko, E. & Wu, H. The CBM signalosome: Potential therapeutic target for aggressive lymphoma? *Cytokine & Growth Factor Reviews* **25,** 175–183. ISSN: 1359-6101 (2014).

99. Muta, T. *et al.* A 13-amino-acid motif in the cytoplasmic domain of FcγRIIB modulates B-cell receptor signalling. *Nature* **368,** 70–73. ISSN: 0028-0836 (1994).

100. O'Keefe, T. L., Williams, G. T., Batista, F. D. & Neuberger, M. S. Deficiency in CD22, a B Cell–specific Inhibitory Receptor, Is Sufficient to Predispose to Development of High Affinity Autoantibodies. *The Journal of Experimental Medicine* **189,** 1307–1313. ISSN: 0022-1007 (1999).

101. McGaha, T. L., Karlsson, M. C. I. & Ravetch, J. V. FcγRIIB Deficiency Leads to Autoimmunity and a Defective Response to Apoptosis in Mrl-MpJ Mice. *The Journal of Immunology* **180,** 5670–5679. ISSN: 0022-1767 (2008).

102. Fukuyama, H., Nimmerjahn, F. & Ravetch, J. V. The inhibitory Fcγ receptor modulates autoimmunity by limiting the accumulation of immunoglobulin G+ anti-DNA plasma cells. English. *Nature Immunology* **6,** 99–106. ISSN: 1529-2908 (2005-01).

103. Jellusova, J. & Nitschke, L. Regulation of B Cell Functions by the Sialic Acid-Binding Receptors Siglec-G and CD22. *Frontiers in Immunology* **2,** 96 (2012).

104. Smith, K. G., Tarlinton, D. M., Doody, G. M., Hibbs, M. L. & Fearon, D. T. Inhibition of the B Cell by CD22: A Requirement for Lyn. *The Journal of Experimental Medicine* **187,** 807–811. ISSN: 0022-1007 (1998).

105. Dustin, L. B. *et al.* Expression of dominant-negative src-homology domain 2-containing protein tyrosine phosphatase-1 results in increased Syk tyrosine kinase activity and B cell activation. *Journal of immunology (Baltimore, Md. : 1950)* **162,** 2717–24. ISSN: 0022-1767 (1999).

106. Ono, M *et al.* Deletion of SHIP or SHP-1 reveals two distinct pathways for inhibitory signaling. English. *Cell* **90,** 293 –301 (July 1997).

107. Liu, W., Sohn, H. W., Tolar, P., Meckel, T. & Pierce, S. K. Antigen-Induced Oligomerization of the B Cell Receptor Is an Early Target of FcγRIIB Inhibition. English. *The Journal of Immunology* **184,** 1977–1989. ISSN: 0022-1767 (Feb. 2010).

108. Ono, M., Bolland, S., Tempst, P. & Ravetch, J. V. Role of the inositol phosphatase SHIP in negative regulation of the immune system by the receptor FeγRIIB. English. *Nature* **383,** 263–266. ISSN: 0028-0836 (1996).

109. Pauls, S. D. & Marshall, A. J. Regulation of immune cell signaling by SHIP1: A phosphatase, scaffold protein, and potential therapeutic target. *European Journal of Immunology* **47,** 932–945. ISSN: 1521-4141 (2017).

110. Bolland, S, Pearse, R. N., Kurosaki, T & Ravetch, J. V. SHIP modulates immune receptor responses by regulating membrane association of Btk. English. *Immunity* **8,** 509 –516 (1998-04).

111. Bryant, P. & Ploegh, H. Class II MHC peptide loading by the professionals. *Current Opinion in Immunology* **16,** 96–102. ISSN: 0952-7915 (2004).

112. Roozendaal, R. *et al.* Conduits Mediate Transport of Low-Molecular-Weight Antigen to Lymph Node Follicles. English. *Immunity* **30,** 264–276. ISSN: 1074-7613 (Feb. 2009).

113. Andrian, U. H. v. & Mempel, T. R. Homing and cellular traffic in lymph nodes. *Nature Reviews Immunology* **3,** 867–878. ISSN: 1474-1733 (2003).

114. Heesters, B. A., Myers, R. C. & Carroll, M. C. Follicular dendritic cells: dynamic antigen libraries. English. *Nature Reviews Immunology* **14,** 495–504. ISSN: 1474-1733 (2014-07).

115. Treanor, B., Depoil, D., Bruckbauer, A. & Batista, F. D. Dynamic cortical actin remodeling by ERM proteins controls BCR microcluster organization and integrity. *Journal of Experimental Medicine* **208,** 1055–1068. ISSN: 0022-1007 (2011).

116. Fleire, S. J. *et al.* B Cell Ligand Discrimination Through a Spreading and Contraction Response. English. *Science* **312,** 738–741. ISSN: 0036-8075 (May 2006).

117. Weber, M. *et al.* Phospholipase C-gamma2 and Vav cooperate within signaling microclusters to propagate B cell spreading in response to membrane-bound antigen. *The Journal of experimental medicine* **205,** 853–68. ISSN: 0022-1007 (2008).

118. Carrasco, Y. R., Fleire, S. J., Cameron, T., Dustin, M. L. & Batista, F. D. LFA-1/ICAM-1 Interaction Lowers the Threshold of B Cell Activation by Facilitating B Cell Adhesion and Synapse Formation. *Immunity* **20,** 589–599. ISSN: 1074-7613 (2004).

119. Carrasco, Y. R. & Batista, F. D. B-cell activation by membrane-bound antigens is facilitated by the interaction of VLA-4 with VCAM-1. *The EMBO journal* **25,** 889–99. ISSN: 0261-4189 (2006).

120. Monks, C. R. F., Freiberg, B. A., Kupfer, H., Sciaky, N. & Kupfer, A. Three-dimensional segregation of supramolecular activation clusters in T cells. English. *Nature* **395.** 10.1038/25764, 82–86. ISSN: 0028-0836 (Sept. 1998).

121. Yuseff, M.-I., Pierobon, P., Reversat, A. & Lennon-Duménil, A.-M. How B cells capture, process and present antigens: a crucial role for cell polarity. English. *Nature Reviews Immunology* **13,** 475–486. ISSN: 1474-1733 (2013-07).

122. Natkanski, E. *et al.* B Cells Use Mechanical Energy to Discriminate Antigen Affinities. English. *Science* **340,** 1587–1590. ISSN: 0036-8075 (June 2013).

123. Hoogeboom, R. *et al.* Myosin IIa Promotes Antibody Responses by Regulating B Cell Activation, Acquisition of Antigen, and Proliferation. *Cell Reports* **23,** 2342–2353. ISSN: 2211-1247 (2018).

124. Chaturvedi, A., Martz, R., Dorward, D., Waisberg, M. & Pierce, S. K. Endocytosed BCRs sequentially regulate MAPK and Akt signaling pathways from intracellular compartments. *Nature Immunology* **12,** 1119–1126. ISSN: 1529-2908 (2011).

125. Eisen, H. N. Roots: Why affinity progression of antibodies during immune responses is probably not accompanied by parallel changes in the immunoglobulin-like antigen-specific receptors on T cells. *BioEssays* **4,** 269–272. ISSN: 1521-1878 (1986).

126. Eisen, H. N. & Siskind, G. W. Variations in Affinities of Antibodies during the Immune Response *. *Biochemistry* **3,** 996–1008. ISSN: 0006-2960 (1964).

127. Steiner, L. A. & Eisen, H. N. SEQUENTIAL CHANGES IN THE RELATIVE AFFINITY OF ANTIBODIES SYNTHESIZED DURING THE IMMUNE RESPONSE. *The Journal of Experimental Medicine* **126,** 1161–1183. ISSN: 0022-1007 (1967).

128. Steiner, L. A. & Eisen, H. N. THE RELATIVE AFFINITY OF ANTIBODIES SYNTHESIZED IN THE SECONDARY RESPONSE. *The Journal of Experimental Medicine* **126,** 1185–1205. ISSN: 0022-1007 (1967).

129. Nieuwenhuis, P. & Opstelten, D. Functional anatomy of germinal centers. *American Journal of Anatomy* **170,** 421–435. ISSN: 1553-0795 (1984).

130. Jacob, J., Kelsoe, G., Rajewsky, K. & Weiss, U. Intraclonal generation of antibody mutants in germinal centres. *Nature* **354,** 389–392. ISSN: 0028-0836 (1991).

131. Küppers, R., Zhao, M., Hansmann, M. & Rajewsky, K. Tracing B cell development in human germinal centres by molecular analysis of single cells picked from histological sections. *The EMBO Journal* **12,** 4955–4967. ISSN: 1460-2075 (1993).

132. Mesin, L., Ersching, J. & Victora, G. Germinal Center B Cell Dynamics. English. *Immunity* **45,** 471–482. ISSN: 1074-7613 (Sept. 2016).

133. Escolano, A., Dosenovic, P. & Nussenzweig, M. C. Progress toward active or passive HIV-1 vaccination. English. *The Journal of Experimental Medicine* **214,** 3–16. ISSN: 0022-1007 (2017-01).

134. Gaebler, C. *et al.* Evolution of antibody immunity to SARS-CoV-2. *Nature* **591,** 639–644. ISSN: 0028-0836 (2021).

135. Batista, F. D. & Harwood, N. E. The who, how and where of antigen presentation to B cells. *Nature Reviews Immunology* **9,** 15–27. ISSN: 1474-1733 (2009).

136. Okada, T. *et al.* Chemokine Requirements for B Cell Entry to Lymph Nodes and Peyer's Patches. English. *The Journal of Experimental Medicine* **196,** 65–75. ISSN: 0022-1007 (July 2002).

137. Yi, T. *et al.* Oxysterol Gradient Generation by Lymphoid Stromal Cells Guides Activated B Cell Movement during Humoral Responses. English. *Immunity* **37,** 535–548. ISSN: 1074-7613 (Sept. 2012).

138. Pereira, J. P., Kelly, L. M., Xu, Y. & Cyster, J. G. EBI2 mediates B cell segregation between the outer and centre follicle. English. *Nature* **460,** 1122–1126. ISSN: 0028-0836 (Aug. 2009).

139. Kelly, L. M., Pereira, J. P., Yi, T., Xu, Y. & Cyster, J. G. EBI2 Guides Serial Movements of Activated B Cells and Ligand Activity Is Detectable in Lymphoid and Nonlymphoid Tissues. English. *The Journal of Immunology* **187,** 3026–3032. ISSN: 0022-1767 (Sept. 2011).

140. Pereira, J. P., Kelly, L. M. & Cyster, J. G. Finding the right niche: B-cell migration in the early phases of T-dependent antibody responses. English. *International Immunology* **22,** 413–419. ISSN: 0953-8178 (2010-06).

141. Cinamon, G. *et al.* Sphingosine 1-phosphate receptor 1 promotes B cell localization in the splenic marginal zone. *Nature Immunology* **5,** 713–720. ISSN: 1529-2908 (2004).

142. Coffey, F., Alabyev, B. & Manser, T. Initial Clonal Expansion of Germinal Center B Cells Takes Place at the Perimeter of Follicles. *Immunity* **30,** 599–609. ISSN: 1074-7613 (2009).

143. Schwickert, T. A. *et al.* A dynamic T cell–limited checkpoint regulates affinity-dependent B cell entry into the germinal center. English. *The Journal of Experimental Medicine* **208,** 1243–1252. ISSN: 0022-1007 (June 2011).

144. Roco, J. A. *et al.* Class-Switch Recombination Occurs Infrequently in Germinal Centers. English. *Immunity* **51,** 337–350.e7. ISSN: 1074-7613 (July 2019).

145. Okada, T., Moriyama, S. & Kitano, M. Differentiation of germinal center B cells and follicular helper T cells as viewed by tracking Bcl6 expression dynamics. English. *Immunological Reviews* **247,** 120–132. ISSN: 1600-065X (Apr. 2012).

146. Huang, C. *et al.* The BCL6 RD2 Domain Governs Commitment of Activated B Cells to Form Germinal Centers. English. *Cell Reports* **8,** 1497–1508. ISSN: 2211-1247 (Sept. 2014).

147. Green, J. A. *et al.* The sphingosine 1-phosphate receptor S1P2 maintains the homeostasis of germinal center B cells and promotes niche confinement. English. *Nature Immunology* **12,** 672–680. ISSN: 1529-2908 (2011-07).

148. Green, J. A. & Cyster, J. G. S1PR2 links germinal center confinement and growth regulation. English. *Immunological Reviews* **247,** 36–51. ISSN: 1600-065X (2012-05).

149. Dent, A. L., Shaffer, A. L., Yu, X., Allman, D. & Staudt, L. M. Control of Inflammation, Cytokine Expression, and Germinal Center Formation by BCL-6. *Science* **276,** 589–592. ISSN: 0036-8075 (1997).

150. Fukuda, T. *et al.* Disruption of the Bcl6 Gene Results in an Impaired Germinal Center Formation. *The Journal of Experimental Medicine* **186,** 439–448. ISSN: 0022-1007 (1997).

151. Klein, U. & Dalla-Favera, R. Germinal centres: role in B-cell physiology and malignancy. *Nature Reviews Immunology* **8,** 22–33. ISSN: 1474-1733 (2008).

152. Green, M. R. *et al.* Transient expression of Bcl6 is sufficient for oncogenic function and induction of mature B-cell lymphoma. English. *Nature Communications* **5,** 3904 (June 2014).

153. Basso, K. *et al.* Integrated biochemical and computational approach identifies BCL6 direct target genes controlling multiple pathways in normal germinal center B cells. *Blood* **115,** 975–984. ISSN: 0006-4971 (2010).

154. Basso, K. & Dalla-Favera, R. Chapter 7 BCL6 Master Regulator of the Germinal Center Reaction and Key Oncogene in B Cell Lymphomagenesis. *Advances in Immunology* **105,** 193–210. ISSN: 0065-2776 (2010).

155. Ranuncolo, S. M. *et al.* Bcl-6 mediates the germinal center B cell phenotype and lymphomagenesis through transcriptional repression of the DNA-damage sensor ATR. English. *Nature Immunology* **8,** 705–714. ISSN: 1529-2908 (2007-07).

156. Phan, R. T. & Dalla-Favera, R. The BCL6 proto-oncogene suppresses p53 expression in germinal-centre B cells. English. *Nature* **432,** 635–639. ISSN: 0028-0836 (Dec. 2004).

157. Shaffer, A. *et al.* BCL-6 Represses Genes that Function in Lymphocyte Differentiation, Inflammation, and Cell Cycle Control. *Immunity* **13,** 199–212. ISSN: 1074-7613 (2000).

158. Tunyaplin, C. *et al.* Direct Repression of prdm1 by Bcl-6 Inhibits Plasmacytic Differentiation. *The Journal of Immunology* **173,** 1158–1165. ISSN: 0022-1767 (2004).

159. Victora, G. D. & Nussenzweig, M. C. Germinal Centers. *Annual Review of Immunology* **30,** 429–457. ISSN: 0732-0582 (2012).

160. Victora, G. D. *et al.* Germinal Center Dynamics Revealed by Multiphoton Microscopy with a Photoactivatable Fluorescent Reporter. English. *Cell* **143,** 592–605. ISSN: 0092-8674 (2010-11).

161. Sander, S. *et al.* PI3 Kinase and FOXO1 Transcription Factor Activity Differentially Control B Cells in the Germinal Center Light and Dark Zones. English. *Immunity* **43,** 1075–1086. ISSN: 1074-7613 (Dec. 2015).

162. Dominguez-Sola, D. *et al.* The FOXO1 Transcription Factor Instructs the Germinal Center Dark Zone Program. English. *Immunity* **43,** 1064–1074. ISSN: 1074-7613 (Dec. 2015).

163. Dickerson, S. K., Market, E., Besmer, E. & Papavasiliou, F. N. AID Mediates Hypermutation by Deaminating Single Stranded DNA. *The Journal of Experimental Medicine* **197,** 1291–1296. ISSN: 0022-1007 (2003).

164. Teng, G. & Papavasiliou, F. N. Immunoglobulin Somatic Hypermutation. English. *Genetics* **41,** 107–120. ISSN: 0066-4197 (2007-12).

165. Wang, Q. *et al.* The cell cycle restricts activation-induced cytidine deaminase activity to early G1. *Journal of Experimental Medicine* **214,** 49–58. ISSN: 0022-1007 (2017).

166. Zhang, J., MacLennan, I. C., Liu, Y.-J. & Lane, P. J. Is rapid proliferation in B centroblasts linked to somatic mutation in memory B cell clones? *Immunology Letters* **18,** 297–299. ISSN: 0165-2478 (1988).

167. Dominguez-Sola, D. *et al.* c-MYC is required for germinal center selection and cyclic re-entry. English. *Nature immunology* **13,** 1083–1091. ISSN: 1529-2908 (2012-11).

168. Calado, D. P. *et al.* MYC is essential for the formation and maintenance of germinal centers. English. *Nature immunology* **13,** 1092–1100. ISSN: 1529-2908 (2012-11).

169. Gitlin, A. D. *et al.* T cell help controls the speed of the cell cycle in germinal center B cells. English. *Science* **349,** 643–646. ISSN: 0036-8075 (Aug. 2015).

170. Vinuesa, C. G., Linterman, M. A., Yu, D. & MacLennan, I. C. Follicular Helper T Cells. English. *Annual Review of Immunology* **34,** 1–34. ISSN: 0732-0582 (May 2016).

171. Vinuesa, C. G. *et al.* A RING-type ubiquitin ligase family member required to repress follicular helper T cells and autoimmunity. *Nature* **435,** 452–458. ISSN: 0028-0836 (2005).

172. Crotty, S. T Follicular Helper Cell Differentiation, Function, and Roles in Disease. English. *Immunity* **41,** 529–542. ISSN: 1074-7613 (Oct. 2014).

173. Linterman, M. A. & Vinuesa, C. G. Signals that influence T follicular helper cell differentiation and function. *Seminars in Immunopathology* **32,** 183–196. ISSN: 1863-2297 (2010).

174. Crotty, S. Follicular Helper CD4 T Cells (TFH). *Annual Review of Immunology* **29,** 621–663. ISSN: 0732-0582 (2011).

175. Nurieva, R. I. *et al.* Bcl6 Mediates the Development of T Follicular Helper Cells. *Science* **325,** 1001–1005. ISSN: 0036-8075 (2009).

176. Ma, X., Nakayamada, S. & Wang, J. Multi-Source Pathways of T Follicular Helper Cell Differentiation. *Frontiers in Immunology* **12,** 621105 (2021).

177. Kerfoot, S. *et al.* Germinal Center B Cell and T Follicular Helper Cell Development Initiates in the Interfollicular Zone. English. *Immunity* **34,** 947–960. ISSN: 1074-7613 (June 2011).

178. Cannons, J. L. *et al.* Optimal Germinal Center Responses Require a Multistage T Cell:B Cell Adhesion Process Involving Integrins, SLAM-Associated Protein, and CD84. English. *Immunity* **32,** 253–265. ISSN: 1074-7613 (2010-02).

179. Moriyama, S. *et al.* Sphingosine-1-phosphate receptor 2 is critical for follicular helper T cell retention in germinal centers. English. *The Journal of Experimental Medicine* **211,** 1297–1305. ISSN: 0022-1007 (June 2014).

180. Xu, H. *et al.* Follicular T-helper cell recruitment governed by bystander B cells and ICOS-driven motility. English. *Nature* **496,** 523–527. ISSN: 0028-0836 (Apr. 2013).

181. Yeh, C.-H., Finney, J., Okada, T., Kurosaki, T. & Kelsoe, G. Primary germinal center-resident T follicular helper cells are a physiologically distinct subset of CXCR5hiPD-1hi T follicular helper cells. *Immunity.* ISSN: 1074-7613 (2022).

182. Weinstein, J. S. *et al.* TFH cells progressively differentiate to regulate the germinal center response. English. *Nature Immunology* **17,** 1197–1205. ISSN: 1529-2908 (2016-10).

183. Shulman, Z. *et al.* T Follicular Helper Cell Dynamics in Germinal Centers. English. *Science* **341,** 673–677. ISSN: 0036-8075 (Aug. 2013).

184. Papa, I. & Vinuesa, C. G. Synaptic Interactions in Germinal Centers. English. *Frontiers in Immunology* **9,** 1858 (2018).

185. Shulman, Z. *et al.* Dynamic signaling by T follicular helper cells during germinal center B cell selection. English. *Science* **345,** 1058–1062. ISSN: 0036-8075 (Aug. 2014).

186. Sage, P. T. & Sharpe, A. H. The multifaceted functions of follicular regulatory T cells. *Current Opinion in Immunology* **67,** 68–74. ISSN: 0952-7915 (2020).

187. Chung, Y. *et al.* Follicular regulatory T (Tfr) cells with dual Foxp3 and Bcl6 expression suppress germinal center reactions. English. *Nature medicine* **17,** 983–988. ISSN: 1078-8956 (July 2011).

188. Wollenberg, I. *et al.* Regulation of the Germinal Center Reaction by Foxp3+ Follicular Regulatory T Cells. English. *The Journal of Immunology* **187,** 4553–4560. ISSN: 0022-1767 (Nov. 2011).

189. Linterman, M. A. *et al.* Foxp3+ follicular regulatory T cells control the germinal center response. English. *Nature Medicine* **17,** 975–982. ISSN: 1078-8956 (2011-08).

190. Aloulou, M. *et al.* Follicular regulatory T cells can be specific for the immunizing antigen and derive from naive T cells. *Nature Communications* **7,** 10579 (2016).

191. Jacobsen, J. T. *et al.* Expression of Foxp3 by T follicular helper cells in end-stage germinal centers. *Science* **373,** eabe5146. ISSN: 0036-8075 (2021).

192. Fontenot, J. D., Rasmussen, J. P., Gavin, M. A. & Rudensky, A. Y. A function for interleukin 2 in Foxp3-expressing regulatory T cells. *Nature Immunology* **6,** 1142–1151. ISSN: 1529-2908 (2005).

193. Botta, D. *et al.* Dynamic regulation of T Follicular Regulatory cell responses by interleukin 2 during influenza infection. English. *Nature immunology* **18,** 1249–1260. ISSN: 1529-2908 (2017-11).

194. Fu, W. *et al.* Deficiency in T follicular regulatory cells promotes autoimmunity. English. *The Journal of Experimental Medicine* **215,** 815–825. ISSN: 0022-1007 (Jan. 2018).

195. Sage, P. T., Francisco, L. M., Carman, C. V. & Sharpe, A. H. The receptor PD-1 controls follicular regulatory T cells in the lymph nodes and blood. *Nature Immunology* **14,** 152–161. ISSN: 1529-2908 (2013).

196. Sage, P., Paterson, A., Lovitch, S. & Sharpe, A. The Coinhibitory Receptor CTLA-4 Controls B Cell Responses by Modulating T Follicular Helper, T Follicular Regulatory, and T Regulatory Cells. English. *Immunity* **41,** 1026–1039. ISSN: 1074-7613 (Dec. 2014).

197. McCarron, M. J. & Marie, J. C. TGF-β prevents T follicular helper cell accumulation and B cell autoreactivity. *Journal of Clinical Investigation* **124,** 4375–4386. ISSN: 0021-9738 (2014).

198. Nossal, G., Ada, G. & Austin, C. M. ANTIGENS IN IMMUNITY: IV. CELLULAR LOCALIZATION OF 125 I- AND 131 I-LABELLED FLAGELLA IN LYMPH NODES. *Australian Journal of Experimental Biology and Medical Science* **42,** 311–330. ISSN: 0004-945X (1964).

199. Ware, C. F. NETWORK COMMUNICATIONS: Lymphotoxins, LIGHT, and TNF. *Annual Review of Immunology* **23,** 787–819. ISSN: 0732-0582 (2005).

200. Allen, C. D. & Cyster, J. G. Follicular dendritic cell networks of primary follicles and germinal centers: Phenotype and function. *Seminars in Immunology* **20,** 14–25. ISSN: 1044-5323 (2008).

201. Wang, X. *et al.* Follicular dendritic cells help establish follicle identity and promote B cell retention in germinal centers. *The Journal of experimental medicine* **208,** 2497–510. ISSN: 1540-9538 (2011).

202. Ansel, K. M. *et al.* A chemokine-driven positive feedback loop organizes lymphoid follicles. *Nature* **406,** 309–314. ISSN: 0028-0836 (2000).

203. Nishikawa, Y. *et al.* Establishment of Lymphotoxin β Receptor Signaling-Dependent Cell Lines with Follicular Dendritic Cell Phenotypes from Mouse Lymph Nodes. *The Journal of Immunology* **177,** 5204–5214. ISSN: 0022-1767 (2006).

204. Kopf, M., Herren, S., Wiles, M. V., Pepys, M. B. & Kosco-Vilbois, M. H. Interleukin 6 Influences Germinal Center Development and Antibody Production via a Contribution of C3 Complement Component. *The Journal of Experimental Medicine* **188,** 1895–1906. ISSN: 0022-1007 (1998).

205. Maeda, K., Kosco-Vilbois, M. H., Burton, G. F., Szakal, A. K. & Tew, J. G. Expression of the intercellular adhesion molecule-1 on high endothelial venules and on non-lymphoid antigen handling cells: interdigitating cells, antigen transporting cells and follicular dendritic cells. *Cell and Tissue Research* **279,** 47–54. ISSN: 0302-766X (1995).

206. Phan, T. G., Green, J. A., Gray, E. E., Xu, Y. & Cyster, J. G. Immune complex relay by subcapsular sinus macrophages and noncognate B cells drives antibody affinity maturation. *Nature Immunology* **10,** 786–793. ISSN: 1529-2908 (2009).

207. Gonzalez, S. F. *et al.* Complement-Dependent Transport of Antigen into B Cell Follicles. *The Journal of Immunology* **185,** 2659–2664. ISSN: 0022-1767 (2010).

208. Heesters, B. *et al.* Endocytosis and Recycling of Immune Complexes by Follicular Dendritic Cells Enhances B Cell Antigen Binding and Activation. English. *Immunity* **38,** 1164–1175. ISSN: 1074-7613 (2013).

209. P. Smith, J., F. Burton, G., G. Tew, J. & K. Szakal, A. Tinigible Body Macrophages in Regulation of Germinal Center Reactions. *Journal of Immunology Research* **6,** 285–294. ISSN: 1044-6672 (1998).

210. Hanayama, R. *et al.* Identification of a factor that links apoptotic cells to phagocytes. *Nature* **417,** 182–187. ISSN: 0028-0836 (2002).

211. Baumann, I. *et al.* Impaired uptake of apoptotic cells into tingible body macrophages in germinal centers of patients with systemic lupus erythematosus. *Arthritis & Rheumatism* **46,** 191–201. ISSN: 1529-0131 (2002).

212. Hanayama, R. *et al.* Autoimmune Disease and Impaired Uptake of Apoptotic Cells in MFG-E8-Deficient Mice. *Science* **304,** 1147–1150. ISSN: 0036-8075 (2004).

213. Hermans, M. H. *et al.* The extent of clonal structure in different lymphoid organs. *The Journal of Experimental Medicine* **175,** 1255–1269. ISSN: 0022-1007 (1992).

214. Kroese, F. G. M., Wubbena, A. S., Seijen, H. G. & Nieuwenhuis, P. Germinal centers develop oligoclonally. *European Journal of Immunology* **17,** 1069–1072. ISSN: 1521-4141 (1987).

215. Kroese, F. G. M., Wubbena, A. S., Seijen, H. G. & Nieuwenhuis, P. Histophysiology of the Immune System, The Life History, Organization, and Interactions of Its Cell Populations. *Advances in Experimental Medicine and Biology,* 245–250. ISSN: 0065-2598 (1988).

216. Tas, J. M. J. *et al.* Visualizing antibody affinity maturation in germinal centers. English. *Science* **351,** 1048–1054. ISSN: 0036-8075 (Mar. 2016).

217. Kuraoka, M. *et al.* Complex Antigens Drive Permissive Clonal Selection in Germinal Centers. English. *Immunity* **44,** 542–552. ISSN: 1074-7613 (Mar. 2016).

218. MacLennan, I. C. M. Germinal Centers. *Annual Review of Immunology* **12,** 117–139. ISSN: 0732-0582 (1994).

219. Allen, C. D. C., Okada, T., Tang, H. L. & Cyster, J. G. Imaging of Germinal Center Selection Events During Affinity Maturation. English. *Science* **315,** 528–531. ISSN: 0036-8075 (Jan. 2007).

220. Schwickert, T. A. *et al.* In vivo imaging of germinal centres reveals a dynamic open structure. English. *Nature* **446,** 83–87. ISSN: 0028-0836 (Mar. 2007).

221. Boscardin, S. B. *et al.* Antigen targeting to dendritic cells elicits long-lived T cell help for antibody responses. English. *The Journal of Experimental Medicine* **203,** 599–606. ISSN: 0022-1007 (Mar. 2006).

222. Kamphorst, A. O., Guermonprez, P., Dudziak, D. & Nussenzweig, M. C. Route of Antigen Uptake Differentially Impacts Presentation by Dendritic Cells and Activated Monocytes. English. *The Journal of Immunology* **185,** 3426–3435. ISSN: 0022-1767 (Sept. 2010).

223. Liu, D. *et al.* T–B-cell entanglement and ICOSL-driven feed-forward regulation of germinal centre reaction. *Nature* **517,** 214–218. ISSN: 0028-0836 (2015).

224. Luo, W., Weisel, F. & Shlomchik, M. J. B Cell Receptor and CD40 Signaling Are Rewired for Synergistic Induction of the c-Myc Transcription Factor in Germinal Center B Cells. English. *Immunity* **48,** 313–326.e5. ISSN: 1074-7613 (Jan. 2018).

225. Tangye, S. G. & Ma, C. S. Regulation of the germinal center and humoral immunity by interleukin-21. *Journal of Experimental Medicine* **217,** e20191638. ISSN: 0022-1007 (2019).

226. Papa, I. *et al.* TFH-derived dopamine accelerates productive synapses in germinal centres. *Nature* **547,** 318–323. ISSN: 0028-0836 (July 2017).

227. Duan, L. *et al.* Follicular dendritic cells restrict interleukin-4 availability in germinal centers and foster memory B cell generation. *Immunity* **54,** 2256–2272.e6. ISSN: 1074-7613 (2021).

228. Gitlin, A. D., Shulman, Z. & Nussenzweig, M. C. Clonal selection in the germinal centre by regulated proliferation and hypermutation. English. *Nature* **509,** 637–640. ISSN: 0028-0836 (May 2014).

229. Finkin, S., Hartweger, H., Oliveira, T. Y., Kara, E. E. & Nussenzweig, M. C. Protein Amounts of the MYC Transcription Factor Determine Germinal Center B Cell Division Capacity. English. *Immunity* **51,** 324–336.e5. ISSN: 1074-7613 (Aug. 2019).

230. Ersching, J. *et al.* Germinal Center Selection and Affinity Maturation Require Dynamic Regulation of mTORC1 Kinase. English. *Immunity* **46,** 1045–1058.e6. ISSN: 1074-7613 (June 2017).

231. Chou, C. *et al.* The Transcription Factor AP4 Mediates Resolution of Chronic Viral Infection through Amplification of Germinal Center B Cell Responses. English. *Immunity* **45,** 570–582. ISSN: 1074-7613 (2016-09).

232. Pae, J. *et al.* Cyclin D3 drives inertial cell cycling in dark zone germinal center B cells. English. *Journal of Experimental Medicine* **218,** e20201699. ISSN: 0022-1007. https://rupress.org/jem/article-pdf/218/4/e20201699/1406609/jem_20201699.pdf (Dec. 2020).

233. Vinuesa, C. G., Sanz, I. & Cook, M. C. Dysregulation of germinal centres in autoimmune disease. *Nature Reviews Immunology* **9,** 845–857. ISSN: 1474-1733 (2009).

234. Brink, R. & Phan, T. G. Self-Reactive B Cells in the Germinal Center Reaction. English. *Annual Review of Immunology* **36,** 1–19. ISSN: 0732-0582 (Apr. 2018).

235. Mietzner, B. *et al.* Autoreactive IgG memory antibodies in patients with systemic lupus erythematosus arise from nonreactive and polyreactive precursors. English. *Proceedings of the National Academy of Sciences* **105,** 9727–9732. ISSN: 0027-8424 (July 2008).

236. Tiller, T. *et al.* Autoreactivity in Human IgG+ Memory B Cells. *Immunity* **26,** 205–213. ISSN: 1074-7613 (2007).

237. Faderl, M. *et al.* Two Distinct Pathways in Mice Generate Antinuclear Antigen-Reactive B Cell Repertoires. *Frontiers in Immunology* **9,** 16. ISSN: 1664-3224 (2018).

238. Wellmann, U. *et al.* The evolution of human anti-double-stranded DNA autoantibodies. *Proceedings of the National Academy of Sciences* **102,** 9258–9263. ISSN: 0027-8424 (2005).

239. Shokat, K. M. & Goodnow, C. C. Antigen-induced B-cell death and elimination during germinal-centre immune responses. English. *Nature* **375,** 334–338. ISSN: 0028-0836 (May 1995).

240. Pulendran, B., Kannourakis, G., Nouri, S., Smith, K. G. C. & Nossal, G. J. V. Soluble antigen can cause enhanced apoptosis of germinal-centre B cells. English. *Nature* **375,** 331–334. ISSN: 0028-0836 (May 1995).

241. Han, S, Zheng, B, Porto, J. D. & Kelsoe, G. In situ studies of the primary immune response to (4-hydroxy-3-nitrophenyl)acetyl. IV. Affinity-dependent, antigen-driven B cell apoptosis in germinal centers as a mechanism for maintaining self-tolerance. English. *The Journal of experimental medicine* **182,** 1635–1644. ISSN: 0022-1007 (Dec. 1995).

242. Reed, J. H., Jackson, J., Christ, D. & Goodnow, C. C. Clonal redemption of autoantibodies by somatic hypermutation away from self-reactivity during human immunization. English. *The Journal of Experimental Medicine* **213,** 1255–1265. ISSN: 0022-1007 (June 2016).

243. Burnett, D. L. *et al.* Germinal center antibody mutation trajectories are determined by rapid self/foreign discrimination. English. *Science* **360,** 223–226. ISSN: 0036-8075 (Apr. 2018).

244. Burnett, D. L., Reed, J. H., Christ, D. & Goodnow, C. C. Clonal redemption and clonal anergy as mechanisms to balance B cell tolerance and immunity. *Immunological Reviews* **292,** 61–75. ISSN: 0105-2896 (2019).

245. Sabouri, Z. *et al.* Redemption of autoantibodies on anergic B cells by variable-region glycosylation and mutation away from self-reactivity. English. *Proceedings of the National Academy of Sciences* **111,** E2567–E2575. ISSN: 0027-8424 (June 2014).

246. Tan, J. *et al.* A LAIR1 insertion generates broadly reactive antibodies against malaria variant antigens. *Nature* **529,** 105–109. ISSN: 0028-0836 (2016).

247. Pieper, K. *et al.* Public antibodies to malaria antigens generated by two LAIR1 insertion modalities. English. *Nature* **548,** 597–601. ISSN: 0028-0836 (Aug. 2017).

248. Mayer, C. T. *et al.* The microanatomic segregation of selection by apoptosis in the germinal center. English. *Science* **358,** eaao2602. ISSN: 0036-8075 (Oct. 2017).

249. Paus, D. *et al.* Antigen recognition strength regulates the choice between extrafollicular plasma cell and germinal center B cell differentiation. English. *The Journal of Experimental Medicine* **203,** 1081–1091. ISSN: 0022-1007 (Apr. 2006).

250. Elsner, R. A. & Shlomchik, M. J. Germinal Center and Extrafollicular B Cell Responses in Vaccination, Immunity, and Autoimmunity. *Immunity* **53,** 1136–1150. ISSN: 1074-7613 (2020).

251. Phan, T. G. *et al.* High affinity germinal center B cells are actively selected into the plasma cell compartment. English. *The Journal of Experimental Medicine* **203,** 2419–2424. ISSN: 0022-1007 (Oct. 2006).

252. Smith, K. G. C., Light, A., Nossal, G. J. V. & Tarlinton, D. M. The extent of affinity maturation differs between the memory and antibody-forming cell compartments in the primary immune response. English. *The EMBO Journal* **16,** 2996–3006. ISSN: 1460-2075 (June 1997).

253. Ise, W. & Kurosaki, T. Plasma cell differentiation during the germinal center reaction. *Immunological Reviews* **288,** 64–74. ISSN: 0105-2896 (2019).

254. Nutt, S. L., Hodgkin, P. D., Tarlinton, D. M. & Corcoran, L. M. The generation of antibody-secreting plasma cells. English. *Nature Reviews Immunology* **15,** 160–171. ISSN: 1474-1733 (Mar. 2015).

255. Klein, U. *et al.* Transcription factor IRF4 controls plasma cell differentiation and class-switch recombination. *Nature Immunology* **7,** 773–782. ISSN: 1529-2908 (2006).

256. Ochiai, K. *et al.* Transcriptional Regulation of Germinal Center B and Plasma Cell Fates by Dynamical Control of IRF4. *Immunity* **38,** 918–929. ISSN: 1074-7613 (2013).

257. Kräutler, N. J. *et al.* Differentiation of germinal center B cells into plasma cells is initiated by high-affinity antigen and completed by Tfh cells. English. *The Journal of Experimental Medicine* **214,** 1259–1267. ISSN: 0022-1007 (Mar. 2017).

258. Chevrier, S. *et al.* The BTB-ZF transcription factor Zbtb20 is driven by Irf4 to promote plasma cell differentiation and longevity. English. *The Journal of Experimental Medicine* **211,** 827–840. ISSN: 0022-1007 (May 2014).

259. Ise, W. *et al.* T Follicular Helper Cell-Germinal Center B Cell Interaction Strength Regulates Entry into Plasma Cell or Recycling Germinal Center Cell Fate. English. *Immunity* **48,** 702–715.e4. ISSN: 1074-7613 (2018-04).

260. Weisel, F., Zuccarino-Catania, G., Chikina, M. & Shlomchik, M. A Temporal Switch in the Germinal Center Determines Differential Output of Memory B and Plasma Cells. English. *Immunity* **44,** 116–130. ISSN: 1074-7613 (Jan. 2016).

261. Sundling, C. *et al.* Positive selection of IgG+ over IgM+ B cells in the germinal center reaction. *Immunity* **54,** 988–1001.e5. ISSN: 1074-7613 (2021).

262. Yang, Z., Sullivan, B. & Allen, C. Fluorescent In Vivo Detection Reveals that IgE+ B Cells Are Restrained by an Intrinsic Cell Fate Predisposition. English. *Immunity* **36,** 857–872. ISSN: 1074-7613 (May 2012).

263. Davidzohn, N. *et al.* Syk degradation restrains plasma cell formation and promotes zonal transitions in germinal centers. English. *Journal of Experimental Medicine* **217,** e20191043. ISSN: 0022-1007. https://rupress.org/jem/article-pdf/217/3/e20191043/861803/jem_20191043.pdf (Dec. 2019).

264. Laidlaw, B. J. & Cyster, J. G. Transcriptional regulation of memory B cell differentiation. *Nature Reviews Immunology* **21,** 209–220. ISSN: 1474-1733 (Oct. 2020).

265. Inoue, T., Moran, I., Shinnakasu, R., Phan, T. G. & Kurosaki, T. Generation of memory B cells and their reactivation. *Immunological Reviews* **283,** 138–149. ISSN: 0105-2896 (2018).

266. Kometani, K. *et al.* Repression of the Transcription Factor Bach2 Contributes to Predisposition of IgG1 Memory B Cells toward Plasma Cell Differentiation. English. *Immunity* **39,** 136–147. ISSN: 1074-7613 (July 2013).

267. Shinnakasu, R. & Kurosaki, T. Regulation of memory B and plasma cell differentiation. English. *Current Opinion in Immunology* **45,** 126–131. ISSN: 0952-7915 (Mar. 2017).

268. Taylor, J. J., Pape, K. A. & Jenkins, M. K. A germinal center–independent pathway generates unswitched memory B cells early in the primary response. English. *The Journal of Experimental Medicine* **209,** 597–606. ISSN: 0022-1007 (Mar. 2012).

269. Viant, C. *et al.* Germinal center–dependent and –independent memory B cells produced throughout the immune response. *Journal of Experimental Medicine* **218,** e20202489. ISSN: 0022-1007 (2021).

270. Suan, D. *et al.* CCR6 Defines Memory B Cell Precursors in Mouse and Human Germinal Centers, Revealing Light-Zone Location and Predominant Low Antigen Affinity. *Immunity* **47,** 1142–1153.e4. ISSN: 1074-7613 (2017).

271. Inoue, T. *et al.* Exit from germinal center to become quiescent memory B cells depends on metabolic reprograming and provision of a survival signal. *Journal of Experimental Medicine* **218,** e20200866. ISSN: 0022-1007 (2020).

272. Laidlaw, B. J. *et al.* The Eph-related tyrosine kinase ligand Ephrin-B1 marks germinal center and memory precursor B cells. English. *The Journal of Experimental Medicine* **214,** 639–649. ISSN: 0022-1007 (Mar. 2017).

273. Shinnakasu, R. *et al.* Regulated selection of germinal-center cells into the memory B cell compartment. English. *Nature Immunology* **17,** 861–869. ISSN: 1529-2908 (2016-07).

274. Laidlaw, B. J., Duan, L., Xu, Y., Vazquez, S. E. & Cyster, J. G. The transcription factor Hhex cooperates with the corepressor Tle3 to promote memory B cell development. English. *Nature Immunology* **21,** 1082–1093. ISSN: 1529-2908 (June 2020).

275. Victora, G. D. & Nussenzweig, M. C. Germinal Centers. *Annual Review of Immunology* **40,** 1–30. ISSN: 0732-0582 (2022).

276. Khalil, A. M., Cambier, J. C. & Shlomchik, M. J. B Cell Receptor Signal Transduction in the GC Is Short-Circuited by High Phosphatase Activity. English. *Science* **336,** 1178–1181. ISSN: 0036-8075 (June 2012).

277. Nowosad, C. R., Spillane, K. M. & Tolar, P. Germinal center B cells recognize antigen through a specialized immune synapse architecture. *Nature immunology* **17,** 870–877. ISSN: 1529-2908 (2016).

278. Kwak, K. *et al.* Intrinsic properties of human germinal center B cells set antigen affinity thresholds. English. *Science Immunology* **3,** eaau6598 (Nov. 2018).

279. Spillane, K. M. & Tolar, P. B cell antigen extraction is regulated by physical properties of antigen-presenting cells. English. *The Journal of Cell Biology* **216,** 217–230. ISSN: 0021-9525 (Jan. 2017).

280. Luo, W. *et al.* The AKT kinase signaling network is rewired by PTEN to control proximal BCR signaling in germinal center B cells. English. *Nature Immunology* **20,** 736–746. ISSN: 1529-2908 (2019-06).

281. Tolar, P. Cytoskeletal control of B cell responses to antigens. English. *Nature Reviews Immunology* **17,** 621–634. ISSN: 1474-1733 (July 2017).

282. Fischer, M. B. *et al.* Dependence of Germinal Center B Cells on Expression of CD21/CD35 for Survival. *Science* **280,** 582–585. ISSN: 0036-8075 (1998).

283. Kraus, M. *et al.* Interference with Immunoglobulin (Ig)α Immunoreceptor Tyrosine–Based Activation Motif (Itam) Phosphorylation Modulates or Blocks B Cell Development, Depending on the Availability of an Igβ Cytoplasmic Tail. *The Journal of Experimental Medicine* **194,** 455–470. ISSN: 0022-1007 (2001).

284. Randall, K. L. *et al.* Dock8 mutations cripple B cell immunological synapses, germinal centers and long-lived antibody production. English. *Nature Immunology* **10,** 1283–1291. ISSN: 1529-2908 (2009-12).

285. Rickert, R. C., Rajewsky, K. & Roes, J. Impairment of T-cell-dependent B-cell responses and B-l cell development in CD19-deficient mice. English. *Nature* **376,** 352–355. ISSN: 0028-0836 (July 1995).

286. Stewart, I., Radtke, D., Phillips, B., McGowan, S. J. & Bannard, O. Germinal Center B Cells Replace Their Antigen Receptors in Dark Zones and Fail Light Zone Entry when Immunoglobulin Gene Mutations are Damaging. English. *Immunity* **49,** 477–489.e7. ISSN: 1074-7613 (2018-09).

287. Mueller, J., Matloubian, M. & Zikherman, J. Cutting Edge: An In Vivo Reporter Reveals Active B Cell Receptor Signaling in the Germinal Center. English. *The Journal of Immunology* **194,** 2993–2997. ISSN: 0022-1767 (Mar. 2015).

288. Rudensky, A. Y., Rath, S., Preston-Hurlburt, P., Murphy, D. B. & Janeway, C. A. On the complexity of self. English. *Nature* **353,** 660–662. ISSN: 0028-0836 (Oct. 1991).

289. Itano, A. A. *et al.* Distinct dendritic cell populations sequentially present antigen to CD4 T cells and stimulate different aspects of cell-mediated immunity. English. *Immunity* **19,** 47 –57 (2003-07).

290. Shih, T.-A. Y., Roederer, M. & Nussenzweig, M. C. Role of antigen receptor affinity in T cell–independent antibody responses in vivo. English. *Nature Immunology* **3,** 399–406. ISSN: 1529-2908 (2002-04).

291. Victora, G. D. *et al.* Identification of human germinal center light and dark zone cells and their relationship to human B-cell lymphomas. *Blood* **120,** 2240–2248. ISSN: 0006-4971 (2012).

292. Huang, C., Bredemeyer, A., Walker, L., Bassing, C. & Sleckman, B. Dynamic regulation of c-Myc proto-oncogene expression during lymphocyte development revealed by a GFP-c-Myc knock-in mouse. *European Journal of Immunology* **38,** 342–349. ISSN: 1521-4141 (2008).

293. Tomayko, M. M. *et al.* Systematic Comparison of Gene Expression between Murine Memory and Naive B Cells Demonstrates That Memory B Cells Have Unique Signaling Capabilities. *The Journal of Immunology* **181,** 27–38. ISSN: 0022-1767 (2008).

294. Dosenovic, P. *et al.* Anti–HIV-1 B cell responses are dependent on B cell precursor frequency and antigen-binding affinity. English. *Proceedings of the National Academy of Sciences* **115,** 201803457. ISSN: 0027-8424 (May 2018).

295. Herman, S. E. M. *et al.* Bruton tyrosine kinase represents a promising therapeutic target for treatment of chronic lymphocytic leukemia and is effectively targeted by PCI-32765. English. *Blood* **117,** 6287–6296. ISSN: 0006-4971 (June 2011).

296. Woyach, J. A., Johnson, A. J. & Byrd, J. C. The B-cell receptor signaling pathway as a therapeutic target in CLL. English. *Blood* **120,** 1175–1184. ISSN: 0006-4971 (Aug. 2012).

297. Honigberg, L. A. *et al.* The Bruton tyrosine kinase inhibitor PCI-32765 blocks B-cell activation and is efficacious in models of autoimmune disease and B-cell malignancy. English. *Proceedings of the National Academy of Sciences* **107,** 13075–13080. ISSN: 0027-8424 (July 2010).

298. Roman-Garcia, S. *et al.* Distinct Roles for Bruton's Tyrosine Kinase in B Cell Immune Synapse Formation. English. *Frontiers in Immunology* **9,** 2027 (2018).

299. Sharma, S., Orlowski, G. & Song, W. Btk Regulates B Cell Receptor-Mediated Antigen Processing and Presentation by Controlling Actin Cytoskeleton Dynamics in B Cells. English. *The Journal of Immunology* **182,** 329–339. ISSN: 0022-1767. http://www.jimmunol.org/content/jimmunol/182/1/329.full.pdf (Dec. 2008).

300. Khan, W. N. *et al.* Defective B cell development and function in Btk-deficient mice. *Immunity* **3,** 283–99. ISSN: 1074-7613 (1995).

301. Petro, J. B., Rahman, S. M., Ballard, D. W. & Khan, W. N. Bruton's tyrosine kinase is required for activation of IkappaB kinase and nuclear factor kappaB in response to B cell receptor engagement. *The Journal of experimental medicine* **191,** 1745–54. ISSN: 0022-1007 (2000).

302. Corneth, O. B. J., Wolterink, R. G. J. K. & Hendriks, R. W. B Cell Receptor Signaling. English. *Current Topics in Microbiology and Immunology* **393,** 67–105. ISSN: 0070-217X (2016).

303. Cheng, S *et al.* Functional characterization of BTKC481S mutation that confers ibrutinib resistance: exploration of alternative kinase inhibitors. English. *Leukemia* **29,** 895–900. ISSN: 0887-6924 (2015-04).

304. Johnson, A. R. *et al.* Battling Btk Mutants With Noncovalent Inhibitors That Overcome Cys481 and Thr474 Mutations. English. *ACS Chemical Biology* **11,** 2897–2907. ISSN: 1554-8929 (Oct. 2016).

305. Woyach, J. A. *et al.* Resistance Mechanisms for the Bruton's Tyrosine Kinase Inhibitor Ibrutinib. English. *The New England Journal of Medicine* **370,** 2286–2294. ISSN: 0028-4793 (June 2014).

306. Bond, D. A. & Woyach, J. A. Targeting BTK in CLL: Beyond Ibrutinib. English. *Current Hematologic Malignancy Reports* **14,** 197–205. ISSN: 1558-8211 (Apr. 2019).

307. Dubovsky, J. A. *et al.* Ibrutinib is an irreversible molecular inhibitor of ITK driving a Th1-selective pressure in T lymphocytes. English. *Blood* **122,** 2539–2549. ISSN: 0006-4971 (Oct. 2013).

308. Schutt, S. D. *et al.* Inhibition of BTK and ITK with Ibrutinib Is Effective in the Prevention of Chronic Graft-versus-Host Disease in Mice. English. *PLoS ONE* **10** (ed Stepkowski, S.) e0137641 (Sept. 2015).

309. Wu, J., Zhang, M. & Liu, D. Acalabrutinib (ACP-196): a selective second-generation BTK inhibitor. *Journal of Hematology & Oncology* **9,** 21 (2016).

310. Bannard, O. & Cyster, J. G. Germinal centers: programmed for affinity maturation and antibody diversification. English. *Current Opinion in Immunology* **45,** 21–30. ISSN: 0952-7915 (2017-04).

311. Mintz, M. A. *et al.* The HVEM-BTLA Axis Restrains T Cell Help to Germinal Center B Cells and Functions as a Cell-Extrinsic Suppressor in Lymphomagenesis. *Immunity* **51,** 310–323.e7. ISSN: 1074-7613 (June 2019).

312. Mandel, T. E., Phipps, R. P., Abbot, A. P. & Tew, J. G. Long-term antigen retention by dendritic cells in the popliteal lymph node of immunized mice. *Immunology* **43,** 353–62. ISSN: 0019-2805 (1981).

313. Szakal, A. K., Gieringer, R. L., Kosco, M. H. & Tew, J. G. Isolated follicular dendritic cells: cytochemical antigen localization, Nomarski, SEM, and TEM morphology. *Journal of immunology (Baltimore, Md. : 1950)* **134,** 1349–59. ISSN: 0022-1767 (1985).

314. Viant, C. *et al.* Antibody Affinity Shapes the Choice between Memory and Germinal Center B Cell Fates. English. *Cell* **183,** 1298–1311.e11. ISSN: 0092-8674 (Nov. 2020).

315. Lagresle, C, Mondière, P, Bella, C, Krammer, P. H. & Defrance, T. Concurrent engagement of CD40 and the antigen receptor protects naive and memory human B cells from APO-1/Fas-mediated apoptosis. *The Journal of experimental medicine* **183,** 1377–1388. ISSN: 0022-1007 (1996).

316. Rathmell, J. C. *et al.* CD95 (Fas)-dependent elimination of self-reactive B cells upon interaction with CD4+T cells. *Nature* **376,** 181–184. ISSN: 0028-0836 (1995).

317. Rothstein, T. L. *et al.* Protection against Fas-dependent Thl-mediated apoptosis by antigen receptor engagement in B cells. *Nature* **374,** 163–165. ISSN: 0028-0836 (1995).

318. Koopman, G *et al.* Adhesion through the LFA-1 (CD11a/CD18)-ICAM-1 (CD54) and the VLA-4 (CD49d)-VCAM-1 (CD106) pathways prevents apoptosis of germinal center B cells. *Journal of immunology (Baltimore, Md. : 1950)* **152,** 3760–7. ISSN: 0022-1767 (1994).

319. Akkaya, M. *et al.* Second signals rescue B cells from activation-induced mitochondrial dysfunction and death. English. *Nature Immunology* **19,** 871–884. ISSN: 1529-2908 (July 2018).

320. Zaretsky, I. *et al.* ICAMs support B cell interactions with T follicular helper cells and promote clonal selection. English. *Journal of Experimental Medicine* **214,** 3435–3448. ISSN: 0022-1007 (Sept. 2017).

321. Inui, M. *et al.* Rapid generation of mouse models with defined point mutations by the CRISPR/Cas9 system. English. *Scientific Reports* **4,** 5396 (June 2014).

322. Pasqual, G., Angelini, A. & Victora, G. D. T follicular Helper Cells, Methods and Protocols. English. *Methods in Molecular Biology* **1291,** 125–134. ISSN: 1064-3745 (2015).

323. Boehmer, L. v. *et al.* Sequencing and cloning of antigen-specific antibodies from mouse memory B cells. English. *Nature Protocols* **11,** 1908–1923. ISSN: 1754-2189 (2016-10).

324. Tiller, T., Busse, C. E. & Wardemann, H. Cloning and expression of murine Ig genes from single B cells. English. *Journal of Immunological Methods* **350,** 183–193. ISSN: 0022-1759 (Oct. 2009).

325. Trombetta, J. J. *et al.* Preparation of Single-Cell RNA-Seq Libraries for Next Generation Sequencing. English. *Current Protocols in Molecular Biology* **107,** 4.22.1–4.22.17. ISSN: 1934-3639 (July 2014).

326. Picelli, S. *et al.* Full-length RNA-seq from single cells using Smart-seq2. English. *Nature Protocols* **9,** 171–181. ISSN: 1754-2189 (2014-01).

327. Islam, S. *et al.* Quantitative single-cell RNA-seq with unique molecular identifiers. English. *Nature Methods* **11,** 163–166. ISSN: 1548-7091 (2014-02).

328. Masella, A. P., Bartram, A. K., Truszkowski, J. M., Brown, D. G. & Neufeld, J. D. PANDAseq: paired-end assembler for illumina sequences. *BMC Bioinformatics* **13,** 31–31 (2012).

329. Bray, N. L., Pimentel, H., Melsted, P. & Pachter, L. Near-optimal probabilistic RNA-seq quantification. English. *Nature Biotechnology* **34,** 525–527. ISSN: 1087-0156 (2016-05).

330. Soneson, C., Love, M. I. & Robinson, M. D. Differential analyses for RNA-seq: transcript-level estimates improve gene-level inferences. *F1000Research* **4,** 1521. ISSN: 2046-1402 (2016).

331. Love, M. I., Huber, W. & Anders, S. Moderated estimation of fold change and dispersion for RNA-seq data with DESeq2. *Genome Biology* **15,** 550. ISSN: 1465-6906 (2014).